The effect of tau hyperphosphorylation on organelle transport

Karthikeyan Swaminathan,
Integrated Program in Neuroscience (IPN),
McGill University,
Montréal, Quebec, Canada

Adam G. Hendricks Laboratory
Department of Bioengineering,
McGill University,
Montréal, Quebec, Canada

Master's research thesis
October 2023

A thesis submitted to McGill University in partial fulfilment of the requirements of the degree of Master of Science, Neuroscience (Thesis option).

Table of contents

Abstract

Tau hyperphosphorylation is strongly linked to neurodegenerative disease, but its impact on intracellular transport is poorly understood. This study aims to understand how aberrant phosphorylation of tau alters its microtubule binding and intracellular transport. Organelle transport is regulated through multiple interdependent mechanisms, which include Microtubule-Associated Proteins (MAPs), post-translational modification of microtubules and MAPs and the organization of microtubules.

Tau is a MAP that bundles and stabilizes microtubules in neuronal axons and regulates intracellular transport. It can be phosphorylated by kinases such as GSK3β, Cdk5 and fyn at multiple sites during tauopathic disease such as Alzheimer's disease. Previously, we discovered that tau differentially regulates the motility of specific cargoes based on the phosphorylation state of tau and the type of motors that carry them. Here, I examined how tau hyperphosphorylation affects microtubule organization and the transport of lysosomes and early endosomes using TIRF microscopy. We exogenously expressed Alzheimer's disease-relevant phosphomimetic tau (E14; mimicking tau hyperphosphorylation by replacing 14 serine/threonine sites with glutamate), phosphoresistive tau (AP14; replacing those same 14 serine/threonine sites to alanine) and wild-type tau (WT) in COS-7 fibroblast cells. COS-7 cells lack endogenous tau expression and possess a flat morphology, and are a useful model for TIRF-based imaging and organelle tracking experiments.

Our findings showed that phosphomimetic E14 tau weakly affected cargo transport dynamics compared to phosphoresistive AP14 tau. E14 tau exhibited a more negative charge state owing to the 14 glutamate sites and so, it experienced repulsion from the negatively charged

microtubules. Because of this, E14 tau predominantly localized in the cytoplasm due to its greater diffusivity, thus drastically affected the formation of microtubule bundles at physiological levels. This contrasts with AP14 tau, which enriched strongly on microtubules and showed greater microtubule bundling. All three tau constructs affected the motility of early endosomes and lysosomes and increased the amount of stationary cargo. AP14 tau strongly inhibited the motility of lysosomes and early endosomes, whereas the organelles were weakly affected by E14 tau.

Our results suggest that the lysosomes and early endosomes are sensitive to AP14 tau and are less sensitive to E14 tau. Since AP14 tau strongly binds to microtubules and could change their properties, it directly hinders cargo transport, whereas E14 tau weakly binds to microtubules and does not directly hinder cargo transport. This shows that hyperphosphorylated tau helps maintain cargo transport by weakly binding to microtubules, reducing competition with motor proteins. Our results support the previous study on Y18E monophosphomimetic tau, where it disrupted the early endosome transport more than lysosomes, similar to what we found in E14 tau, but the effects were weaker. Further research on iPSC-derived tau knockout neurons could provide new insights in axonal transport. This work was supported by NIH, Mitacs and Healthy Brains Healthy Lives (HBHL).

Résumé

L'hyperphosphorylation du tau est fortement liée aux maladies neurodégénératives, mais son impact sur le transport intracellulaire est mal compris. Cette étude vise à comprendre comment la phosphorylation aberrante du tau modifie sa liaison aux microtubules et son transport intracellulaire. Le transport des organites est régulé par de multiples mécanismes interdépendants, dont les protéines associées aux microtubules (MAP), la modification post-traductionnelle des microtubules et des MAP et l'organisation des microtubules.

Tau est un PAM qui regroupe et stabilise les microtubules dans les axones neuronaux et régule le transport intracellulaire. Elle peut être phosphorylée par des kinases telles que GSK3β, Cdk5 et fyn sur de multiples sites au cours d'une maladie tauopathique telle que la maladie d'Alzheimer. Précédemment, nous avons découvert que tau régule de manière différentielle la motilité de cargaisons spécifiques en fonction de l'état de phosphorylation de tau et du type de moteurs qui les transportent. Ici, j'ai examiné comment l'hyperphosphorylation de tau affecte l'organisation des microtubules et le transport des lysosomes et des endosomes précoces à l'aide de la microscopie TIRF. Nous avons exprimé de façon exogène de la tau phosphomimétique (E14 ; imitant l'hyperphosphorylation du tau en remplaçant 14 sites sérine/thréonine par du glutamate), de la tau phosphoresistive (AP14 ; remplaçant ces mêmes 14 sites sérine/thréonine par de l'alanine) et du tau de type sauvage (WT) dans des cellules de fibroblastes COS-7. Les cellules COS-7 n'expriment pas de tau endogène et possèdent une morphologie plate. Elles constituent un modèle utile pour l'imagerie TIRF et les expériences de suivi des organites.

Nos résultats ont démontré que la phosphomimétique E14 tau affectait faiblement la dynamique du transport de fret par rapport à la phosphorésistive AP14 tau. La tau E14 présente

une charge plus négative en raison de ses 14 sites de glutamate et est donc repoussée par les microtubules chargés négativement. Pour cette raison, la tau E14 se localise principalement dans le cytoplasme en raison de sa plus grande diffusivité, ce qui affecte considérablement la formation de faisceaux de microtubules à des niveaux physiologiques. Ceci contraste avec le tau AP14, qui s'est fortement enrichie en microtubules et a montré une plus grande formation de faisceaux de microtubules. Les trois constructions tau ont affecté la motilité des endosomes précoces et des lysosomes et ont augmenté la quantité de cargaison stationnaire. La tau AP14 a fortement inhibé la motilité des lysosomes et des endosomes précoces, tandis que les organites ont été faiblement affectés par le tau E14.

Nos résultats suggèrent que les lysosomes et les endosomes précoces sont sensibles à la AP14 tau et moins sensibles à la E14 tau. Comme la AP14 se lie fortement aux microtubules et peut modifier leurs propriétés, elle entrave directement le transport des cargaisons, alors que la E14 se lie faiblement aux microtubules et n'entrave pas directement le transport des cargaisons. Cela montre que la tau hyperphosphorylée aide à maintenir le transport des cargaisons en se liant faiblement aux microtubules, réduisant ainsi la compétition avec les protéines motrices. Nos résultats confirment l'étude précédente sur le tau monophosphomimétique Y18E, qui perturbait davantage le transport des endosomes précoces que celui des lysosomes, comme nous l'avons constaté avec le tau E14, mais les effets étaient plus faibles. D'autres recherches sur les neurones knock-out tau dérivés d'iPSC pourraient fournir de nouvelles informations dans le contexte du transport axonal. Ce travail a été soutenu par les NIH, Mitacs et Healthy Brains Healthy Lives (HBHL).

Acknowledgments

I extend my heartfelt gratitude to my esteemed supervisor, Dr. Adam Hendricks, whose unwavering encouragement and instrumental support helped me complete this project. Even amidst the challenges posed by the pandemic, Dr. Hendricks provided me with a remarkable opportunity within his laboratory, initially as a McGill SURE intern and subsequently as an IPN Master's student. His guidance and expertise have not only helped me complete my project and side projects I had, but have also instilled within me invaluable skills and a heightened acumen for critical thinking. My appreciation for your unwavering assistance knows no bounds. Thank you so much for everything!

I am indebted to my lab colleagues, with special mention to Brooke Turkalj, Sahil Nagpal, Emily Prowse, Magda Giovanna Sanchez, Omar Kabalan, Samuel Wang, Zhu Liu, Sofia Cruz Tetlalmatzi, and Daniel Beaudet for their endless knowledge, motivation, and shared laughter! I express my gratitude to Dr. Linda Balabanian for her initial support, which set the foundation for my project. My profound acknowledgments extend to my esteemed committee members, Dr. Gary Brouhard and Dr. Maria Vera Ugalde, whose feedback and wealth of knowledge has been pivotal in advancing my project.

I thank the National Institute of Health (NIH), Mitacs, and Healthy Brains Healthy Lives (HBHL) for their generous funding of my project. I sincerely thank the McGill Integrated Program in Neuroscience team for their steadfast support during my master's program.

I am elated by the support of my cherished friends in India, notably Prem Kumar, Santhosh Raj, Shankar Narayanan, Menjith, Vinodh Kumar, Shabnam Shajahan, and Mary Vincy Joseph! I am also profoundly thankful for my dear companions in Montreal – François Jarry,

Nathanaël Beaulieu, Alexander Bailey, Maria Vittoria Gugliuzza, Flavie Laliberté, Mayank Shrivastava, Pranjal Wadhwa, Maria Haddad, Theresa Degenhard, Manisha Aindrila, Pranab Kumar Saha, Franziska Hildesheim, and numerous others who have genuinely made me feel Montreal like a second home!

My gratitude extends to the mentees I had the privilege of guiding through the Mitacs Globalink Research Internship program. Their enthusiasm allowed me to revisit the transformative experience of my own internship in 2019 and illuminated the milestones I achieved along my journey. I also extend my appreciation to the dedicated staff members of HBHL, particularly Dr. Andrzej Tereszkowski and Dr. Adrienne Crampton, whose belief in my potential facilitated interactions with neuroscience researchers and industrial representatives, affording me insights into the boundless horizons of my field, which I hope will shape my future career.

Most importantly, I am profoundly thankful for my brother, Viswanathan Swaminathan, my sister-in-law, Gayatri Madhukumar, and my father, Swaminathan Gobichettipalayam Ramarathinam, whose unwavering support and encouragement have been pivotal during my master's program! In moments of difficulty, their belief in me acted as a guiding light, urging me to aspire higher. Finally, I dedicate my deepest gratitude to my late mother, Parvathy Swaminathan, whose past actions, compassion, and unyielding pursuit of excellence continue to inspire me. Though physically absent, her spirit endures, urging me to fulfill her vision of me being a better human being.

Contribution of Authors

This study was designed and supervised by Dr. Adam Hendricks. This thesis, along with images and plots, was done by Karthikeyan Swaminathan. Some images in the literature review and methodology were taken from research papers with permission and were cited properly. Dr. Adam Hendricks reviewed the thesis and provided feedback and comments.

Introduction and Literature Review – Written by Karthikeyan Swaminathan, and reviewed and edited by Dr. Adam Hendricks.

Methodology – Adapted based on the protocol my previous lab colleague, Dr. Linda Balabanian, provided. MATLAB codes used for the analysis were inspired by the codes developed by Dr. Linda Balabanian, Dr. Abdullah Chaudhary and Emily Prowse or written completely by Karthikeyan Swaminathan with suggestions from Dr. Adam Hendricks.

Results – Karthikeyan Swaminathan performed all the experiments, analyzed all the data, and compiled and plotted them with guidance and feedback from Dr. Adam Hendricks.

Discussion – Written by Karthikeyan Swaminathan and reviewed and edited by Dr. Adam Hendricks.

Conclusion and Future Direction – Written by Karthikeyan Swaminathan, and reviewed and edited by Dr. Adam Hendricks.

Contribution to other projects – The first project was done with Dr. Linda Balabanian. Karthikeyan Swaminathan performed the experimental work and data collection and then shared the data with Dr. Linda Balabanian for lysosome motility analysis. The second project was done with Sahil Nagpal. Karthikeyan Swaminathan developed the MATLAB velocity codes based on the data provided by Sahil Nagpal. Sahil Nagpal used the code for the data analysis.

List of figures

Abbreviations

AD – Alzheimer's Disease

AIC - Akaike Information Criterion

AP14 – Phosphoresistive tau (mutated to Alanine)

DMEM - Dulbecco's Modified Eagle Medium

EGFP – Enhanced Green Fluorescent Protein

E14 – Phosphomimetic tau (mutated to glutamate)

FBS – Fetal Bovine Serum

GMM - Gaussian Mixture Model

iPSC - Induced Pluripotent Stem Cells

LAP - Linear Assignment Problem

LoG - Laplacian of Gaussian

MSD – Mean Squared Displacement

OT – Optical Trapping

Qdot – Quantum Dot (Qdot 565)

Rg – Radius of Gyration

SIM – Structured Illumination Microscopy

TIRF - Total Internal Reflection Fluorescent

WT – Wild type

Chapter 1

1.1. Introduction:

Alzheimer's disease (AD) is a progressive neurodegenerative disorder affecting millions of individuals worldwide, primarily those over 65. It accounts for approximately 70% of dementia (Tarawneh & Holtzman, 2012). The hallmark feature of AD is the accumulation of abnormal protein aggregates in the brain, including senile beta-amyloid plaques (comprising amyloid β peptide - Aβ) (Duquette et al., 2021; Kent et al., 2020; Tarawneh & Holtzman, 2012) and neurofibrillary tangles (consisting of Tau) (Ballatore et al., 2007; Combs et al., 2019; Xia et al., 2021a). While many previous studies have focused on how Aβ and tau form plaques and tangles that could induce neurodegeneration, less is known about tau's role in regulating intracellular transport. In this project, we show how misregulated tau through hyperphosphorylation weakly binds to microtubules and affects cell organelle transport compared to unphosphorylated tau, suggesting that hyperphosphorylation may protect the transport process rather than disrupt it.

Tau hyperphosphorylation is a critical event in the progression of tauopathic diseases such as Alzheimer's Disease, as phosphorylation alters the normal function of tau in maintaining and stabilizing cytoskeletal structures and regulating intracellular cargo transport (Hamano et al., 2021; Yang et al., 2023). However, the actual mechanism of how the aberrantly phosphorylated tau forms and how it affects intracellular transport is still under research. It is proposed that tau hyperphosphorylation can lead to the destabilization of microtubules and which will directly impact the transport (Baas & Qiang, 2019; Rodríguez-Martín et al., 2013; Shahpasand et al., 2012). Still, only a few research studies were performed to address this issue of how impaired transport is linked to neurodegeneration, making it crucial to investigate in-depth. Hence, in

our research, we specifically focused on understanding microtubule-based cargo transport and its regulation, which are some of the primary functions of the cytoskeleton affected during the disease condition, especially in tau hyperphosphorylation.

Cells need to transport organelles, proteins, and other biological materials from one part of the cell to another. This process is facilitated by cytoskeletal structures like microtubules, which act as tracks for motor proteins, such as kinesins and dyneins (Aiken & Holzbaur, 2021; Balabanian et al., 2018; Hirokawa & Tanaka, 2015; Scholey, 2013). Microtubules, composed of αβ-tubulin, are highly dynamic as they grow by adding GTP-tubulin dimers to the microtubule ends where a stabilizing cap is present. The GTP-tubulin below this cap is hydrolyzed to GDP-tubulin because of the GTPase activity of the tubulin. Proteins such as polymerases, depolymerases, and regulatory kinesins interact with the microtubule ends, influencing their growth or shrinkage. Loss of the cap triggers rapid shrinking or catastrophe. Sometimes the microtubule shrinkage is stopped and is rescued to switch back to a growth state. This dynamic switch between growing and shrinking is called dynamic instability (Mitchison & Kirschner, 1984). It is employed by cells for tasks like exerting forces during mitotic chromosome segregation or to help navigate cells extracellularly (Brouhard & Rice, 2018). This dynamic nature of microtubules affects cargo transport, mostly through microtubule-associated proteins (MAPs) (Aiken & Holzbaur, 2021; T. Guo et al., 2017; Xia et al., 2021a), post-translational modifications (PTMs) (Harada et al., 1994; Martin et al., 2013) and microtubule configuration (Bechstedt et al., 2014; Muroyama & Lechler, 2017; Samsonov et al., 2004; Yogev et al., 2016). Understanding the disease progression becomes complicated when considering all these modes of regulations simultaneously. So, we focused on the microtubule-associated protein-based regulation alone, focusing on tau hyperphosphorylation through tau transfection study using COS-7 as the model cell line. COS-7 lacks endogenous

tau, which makes it ideal for isolating the effects of hyperphosphorylated tau on cargo transport upon transfecting tau constructs into the cells (Balabanian et al., 2022). Through cell model studies, we focused on microtubule organization and also the spatiotemporal motility of cargo transport in real time, especially in hyperphosphorylated tau. This approach can yield more profound insights into the influence of hyperphosphorylated tau on the defective transport observed in neurodegenerative diseases such as Alzheimer's.

The reason to focus on phosphorylation is that it is the most common post-translational modification found in tau isolates from Alzheimer's Disease patients and is associated with tau aggregation (Goedert et al., 2017; Xia et al., 2020). Tau, primarily found in neurons, plays an essential role in maintaining the structural integrity of microtubules (Gendron, 2009; Hoover et al., 2010; Rodríguez-Martín et al., 2013). Through hyperphosphorylation, aberrant tau can disrupt microtubule function, destabilize neuronal structure, and increase the propensity to form aggregates. Misregulation of tau could ultimately lead to cell death and cognitive decline, emphasizing that hyperphosphorylated tau may be the driving factor for neurotoxicity in Alzheimer's Disease (Xia et al., 2021a).

Disrupting the cytoskeleton is a hallmark of neurodegenerative diseases (Aiken & Holzbaur, 2021; Gendron, 2009). Tau dysfunction through hyperphosphorylation could be a significant factor contributing to this hallmark (Fig. 1). Disruption to axonal transport could be an early indicator of several neurodegenerative diseases (Hoover et al., 2010; Rodríguez-Martín et al., 2013). But how they affect axonal transport remains a question. Thus, knowing that tau can modulate cargo transport through different states of tau (static and diffusive), posttranslational modifications (phosphorylation), and motor proteins (at different combinations of kinesins and dyneins), we aim to understand how hyperphosphorylated tau affect the microtubule

organization and the cargo transport, and this will help us explain the mechanisms underlying tau's dysregulation of axonal transport in disease like Alzheimer's disease.

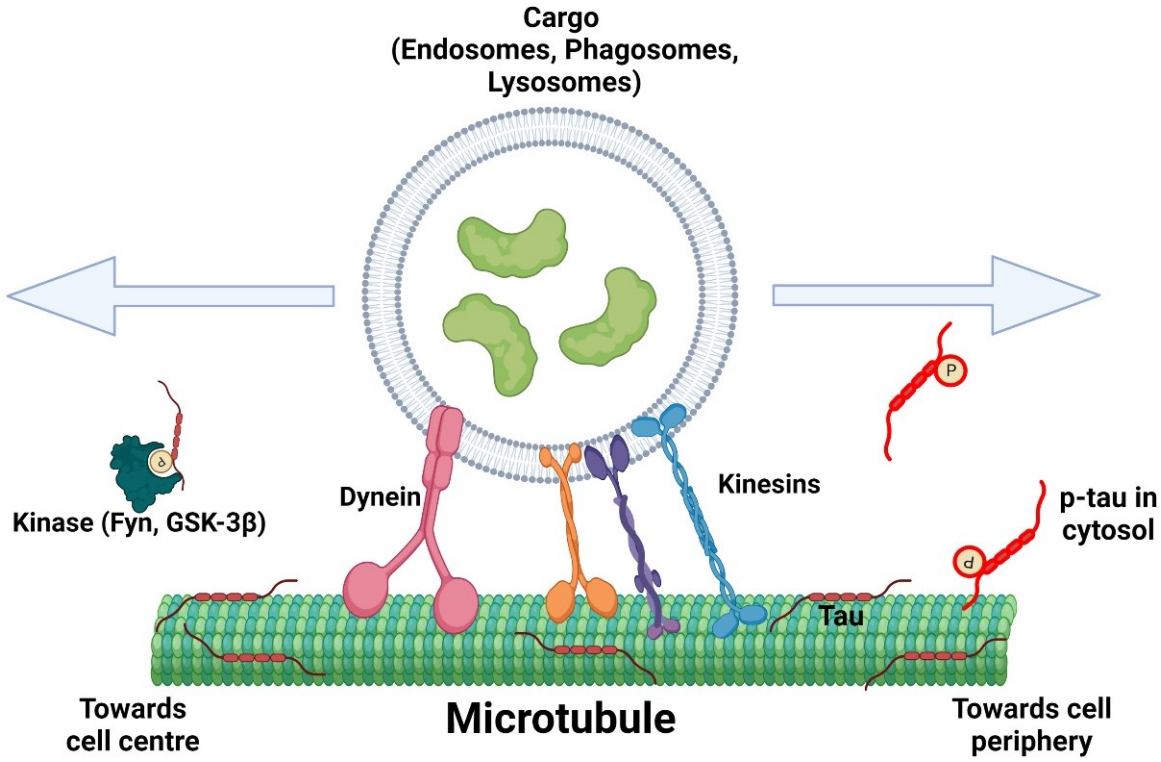

Figure 1: Study of intracellular transport with a focus on tau. Cargoes such as endosomes, lysosomes and phagosomes are transported by kinesins and dyneins, which run in opposite directions to each other, resulting in a tug-of-war. Tau binds to the microtubules statically and helps regulate the cargo transport by inhibiting kinesins (kinesin-1 and kinesin-3) more than dyneins. Since each cargo has different sets and combinations of kinesins and dyneins, some cargoes are more sensitive to tau than others. Kinases such as Fyn and GSK-3β help phosphorylate tau, which alters the tau structure and their ability to bind to the microtubules. The addition of the phosphate group makes the tau more diffusive into the cytosol, thereby, these phosphotau have different effects on cargo transport compared to the static tau. With tauopathic diseases like Alzheimer's, we hypothesize that hyperphosphorylated tau leads to defective cargo transport along the microtubules along the axon. [Image created using Biorender]

I investigated the regulation of microtubule organization and intracellular transport through tau hyperphosphorylation using phosphomimetic tau constructs that mimic the Alzheimer's disease tau. The subsequent section delves into our research objectives on understanding the role of hyperphosphorylated tau in organizing the microtubules and affecting the organelle transport of lysosomes and early endosomes. Chapter 2 is dedicated to a comprehensive literature review of the cellular transportation system, the involvement of tau in cytoskeletal functions, and its influence on motor protein-driven transport. This literature review underscores the significance

of our research in uncovering the role of hyperphosphorylated tau in cargo transport. In Chapter 3, we detail the methodology employed in our study. We also interpret our findings in previous studies on hyperphosphorylated tau, further explored in Chapters 5 and 6. Our research contributes to understanding tau hyperphosphorylation and its disruptive impact on axonal transport, thus shedding light on the underlying pathophysiology of Alzheimer's disease. In the concluding chapter, Chapter 6, I discuss potential future research avenues to solidify our comprehension of how hyperphosphorylated tau influences cargo transport. Furthermore, I elaborate on my contributions to collaborative projects in Chapter 7, where I examined the effect of normal tau phosphorylation on motor proteins and transport. Additionally, I outlined the development of a MATLAB script designed to quantify the directionality switch resulting from motor protein inhibition using the optogenetic system.

In summary, my thesis offers valuable insights into the role of hyperphosphorylated tau in cargo transport. It provides a way for further investigations in tau-related pathologies and cellular transport dynamics.

1.2. Objectives

Axonal transport plays a critical role in maintaining neuronal health and function. Defects in axon transport have been associated with various neurodegenerative diseases, including Alzheimer's, Parkinson's, and Huntington’s disease. Impaired transport can arise from many factors, such as the accumulation of toxic protein aggregates, mitochondrial dysfunction, autophagy dysregulation, endoplasmic reticulum stress and impairment in adaptor recruitment and motor protein binding (Guha et al., 2020; Guo et al., 2020; Iqbal et al., 2016). Mutations in motors, microtubule-associated proteins (MAPs), and adaptors can also contribute to neurodegenerative diseases (Hirokawa et al., 2010; Nagano & Araki, 2021). For example,

Amyotrophic lateral sclerosis (ALS) and Alzheimer's disease are linked to defects in KIF5A (kinesin-1 family), which disrupts anterograde axonal mitochondrial transport (Pant et al., 2022; Wang et al., 2019). Perry syndrome, a rare neurodegenerative disease, is associated with Dynactin 1 (DCTN1) mutations which affects the dynein activity (Farrer et al., 2009). And Huntington's disease involves mutant Huntingtin (mHTT) promoting vesicle detachment from microtubules, thereby reducing transport efficiency (Vitet et al., 2020). There are over 50 pathogenic mutations in MAP tau alone, which could induce microtubule instability and increased propensity to form aggregates that could disrupt the cargo transport in neurons (Strang et al., 2019). These factors and examples show that defects in intracellular components could disrupt the delivery of essential cellular materials to distant parts of neurons and ultimately lead to neuronal dysfunction and degeneration.

Despite all the progress made in tau mutations and their role in neurodegenerative diseases, there is a significant gap in our understanding of how tau regulates axonal transport in healthy neurons and how this regulation becomes disrupted in various tauopathies. To address this gap comprehensively, this thesis focuses on two main objectives:

1) **Investigating the impact of tau hyperphosphorylation on microtubule organization:**

This objective centers on understanding how hyperphosphorylated tau alters microtubule organization. Specifically, we will closely examine the microtubule binding properties of hyperphosphorylated tau, comparing them to those of other tau variants such as wild-type tau (WT tau) and the phosphoresistive tau model.

2) **Analyzing the effect of tau hyperphosphorylation on lysosomal and early endosomal cargo transport:**

The second objective aims to determine how the presence of hyperphosphorylated tau affects the transport of lysosomes and early endosomes within cells. Our analysis will focus on key biophysical parameters, including mean squared displacement (MSD), radius of gyration (Rg), diffusive coefficient (α), and velocity. These parameters provide insights into how hyperphosphorylated tau impacts cargo transport dynamics. Directionality and localization analyses will also be performed to detect any bias in cargo transport in the presence of the hyperphosphorylated tau.

These objectives aim to model a pathogenic phosphorylation state of tau which can help us dissect how the microtubule organization and the trafficking of different intracellular cargoes are affected by the misregulated hyperphosphorylated tau.

To achieve these objectives, live-cell imaging using Total Internal Reflection Fluorescent (TIRF) microscopy will be conducted on COS-7 cell lines expressing tau constructs. TIRF is a valuable tool used to study molecular events happening at a thin plane near the cell membrane. It relies on the phenomenon of total internal reflection, where excitation light generates an evanescent wave at the solid-liquid interface. This evanescent wave excites only a thin slice (~100 nm) of the sample, minimizing background from out-of-focus light to observe and analyze the dynamic and spatial organization of fluorophores. Thus, TIRF microscopy provides valuable insights into cellular processes occurring at the thin section of the cell (Fish, 2022). In our research, TIRF will be employed to track cargo movement and quantify the influence of tau on cargo behaviour (Fig. 2). COS-7 cells are ideal for this research as they can be cultured quickly, and their flat morphology is suitable for imaging lysosomes and early endosomes at higher signals under TIRF. As COS-7 cells lack endogenous tau expression, we can exclusively examine the effects of tau by transfecting them with tau constructs. Our strategy involves

transfecting cells with tau constructs (WT tau, phosphomimetic E14 tau, and phosphoresistive AP14 tau), all tagged with enhanced Green Fluorescent Protein (eGFP) markers.

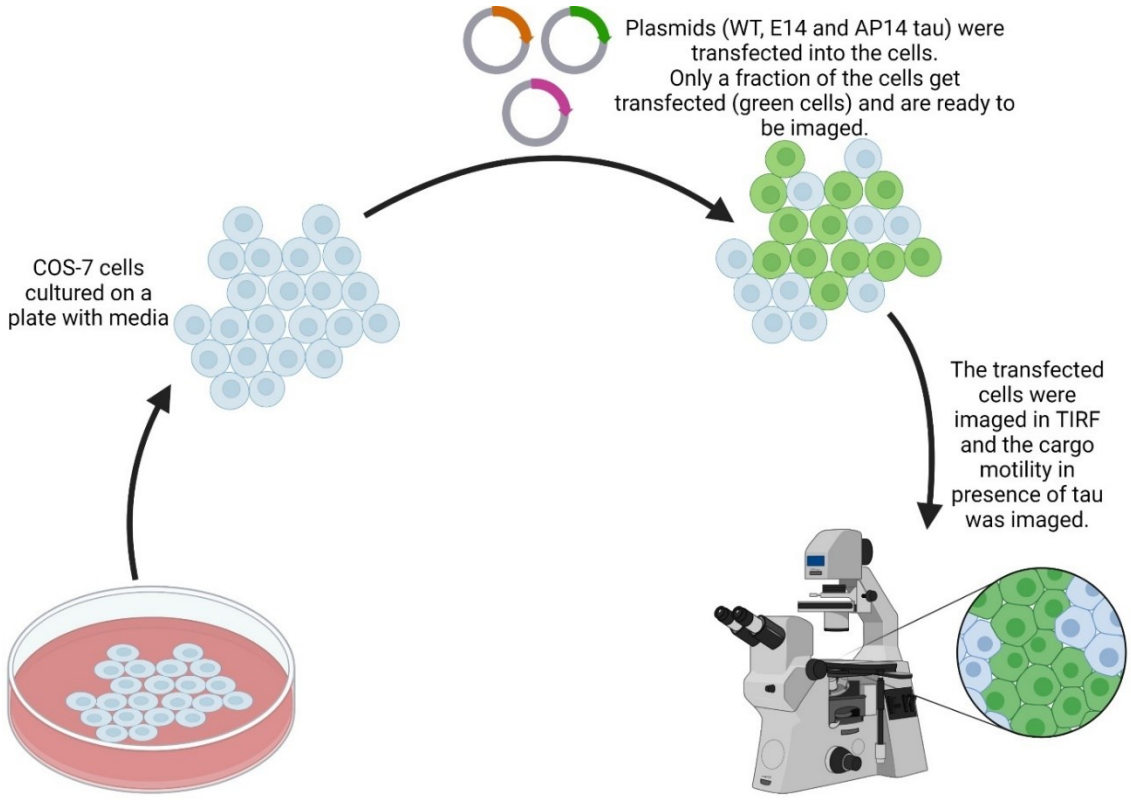

Figure 2: Live cell imaging on tau transfected cells. A schematic methodology workflow of culturing COS-7 cells, transfecting them with eGFP-tau plasmids and then imaging them under total internal reflection fluorescence (TIRF) microscopy after expressing the tau protein and adding lysotracker (for labelling lysosomes) or quantum dot-EGF (for labelling early endosomes). [Image created using Biorender]

Phosphomimetic tau refers to the substitution of serine or threonine residues with glutamic acid (E) or aspartic acid (D). These substitutions mimic the negative charge of a phosphorylated serine or threonine that is usually phosphorylated by kinases (Anthis et al., 2009). This alteration could mimic the behaviour of phosphorylated tau found in normal and abnormal conditions. Conversely, phosphoresistive tau in my thesis refers to the substitution of phosphorylatable serine or threonine residues with alanine (A). Alanine lacks the phosphate group found in serine or threonine, making it less prone to phosphorylation by kinases at the key sites (Alzheimer's disease-relevant sites) (Anthis et al., 2009). These substitutions allow

the study of the functional consequences of tau phosphorylation and its role in neurodegenerative diseases like Alzheimer's. Quantification of tau expression will be based on their fluorescence intensity. E14 tau has 14 Alzheimer's disease-relevant phosphorylated sites (check the methodology), which are used to mimic the hyperphosphorylation of tau by GSK-3β as found in Alzheimer's disease (Hoover et al., 2010).

1.3. Literature review

This literature review delves into the complex cellular transport system, exploring how cells efficiently move biomolecules and organelles within their structures. This review will also explore the functions of both normal and phosphorylated tau in microtubule organization, their interactions with motor proteins, and the consequent impact on intracellular transport. The interaction of tau with microtubules is governed by its distinct regions, which enables tau to interact with tau and other MAPs, affecting the microtubule lattice properties such as spacing, compaction and expansion of tubulins in the lattice and bundling of microtubules. Importantly, tau influences motor protein activities, which enables them to regulate transport. Phosphorylation could affect all the mentioned properties of microtubules and motor proteins. However, the specific consequences of hyperphosphorylated tau, especially in cargo transport regulation, remain less explored, forming our research's central focus. By leveraging the insights gained from our examination of normal tau, we aim to decipher the altered behaviour and functionalities of hyperphosphorylated tau. This will provide valuable insights into the mechanisms underlying transport defects during Alzheimer's disease. Through this review, we bridge the gap between the known functions of tau and the potential disruptions caused by hyperphosphorylation, ultimately enhancing our understanding of cellular transport systems in disease conditions.

1.3.1. Intricate intracellular transportation system

The dynamic cytoskeletal elements in the cells include actin, intermediate filaments, and microtubules, and they play a pivotal role in maintaining cell structure, cell division, motility, and intracellular transport. The intricate intracellular transportation system is essential for transporting biomolecules, organelles, and cellular components within the cell to the correct

target destination, ensuring proper cellular function, and maintaining homeostasis (Aiken & Holzbaur, 2021; Balabanian et al., 2018). For example, the endocytic pathway is a process by which cells internalize substances from the extracellular environment into membrane-bound vesicles for transport to various cellular destinations, such as lysosomes or recycling back to the plasma membrane (Hyttinen et al., 2013). Like actin, microtubules are stiffer and most dynamically assembled and disassembled structures (Fletcher & Mullins, 2010). This unique characteristic allows individual microtubules to serve as nearly linear tracks spanning the entire length of a typical animal cell, providing a physical framework for the efficient and precise transport of vesicles and organelles to their target locations within the cell. Thus, understanding microtubules is critical to understanding the intracellular transportation system, which will aid us in comprehending our results in transport defects during disease conditions.

1.3.2. Microtubules: Its components, regulations, and functions

Microtubules are long, hollow and polar structures composed of 13 protofilaments. Each protofilament comprises two tubulin heterodimer subunits, α- and β- tubulin. The significance of microtubules extends beyond acting as tracks, as they play critical roles in cell division, migration, structural integrity, and intracellular transport (Aiken & Holzbaur, 2021; Balabanian et al., 2018; Brouhard & Rice, 2018; Muroyama & Lechler, 2017; Yogev et al., 2016). Microtubules exhibit dynamic behaviour as they elongate by incorporating GTP-tubulin into their structure, which is capped by a stabilizing cap. Below this cap, GTP-tubulin undergoes hydrolysis, converting it into GDP-tubulin due to the GTPase activity of tubulin. This hydrolysis process, coupled with interactions of microtubule ends with proteins like polymerases, depolymerases, and regulatory kinesins, affects the growth or shrinkage of microtubules. If the cap is lost, it leads to rapid shrinkage, a phenomenon termed catastrophe. Occasionally, microtubule shrinkage is halted, and the structure returns to a growing state, a

phenomenon termed rescue. This dynamic interplay of growth and shrinkage is called dynamic instability (Horio & Murata, 2014; Mitchison & Kirschner, 1984). It is employed by cells for tasks like exerting forces during mitotic chromosome segregation or to help navigate cells extracellularly (Brouhard & Rice, 2018). However, the alternate growth and shrinkage of microtubules can impact their lattice properties, affecting the protein interactions on the microtubule surface. For example, Cryo-EM studies found that when GTP-tubulin undergoes hydrolysis to form GDP-tubulin, the lattice can undergo compaction along the longitudinal interface (Alushin et al., 2014). Thus, the expanded GTP-lattice (~8.4 nm/tubulin) contracts to compacted GDP-lattice (~8.2 nm/tubulin) (Verhey & Ohi, 2023). This structural change can influence the binding of proteins, such as MAPs, which can further influence the lattice properties (Castle et al., 2020; Kellogg et al., 2018; Siahaan et al., 2022).

The microtubules are polarized due to their heterodimer tubulin subunits. Hence, they have two distinct ends. The plus end of the microtubule generally polymerizes toward the cell periphery, and the minus end of the microtubule is positioned in the microtubule-organizing center (MTOC). Microtubules serve as a highway for the intracellular transport of cargo with the help of motor proteins such as kinesins and dyneins, which are ATP hydrolases as they convert the chemical energy of ATP to motion. Kinesins -1, -2, and -3 are anterograde motors as they carry cargo towards the plus-end of the microtubule (Hirokawa & Tanaka, 2015), while cytoplasmic dynein is considered a retrograde motor as it carries towards the minus-end of the microtubule (Maday et al., 2012). Cargoes can have different ratios of kinesins and dyneins, which help them move the cargo unidirectional or bidirectional along the microtubules. The motors are regulated by numerous proteins and factors (Aiken & Holzbaur, 2021; Tarhan et al., 2013). Defects in microtubule-based transport and their regulation can lead to a variety of diseases and disorders, including cancer, developmental disorders, and

neurodegenerative diseases (Ballatore et al., 2007; Gendron, 2009; Noble et al., 2013; Xia et al., 2021a).

In neurons, the microtubules are long-lived and can support the axonal structures for performing intracellular trafficking, such as transporting mitochondria, vesicles for neurotransmitters, ion channels, scaffolding proteins, and other proteins from the cell body to the axon terminals or dendrites and vice versa (Aiken & Holzbaur, 2021; Balabanian et al., 2018.; Chaudhary et al., 2018a)**.** This transport to and from synaptic sites is crucial for neuronal communication, so defects in this transport could cause malfunctioning of synaptic communication, leading to synaptic degeneration. The mechanism of cargo transport and regulation is still an ongoing research interest due to the complex nature of the cytoskeleton (Kametani & Hasegawa, 2018). Moreover, several mechanisms can affect motor protein motility, such as post-translational modifications (PTMs), organization of microtubules and multiple proteins that regulate microtubules and motors, and all these mechanisms are interconnected in their functions (Aiken & Holzbaur, 2021; Balabanian et al., 2018) (Fig. 3)**.** This review provides information on the role of a microtubule-associated protein called tau and its impact on microtubule organization and intracellular transport in normal conditions. This review will provide us with more context, which will help us understand how hyperphosphorylated tau affects the intracellular processes based on our experimental results, providing valuable insights into the mechanisms underlying Alzheimer's disease.

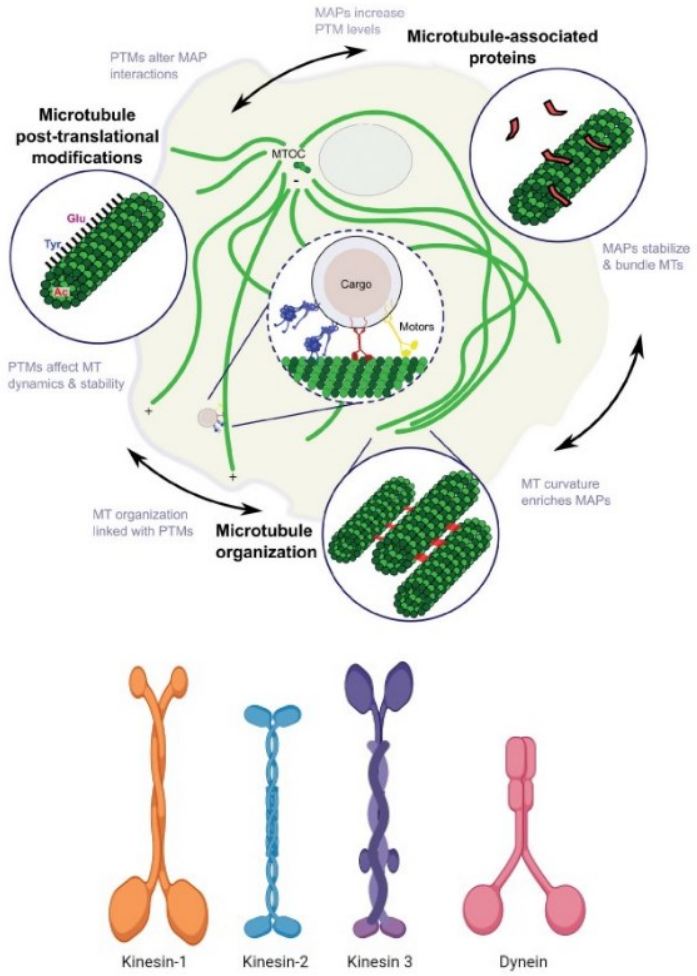

Figure 3: Regulation of microtubule and microtubule-based transport. A. There are multiple ways in which motor protein activity is regulated. They include 1) post-translational modification (PTMs) – such as Acetylation, tyrosination, and they are involved in the dynamics and stability of microtubules which affects the motor protein activity; 2) microtubule-associated proteins (MAPs) – such as tau, MAP7, MAP2, DCX, which also involved in stabilizing and bundling microtubules and they can have a direct effect on motors by either blocking their path or promoting binding to the microtubules; 3) Organization of microtubule networks – Curvature, microtubule orientation (uniform in axons and mixed in dendrites) [Image sourced from Balabanian et al., 2018]. B. There are 2 major types of motor proteins – kinesins (kinesin-1, kinesin-2, kinesin-3, and numerous others) and dyneins. They act in opposite directions and are often associated with the cargoes at different combinations. [Image created using Biorender]

1.3.3. Microtubule-associated protein tau

Tubulin Associated Unit (Tau) is an intrinsically disordered neuronal MAP predominantly found in the neurons of the central nervous system with a concentration greater in axons than in somatodendritic sites. It is also found in other cell types like glial and neuroendocrine cells and other parts of the body, such as the kidney and skeletal muscles (Chapelet et al., 2023; Duquette et al., 2021; Kent et al., 2020; Wang & Mandelkow, 2016; Xia et al., 2021a). Tau is a hydrophilic, unfolded protein encoded by the MAPT gene in chromosome 17. There are six isoforms of Tau in the brain based on the mRNA splicing of exons 2, 3, and 10. These isoforms differ by the absence or presence of 1 or 2 acidic inserts at the N-terminal and whether they contain 3 or 4 repeats of the tubulin-binding motif at the C-terminal region. So 4R-tau is based

on the inclusion of exon 10, and 3R-tau is based on the exclusion of exon 10. The repeat region within the microtubule-binding domain binds to microtubules and promotes their assembly (Ballatore et al., 2007; Mueller et al., 2021; Xia et al., 2021a). Each isoform has a different affinity towards the microtubules, and it was found that 3R-tau can bind with greater affinity than 4R-tau (Gendron, 2009; McVicker et al., 2014a). The ratio of 3R:4R tau is about 1:1, with an expression level of 3R-tau being higher in fetal development, followed by the expression of 4R-tau later in post-natal. The activity of tau can be modulated by adding functional groups to tau, which modifies their structure, which in turn modifies their function.

Tau can undergo various post-translational modifications, including phosphorylation, acetylation, ubiquitination, and glycosylation, which can regulate its function and stability. One of the most extensively studied modifications of tau is phosphorylation which is catalyzed by enzymes called kinases such as fyn, glycogen synthase kinase 3 beta (GSK3β), cyclin-dependent kinase 5 (CDK5), and mitogen-activated protein kinase (MAPK) (Aiken & Holzbaur, 2021; Gendron, 2009). In neurons, tau is phosphorylated at specific sites, which regulates its binding to microtubules and its ability to promote microtubule assembly and stability. However, in neurodegenerative diseases such as Alzheimer's, tau becomes abnormally hyperphosphorylated, meaning it is phosphorylated at many more sites than in normal conditions. This could affect the tau function negatively and promotes the formation of neurofibrillary tangles, which is the hallmark of neurodegenerative diseases such as Alzheimer's disease (Ballatore et al., 2007; Gendron, 2009; Martin et al., 2013).

We will first focus on how normal tau influences microtubule stability and the intracellular transport of organelles. This will provide us support in understanding how the hyperphosphorylated tau might affect microtubules and organelle transport.

1.3.4. Role of tau in organizing and stabilizing the microtubules

Tau both statically binds to microtubules and diffuses along the microtubule surface in a dynamic equilibrium. This happens in an isoform-specific manner, with 4R-tau being more diffusive than 3R-tau (Hinrichs et al., 2012; McVicker et al., 2014b). The mechanism of how tau interacts with microtubules suggests that the acidic (negative) N-terminal projection region of tau is repulsed from the negatively charged surface of the microtubules, and the positively charged proline-rich region and the sites in the C-terminal region of tau promote strong binding to the microtubules longitudinally (Chong et al., 2018; D'Souza & Schellenberg, 2005; Gendron, 2009; Goedert et al., 1989; Kellogg et al., 2018; McVicker et al., 2014a). It was shown that the polyglutamylation of tubulin enhances the affinity of tau for microtubules (Genova et al., 2023). Tau has higher preferences in binding to a specific organization of the microtubules and influences microtubule properties to provide structural rigidity to the cells.

Tau prefers binding to the microtubule curvatures at a higher concentration due to the affinity of tau towards the compacted microtubule lattice upon GTP to GDP tubulin hydrolysis (Balabanian et al., 2017; Bechstedt et al., 2014; Samsonov et al., 2004). Tau can also help remodel the microtubules into bundles (Balabanian et al., 2017; Breuzard et al., 2013), and this bundle formation is regulated through the N-terminal projection region of tau (Chen et al., 1992; Kanai et al., 1992). It was suggested that N-terminal projection and proline-rich region of tau influence the microtubule bundle spacing (Rosenberg et al., 2008). Microtubules are dynamic, so tau prefers to bind to some areas of the microtubule to influence the microtubule dynamics.

Tau plays a critical role in maintaining and stabilizing the structural integrity of microtubules in neurons (Aiken & Holzbaur, 2021; Rodríguez-Martín et al., 2013). In axonal microtubules,

tau is more abundant in the dynamic plus tip (Qiang et al., 2018). Depletion of tau reduced the length of the dynamic plus tip, so tau is crucial in maintaining and stabilizing this region for further elongation of the dynamic microtubules. (Qiang et al., 2018). Therefore, tau can be considered a nucleating and stabilizing MAP (Cario & Berger, 2023). Furthermore, it was shown that tau avoids the GTP cap at the dynamic plus tip as tau recognizes and binds preferentially to the unstable GDP-tubulin lattice (Castle et al., 2020). It was proposed that cap avoidance by tau could enable it to selectively influence microtubule dynamics during shortening, potentially regulating polymer loss without impeding growth, thus facilitating the dynamic exploration of the cell in the extracellular space (Castle et al., 2020) Tau also forms envelopes along the microtubule surface, influencing microtubule stability and dynamics.

Siahaan et al. (2022) uses in vitro assays to show that tau forms cohesive envelopes on the microtubule surface distinct from individual diffusing tau. These envelopes shield microtubules from severing enzymes such as katanin, alter microtubule lattice spacing, and selectively regulate access of other MAPs to the microtubule lattice. Tau was suggested to influence the structural dynamics of microtubules by recognizing and modifying their compaction state, which refers to the localized compression and tightening of the tubulins in the microtubule. The prevailing microtubule lattice in mammalian cells is thought to be homogeneously compacted due to the GDP lattice. However, the research suggests that the lattice is non-uniform and constantly undergoing the addition and release of GTP-tubulin units to the lattice, possibly tied to responses such as mechanical stress and repair. Thus, tau can recognize and alter the confirmation of the lattice by forming envelopes on the lattice. Despite increased tau affinity towards microtubule curvatures, these tau envelopes are not found in curvatures. Instead, tau envelopes straighten the curved regions of the microtubules. These findings suggest that an interplay between lattice spacing and cooperative envelope formation

is the molecular basis for spatial regulation of microtubule-related processes. (Siahaan et al., 2019, 2022). Previous research on R5L mutation points out that modifications in the N-terminal region can impact the ability of tau to form patches which increases the shrinkage rate of microtubules (Cario et al., 2022).

On top of regulating microtubule assembly, tau is also suggested to be involved in various functions, such as affecting actin polymerization, regulation of transcription, neurogenesis and synaptogenesis, signal transduction and intracellular transport (Barbier et al., 2019; Gendron, 2009; Mueller et al., 2021; Stern et al., 2017; Wang & Mandelkow, 2016). Tau is suggested to compete with motor proteins and other MAPs for binding to the microtubule, enabling tau to regulate the motor protein activity (Beaudet et al., 2023; Stern et al., 2017).

1.3.5. Effect of tau on the motor proteins and motility of organelles

Tau regulates axonal transport, which involves various motor proteins, including kinesin-1, kinesin-2, kinesin-3, and dynein (Aiken & Holzbaur, 2021; Balabanian et al., 2022; Beaudet et al., 2023; Chaudhary et al., 2018; Dixit et al., 2008; Hanger & Noble, 2011; McVicker et al., 2014a; Stern et al., 2017). Tau differentially affects motor proteins, which impacts organelle transport (Dixit et al., 2008; McVicker et al., 2011). For example, in vitro studies on taxol-stabilized microtubules have shown that static 3RS-tau reduces the processivity more strongly for kinesin-1 than the 4R-tau isoform. However, in GMPCPP-stabilized microtubules, the inhibitory effects of the 3RS-tau were reduced because tau was more diffusive than the taxol-stabilized microtubules (McVicker et al., 2011, 2014a). However, the static 3RS-tau has less effect on kinesin-2, KIF1A (kinesin-3), and KIF18A (kinesin-8) because their extended neck-linker region helps them navigate tau on the microtubule surface (Hoeprich et al., 2014, 2017; Lessard et al., 2019). Interestingly, 3RS-tau, in its diffusive form, disrupts the pauses that

KIF1A (kinesin-3) takes for its successful processive runs as the diffusive tau competes with KIF1A for binding with the polyglutamylated C-terminal tail of the tubulin, and thereby leading to its inhibition. This inhibition is unique to kinesin-3 (Lessard et al., 2019). Although heavily present in axonal microtubules, tau does not entirely inhibit kinesin-based transport. However, it biases the direction towards the retrograde direction by selectively inhibiting kinesin-1 and kinesin-3 (Balabanian et al., 2022).

Tau inhibits kinesins at physiological levels and affects the on-rate of kinesin-1 and dynein-dynactin microtubule binding (Dixit et al., 2008). While dyneins are affected at higher concentrations of 3RS-tau (≥ 0.2 tau/tubulin dimer), which reduces their attachment rate to microtubules and processivity (Vershinin et al., 2008). However, when dynein interacts with dynactin to form the co-complex, they can pass through tau or step back to reorient and then move when they face 3RS-tau on microtubules (Balabanian et al., 2022; Chaudhary et al., 2018; Dixit et al., 2008; Tan et al., 2019). These findings suggest that tau can act as a barrier for specific motors or allow other motors to pass through, depending on its state, the ability to influence the microtubule lattice and the motor protein nature. (Beaudet et al., 2023; Chaudhary et al., 2018; McVicker et al., 2014a; Monroy et al., 2018). Tau envelopes influence the conformational behaviour of the lattice, which can help to differentially regulate kinesin activity by spatially gating its access to the microtubule surface while having less impact on dyneins (Siahaan et al., 2022). However, a single motor does not define the motility of the cargo in a cell. Instead, it is determined by a combination of different types and sets of motors that provide the cargo with the ability to navigate in the complex intracellular environment (Beaudet et al., 2023; Chaudhary et al., 2018; Vershinin et al., 2007). Therefore, the impact of tau can vary depending on the teams of motors carrying the cargo.

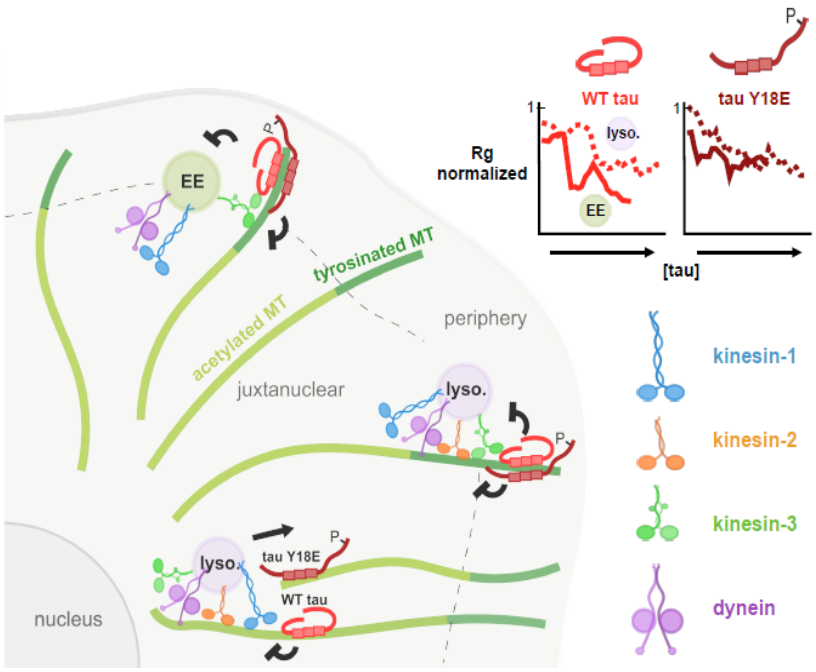

Figure 4: Differential regulaton of cargo transport by 3RS WT and Y18E tau. This image illustrates the impact of tau Y18 phosphorylation on vesicle transport regulation. While kinesin-1 and kinesin-2 driven lysosome transport were less sensitive to phosphomimetic Y18E tau, both WT and phosphomimetic Y18E tau inhibit kinesin-1 and kinesin-3 driven transport of early endosomes and peripheral lysosomes. Image taken from Balabanian et al., 2022.

Through in vitro and optical trapping experiments, early phagosomes carried by fewer kinesins were more susceptible to tau inhibition remarkably. (Beaudet et al., 2023; Chaudhary et al., 2018). Nevertheless, early phagosomes also have fewer dyneins, which were expected to drive the cargo retrograde, but there was a reduction in retrograde transport. This shows that, like kinesins, the number of engaged dyneins also influences the transport of organelles. Similarly, since late phagosomes possess many kinesins and dyneins, they are bidirectional in nature and, upon introducing tau, they become biased toward the retrograde direction. This is because tau inhibits kinesin-1, leading to dynein taking over cargo motility and biasing the directionality towards the retrograde direction (Beaudet et al., 2023; Chaudhary et al., 2018). It was also shown that 3RS tau can reduce the motility of teams of motors driving the cargo significantly compared to 4RL-tau (Vershinin et al., 2007). Additionally, the location of the cargo within the cell can also influence tau's inhibitory effect due to the differences in the post-translational modification of microtubules in the different cell regions. For example, WT Tau and Y18E monophosphorylated Tau inhibit lysosome driven by kinesin-3 in peripheral tyrosinated microtubules (Aiken & Holzbaur, 2021; Katrukha et al., 2021). Furthermore, WT tau inhibits

lysosomes driven by kinesin-1 in the perinuclear and juxtanuclear space of the cell (Aiken & Holzbaur, 2021; Balabanian et al., 2018, 2022; Katrukha et al., 2021).

With our understanding of the role of tau in modulating microtubule properties and regulating motor protein transport, we now focus on tau phosphorylation and the need to understand the role of tau hyperphosphorylation, especially in cargo transport, which is the objective of our project.

1.3.6. Tau phosphorylation and its effects on microtubules and cargo transport

Tau can be phosphorylated with over 85 putative phosphorylation sites, marked on either serine, threonine, or tyrosine residues in the longest tau isoform (2N4R) (Gendron, 2009; Xia et al., 2021a) (Fig. 5). Phosphorylation of tau means that tau has additional negative charges, which can reduce the affinity towards the microtubules and decrease the repulsion with positively charged motor domains of kinesins. Thus, tau can be modulated between the static and diffusive state depending on the phosphorylation status of tau, as the addition of negative charges in the form of phosphorylation can affect the microtubule-binding ability of tau and can help in differentially regulate the motility of cargoes (Balabanian et al., 2022; Beaudet et al., 2023; Hinrichs et al., 2012)**.** Phosphorylation at S214, S262/356 or T231 can reduce the microtubule-binding affinity, whereas phosphorylation in S202, T205 or S208 increases the ability of tau to form aggregates (Review from Cario & Berger, 2023). Recently, it was found that phosphorylated tau can participate in tau envelope formation on the microtubule surface, but slows their formation and ultimately destabilizes the envelopes. It can also destabilize pre-existing envelopes on the microtubules, conferring less protection from severing enzymes such as katanin (Siahaan et al., 2019, 2022). This also suggests that tau envelopes will have less impact on the lattice compaction, thereby, may have less impact on the kinesin-driven cargo

transport (Karhanová & Lánský, 2023). Hence, tau phosphorylation can impact its ability to bind to microtubules and modulate the microtubule properties.

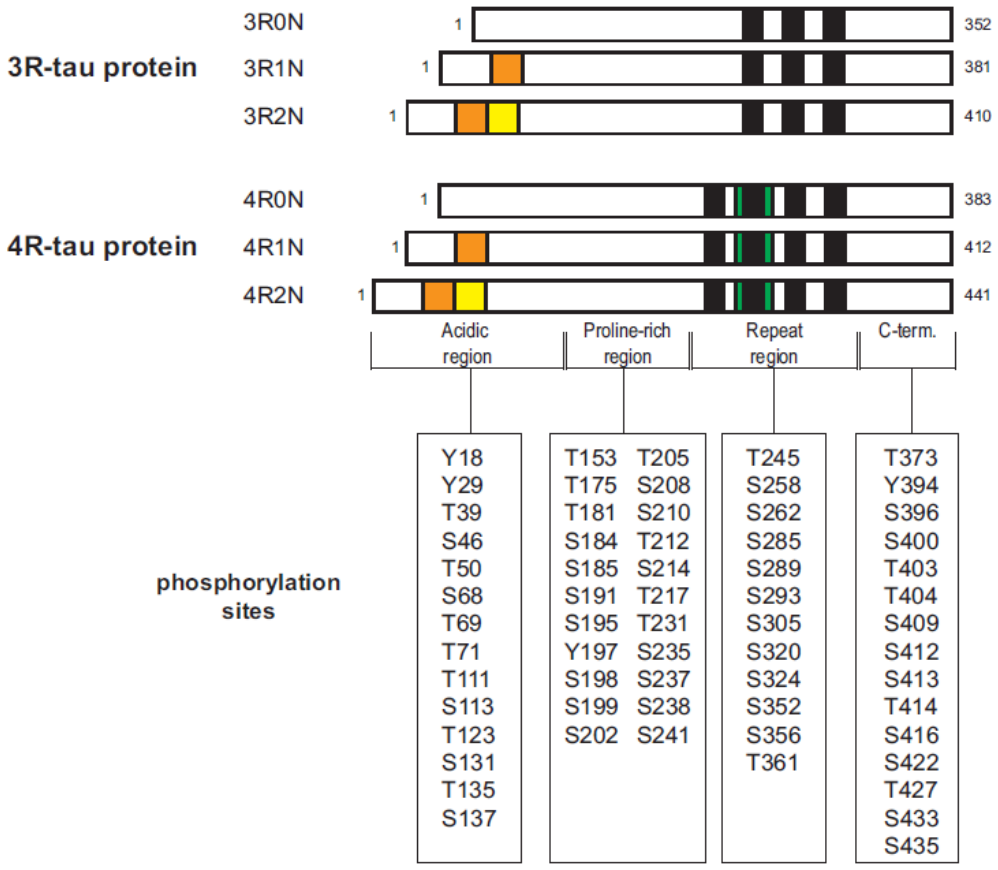

Figure 5: Different isoforms of Tau and their phosphorylation sites. Tau is phosphorylated in multiple sites by many kinases such as fyn, glycogen synthase kinase three beta (GSK3β), cyclin-dependent kinase 5 (CDK5), and mitogen-activated protein kinase (MAPK). Some sites are phosphorylated in the AD brain, some in the normal brain and some in both the AD and the normal brain. Image taken from Gendron, 2009.

Few studies also focused on how tau phosphorylation can affect cargo transport. Previous studies on fyn and phosphomimetic Y18E tau in our lab have shown that tau is involved in differentially regulating the transport of early endosomes and lysosomes based on their properties and positioning (Balabanian et al., 2022). It was found that kinesin-3 was strongly inhibited by monophosphomimetic Y18E tau, so peripheral lysosomes and early endosomes were inhibited as kinesin-3 dominated sets of motor proteins drove them. This inhibition could be attributed to the enhanced diffusivity of the phosphomimetic tau, enabling it to interact with a larger number of tubulin C-terminal tails across a broader microtubule surface. Consequently,

this interaction limits the ability of kinesin-3 to pause, reducing its overall run lengths over extended distances.(Balabanian et al., 2022; Stern et al., 2017)**.** Another study focused on the overexpression of AT8 phosphomimetic 3D tau (Ser199, Ser202, and Thr205 AD relevant sites mutated to aspartic acid to mimic the phosphorylation) in PC12 cells and mouse cortical neurons and found that kinesin-antegrade transport of mitochondria was inhibited. It was found that 3D tau expanded the microtubule spacing by extending the projection domain away from the microtubules more than WT or 3A phosphoresistive tau. This change in inter-microtubule distance was considered the reason for mitochondria motility inhibition (Shahpasand et al., 2012).

1.3.7. Tauopathic diseases

Primary tauopathic diseases such as PSP, corticobasal degeneration (CBD) and some Frontotemporal Dementia (FTD) are considered 4R-tauopathic diseases because of the accumulation of 4R-tau precisely. In contrast, diseases such as Alzheimer's are considered mixed tauopathic diseases as they initially begin as 4R-tau predominant and later transition into 3R predominant disease (Bowles et al., 2023). It is suggested that the early dysfunctional 4R-tau has implications for understanding the risk and pathogenesis of neurodegenerative diseases. In these neurodegenerative diseases, tau becomes abnormally modified due to hyperphosphorylation at multiple sites, forming insoluble aggregates (Duquette et al., 2021) But how tau aggregation leads to neuronal dysfunction and death is unclear. So, understanding tau hyperphosphorylation can help us understand the tauopathic disease progression, such as Alzheimer's, as it is considered a key pathological event.

1.3.8. Tau hyperphosphorylation and its role in neurodegeneration

Tau hyperphosphorylation is believed to be caused by an imbalance between increased kinase activity and decreased phosphatase activity (Hanger & Noble, 2011; Noble et al., 2013). In tau pathology, phosphorylation can occur in a temporally specific sequence (Armstrong et al., 2013), and the earliest phosphorylation changes in Tau occur at sites S199 and T231 (Bertrand et al., 2010; Maurage et al., 2003). It was shown that increased tau phosphorylation could lead to the detachment of tau from microtubules regardless of the phosphorylated sites, which can disrupt microtubule stability and neuronal cytoskeleton (Noble et al., 2013). Further destabilization of microtubules can occur when the accumulated phosphorylated tau sequesters normal tau and other MAPs bound to microtubules (Noble et al., 2013).

Elevated levels of tau phosphorylation have shown an increase in the rate of tau transport in axons in neurons, but inhibiting GSK-3β kinase activity reduces tau motility and tau aggregation in neurons (Rodríguez-Martín et al., 2013). It was also shown that the tau aggregates were not degraded in disease conditions, leading to increased tau accumulation and could further interfere with cargo transport (Gendron, 2009; Rodríguez-Martín et al., 2013). Hyperphosphorylated tau can also interact with the nuclear pore protein complexes such as nucleoporins (Nups) and disrupt their normal functioning of nuclear-cytoplasmic transport (Tripathi et al., 2019). So, it can be noted that tau-mediated neurodegeneration could result from a combination of toxic gain of functions and loss of normal function of tau and proteasome and autophagy-based tau degradation that reduces tau clearance mechanism in the brain (Rodríguez-Martín et al., 2013). However, only a few studies were done on how tau hyperphosphorylation might affect cargo transport, which may lead to defective transport observed in neurodegenerative diseases.

The hyperphosphorylation of tau was also observed during fetal and postnatal-brain development in humans and rodents at sites like those found in AD. However, this does not correlate with neurodegeneration. This is still unclear as only a few studies confirm this, and the methods of obtaining the phosphorylation sites of tau in the fetal brain are disputed (Duquette et al., 2021; Jovanov-Milošević et al., 2012; Yu et al., 2009). However, this shows that hyperphosphorylation may not be toxic as expected. Instead, its toxicity is because of the specific phospho-residues and the cellular context for phosphorylation that eventually leads to neurodegeneration. However, research needs to be done to prove this stance.

1.3.9. Tau point mutations and phosphomimetic tau

Different tau point mutants, including P301L, P301S, P301T, and R5L, have been instrumental in elucidating and modeling the pathological roles of tau in microtubule assembly, binding, and aggregation (Guha et al., 2020; Strang et al., 2019). Over 50 pathogenic missense, silent, and intronic mutations within the MAPT gene have been identified, demonstrating the pivotal role of tau in neurodegeneration (Strang et al., 2019). Modifications to tau disrupt its interactions with microtubules, leading to microtubule instability and an increased propensity for aggregation. These alterations also impact the diverse physiological functions of tau, encompassing neurodevelopment, cognition, behaviour, and motor activity (Cario & Berger, 2023; Chang et al., 2021; Strang et al., 2019). For example, tau mutants such as P301L, V337M, R406W, and N279, reduce microtubule assembly, contributing to the stabilization of paired helical filaments (PHFs) and the formation of neurofibrillary tangles (NFTs) (Barghorn et al., 2000). Additionally, intronic mutations around exon 10 results in an imbalance of proportion between 4R- and 3R-tau isoforms that are observed in tauopathic diseases (Liu & Gong, 2008; Strang et al., 2019).

It is important to note that not all pathogenic tau mutations diminish microtubule affinity or enhance aggregation. For instance, the R5L mutation in the N-terminal projection domain maintains microtubule affinity (Cario et al., 2022). Some mutations, like N279K and S305N, have no impact on microtubule interactions or assembly, while others, such as Q336H and E342V, actually was known to promote microtubule assembly (Cario & Berger, 2023; Fernández-Nogales & Lucas, 2020). Thus, each disease-associated mutation or aberrant posttranslational modification represents a distinct pathology with its unique molecular mechanisms. Therefore, comprehending how each of these mutations or modifications affects the diverse cellular functions of tau is crucial for defining the molecular underpinnings of various tauopathies (Cario & Berger, 2023).

Phosphorylation of tau is a key aspect of its regulation and involvement in neurodegenerative diseases. Phosphomimetic tau mutants, which replicate phosphorylation events, have been invaluable in studying the effects of tau phosphorylation and hyperphosphorylation on cellular functions such as cargo transport, cell signaling, and protein degradation (Chang et al., 2021). For example, experiments involving large unilamellar vesicles (LUVs) have provided insights into tau's interaction with PI(4,5)P2 and its importance in membrane binding (Katsinelos et al., 2018). In another study, pseudo-phosphorylated tau known as tau441PHP exhibited a fivefold decrease in its association rate with microtubules, while its dissociation rate remained unaffected (Kent et al., 2020; Niewidok et al., 2016).

Phosphomimetic tau mutants, E18 and E27, which mimic the phosphorylation of 18 and 27 serine/threonine sites, were used to correlate between tau phosphorylation and its microtubule binding capacity. Notably, increasing tau phosphorylation reduced its binding to microtubules and improved axonal transport kinetics. Furthermore, autophagy was found to be the primary

route for clearing phosphorylated tau in neurons, suggesting a potential link between defective autophagy and tau accumulation in neurodegenerative diseases (Rodríguez-Martín et al., 2013a). While it is hard to actually use kinases for experiments which can phosphorylate tau and other proteins at the same time, the use of phosphomimics could help us isolate the effects of phosphorylated tau and understand their role in cellular processes.

In our study, we specifically examined the effect of E14 tau, which mimics 14 Alzheimer's disease-relevant phosphorylation sites (Hoover et al., 2010) in COS-7 cell models. This tau variant serves as a simple yet valuable model as it replicates the key phosphorylation sites observed in Alzheimer's disease, spanning different regions of tau. This tau model could provide us with insights into the pathogenic mechanisms associated with hyperphosphorylated tau. E14 tau was used in other studies on tau hyperphosphorylation as well. For example, studies using fluorescently labelled E14 phosphomimetic tau aggregates demonstrated effective propagation from neuron to neuron without causing detrimental effects on neuronal survival, presynaptic terminals, fundamental electrophysiological characteristics, or neuronal activity (Hallinan et al., 2019). Other research focused on the effect of E14 tau on mitochondria, tau mislocalization in neurons and tau toxicity studies on Drosophila flies (Guha et al., 2020; Iqbal et al., 2016; Strang et al., 2019).

Despite our increased understanding of how phosphorylated and hyperphosphorylated tau affect cellular functions, there is not much focus on microtubule organization and cargo transport at varying levels of hyperphosphorylated. So, our thesis aims to bridge the gap between known disease-related tau phosphorylation mimics (i.e. E14 tau) and their functional consequences on microtubule organization and cargo transport.

1.3.10. Why study tau hyperphosphorylation on its effect on cargo transport?

Tau hyperphosphorylation is the hallmark of neurodegenerative diseases such as Alzheimer's disease. Hyperphosphorylation of tau may negatively affect microtubule stabilization and regulation of motor proteins (Avila et al., 2012; Toral-Rios et al., 2020). These changes can disrupt axonal transport in neurons, potentially leading to neuronal degeneration due to impaired transport mechanisms (Hoover et al., 2010). But how hyperphosphorylated tau affects cargo transport during disease conditions is not well-researched. The physiological relevance of tau hyperphosphorylation is yet to be fully determined, and its involvement in Alzheimer's disease makes it an area of great interest and importance.

Our research aims to address this gap by focusing on understanding the influence of hyperphosphorylated tau on motor proteins and building a model to describe how their regulation affects intracellular transport. We hypothesize that tau plays a central role in regulating this transport process and that its dysregulation, caused by hyperphosphorylation, results in defects in axonal transport due to microtubule destabilization (Fig. 6).

We know that tau regulation of motor protein motility is complex as it involves the microtubule dynamics, the behaviour and phosphorylation status of tau and the number, type and localization of the motors carrying the cargo in a cell (Balabanian et al., 2022; Beaudet et al., 2023; Dixit et al., 2008; McVicker et al., 2014a; Siahaan et al., 2019; Stern et al., 2017). Thus, to explore the pathogenesis of Alzheimer's disease, we will mimic disease-relevant sites on tau to investigate the effect of hyperphosphorylated tau on the transport of cargoes, including lysosomes and early endosomes.

Lysosomes and early endosomes are integral components of the endocytic pathway, playing pivotal roles in waste clearance, degradation of misfolded proteins, plasma membrane repair, exosome release, cell adhesion, migration, apoptosis, metabolic signaling, and gene regulation (Loubéry et al., 2008; Pu et al., 2016). It was found that many of their functions are influenced based on their positioning and motility within the cells. Thus, dysregulation of lysosomal and endosomal transport has been implicated not only in lysosomal storage diseases but also in neurodegenerative diseases, such as Alzheimer's disease, Parkinson's and Huntington's disease (Pu et al., 2016). Additionally, studying lysosomes and early endosomes is advantageous as they can be investigated using simple reagents like Lysotracker and Quantum Dots (Balabanian et al., 2022).

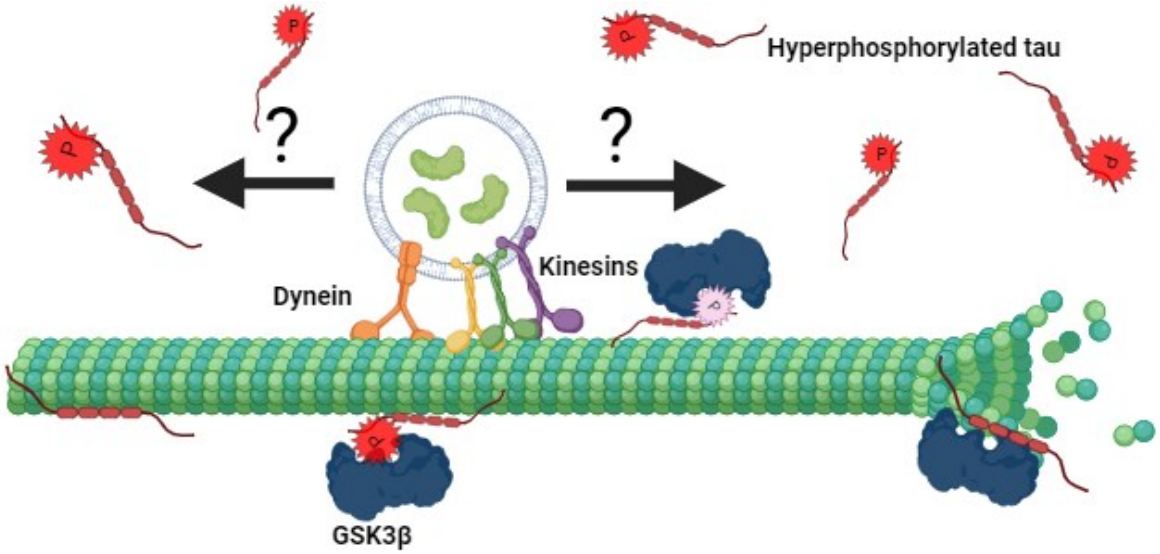

Figure 6: How does hyperphosphorylated tau affect the microtubule organization and motility of organelles? Different cargo has different sets of motors carrying them, and each motor has varying sensitivity to tau and phosphorylated tau. It is poorly understood how hyperphosphorylated tau can affect cargo transport, as this can help us understand the reasons for defective transport found in Alzheimer's disease. GSK-3β is widely studied for its involvement in Alzheimer's, as they are known to phosphorylate multiple sites in tau. We hypothesize that hyperphosphorylated tau results in the destabilization of the microtubules due to their poor binding ability and, thus, will negatively affect the transport. [Image created using Biorender]

In our study, we focus primarily on the impact of hyperphosphorylated tau on microtubule stability and cargo transport using COS-7 cells. While neurons possess a highly specialized and compartmentalized architecture with distinct axonal and dendritic microtubule

organization (Aiken & Holzbaur, 2021), we have chosen to utilize COS-7 cells as a simplified cellular model. Although neurons and COS-7 cells differ significantly, COS-7 cells offer several advantages, including ease of culturing and a flat morphology suitable for imaging. Importantly, COS-7 cells lack endogenous tau expression, allowing us to exclusively study the effects of tau by transfecting them with tau constructs. Our research using COS-7 cells will provide valuable insights into the role of hyperphosphorylated tau in cargo transport, offering an understanding of the mechanisms that may contribute to transport defects observed in neurodegenerative diseases. Subsequent research can further build upon these insights by employing neuron-specific models.

Chapter 2

2. Methods

2.1. Preparation of tau plasmid constructs

The plasmid constructs, WT tau (#46904), E14 Tau (#46907), and AP14 tau (pRK5-EGFP-Tau AP (#46905), were acquired from Addgene. The constructs were expressed in the pRK5 vector containing the cytomegalovirus (CMV) promotor and tagged with eGFP (enhanced Green Fluorescent Protein) at the N terminus. These constructs encode the four repeats, lack the N-terminal sequence (4R0N), and contain exons 1, 4 and 5, 7, and 9–13, intron 13, and exon 14. The E14 and AP14 tau constructs were generated based on the WT construct, and the 14 sites (T111, T153, T175, T181, S199, S202, T205, T212, T217, T231, S235, S396, S404, and S422) were mutated to alanine (AP14 tau - phosphoresistive) or glutamate (E14 Tau - phosphomimetic) (Hoover et al., 2010). The plasmids were obtained through a mini-prep procedure and subsequently purified using anion-exchange gravity flow chromatography (Qiagen, Hilden, Germany).

2.2. COS-7 cell culture and transfection

COS-7 fibroblast cells were sourced from the American Type Culture Collection (ATCC, Manassas, VA) for the research study. To ensure their viability and proper growth, the cells were cultured in T-25 Cell culture flasks (Sarstedt) for maintenance and subsequently transferred onto MatTek No. 1.0 coverslip glass bottom dishes (MatTek Corporation) for imaging purposes. The cell culture media used for sustaining the cells consisted of DMEM basal media (Gibco) supplemented with 1% (v/v) glutamax (Gibco) and 10% (v/v) fetal bovine serum (Gibco). For passaging, the cells were treated with 0.25% trypsin-EDTA and seeded

onto the glass bottom dishes, followed by incubation at 37°C with 5% CO2 for 24 hours before transfection. The transfection involved introducing approximately 400 ng of DNA plasmid, prepared in OPTI-MEM Reduced Serum (Gibco), into the cells. Lipofectamine LTX with Plus-Reagent, as per the manufacturer's instructions (Invitrogen), was utilized for efficient transfection. The transfected cells were then kept in the transfection media, containing DNA-lipid complexes, at 37°C for 4 hours before being replaced with fresh, complete DMEM media. Subsequently, the cells were maintained overnight (~12 h) at 37°C to allow for optimal expression of the transfected DNA before proceeding with imaging. For experiments involving nocodazole as a baseline measurement, the cells were treated with 10 μM nocodazole for a duration of 15 minutes.

2.3. Microscopy and live cell imaging

Live-cell imaging was done using a custom Total Internal Reflection Fluorescence (TIRF) microscopy set-up built on an Eclipse Ti-E inverted microscope (Nikon), with an EMCCD camera (iXon U897, Andor Technology) and a 1.49 numerical aperture oil-immersion 100x objective (Nikon) using diode lasers (100 mW maximum power) (Coherent). The pixel size was 0.160 μm for all imaging experiments.

A) Lysosomes:

Cells in the glass bottom dishes were incubated with 50 nM Lysotracker Deep Red (Invitrogen) in complete DMEM media for 10 minutes. Cells were then washed and imaged in Leibovitz's L-15 Medium (no phenol red) (Gibco) supplemented with 10% (v/v) FBS, at 37°C, using the TIRF microscope. To achieve the desired fluorescence excitation, a 488nm laser (1 mW) was employed for exciting tau-EGFP, and a 647 nm laser (1 mW) was used for exciting Lysotracker Deep Red, along with the appropriate emission filters. The time-lapse imaging was performed at a frame rate of 302 ms per frame, allowing for the capture

of dynamic lysosome motility. Cells were imaged within 1 hour following Lysotracker staining.

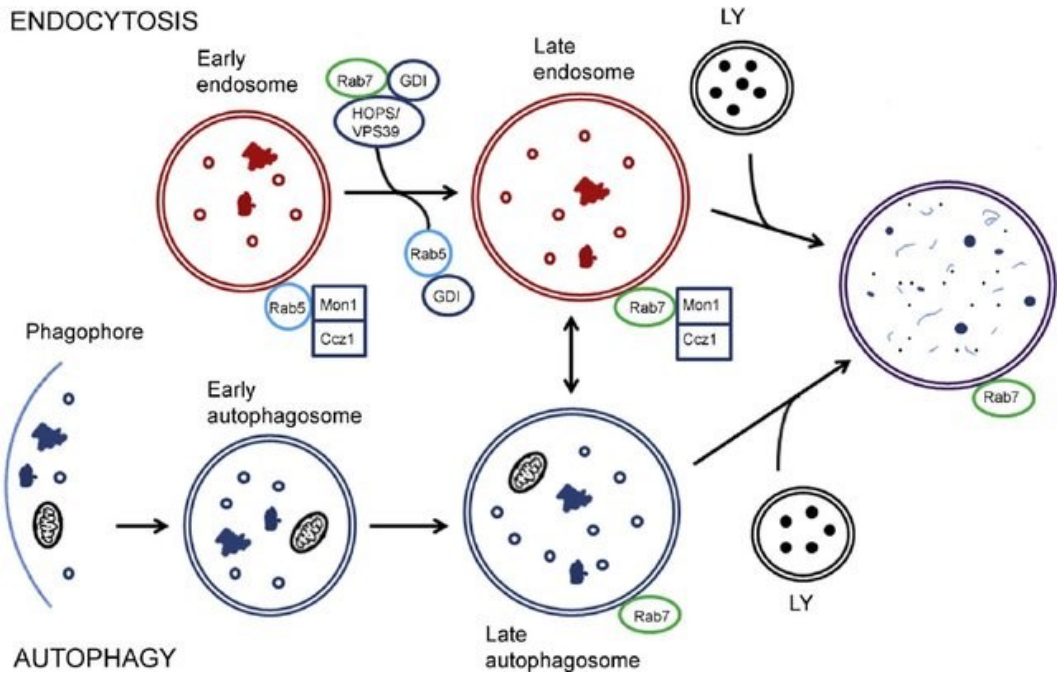

Figure 7: The endocytic cargo maturation and fusion with the lysosome. Endocytosis degrades foreign materials external to the cell, whereas autophagy involves degrading cellular components and defective organelles. In endocytosis, early and late endosomes are characterized by marker proteins Rab5 and Rab7, respectively. Early endosome matures into late endosome and then fuses with the lysosome to form endolysosome, which is highly acidic and has hydrolases, so the materials inside the endolysosome are degraded. A similar process happens with autophagy for degrading cellular debris. Image taken from (Hyttinen et al., 2013).

B) Early Endosomes:

Streptavidin-conjugated quantum dots (Qdot 565, Invitrogen) at a concentration of 0.02 µM were used to visualize early endosomes. The streptavidin-conjugated Qdots were coated with Biotin-conjugated Epidermal Growth Factor (EGF) (Invitrogen) at a concentration of 2.4 µg/mL in Qdot Incubation Buffer (50 mM borate buffer, pH 8.3, 2% BSA) (Invitrogen). The coating process was performed by incubating the Qdots with EGF for 30 minutes on ice in a dark chamber (Zajac et al., 2013)**.** Cells were then incubated with a solution of 2.2 µL Qdot preparation in a total of 200 µL complete DMEM media on an orbital shaker for 10 minutes. Cells were then washed and imaged in Leibovitz's L-15

(supplemented with 10% FBS) before 1-hour post-internalization of Qdots. The imaging was carried out at 37°C using TIRF. Time-lapse movies were captured at a frame rate of 300 ms per frame. A 488nm laser (1 mW) was used to excite tau-EGFP, and a 405 nm laser (3 mW) was used for exciting the Qdots. The setup included appropriate emission filters to prevent signal cross-bleeding between tau and Qdot emissions. A dichroic mirror (BP 650) was placed in the emission path to separate the Qdot and Tau-GFP emission. Cells were imaged within 1 hour following Qdot internalization.

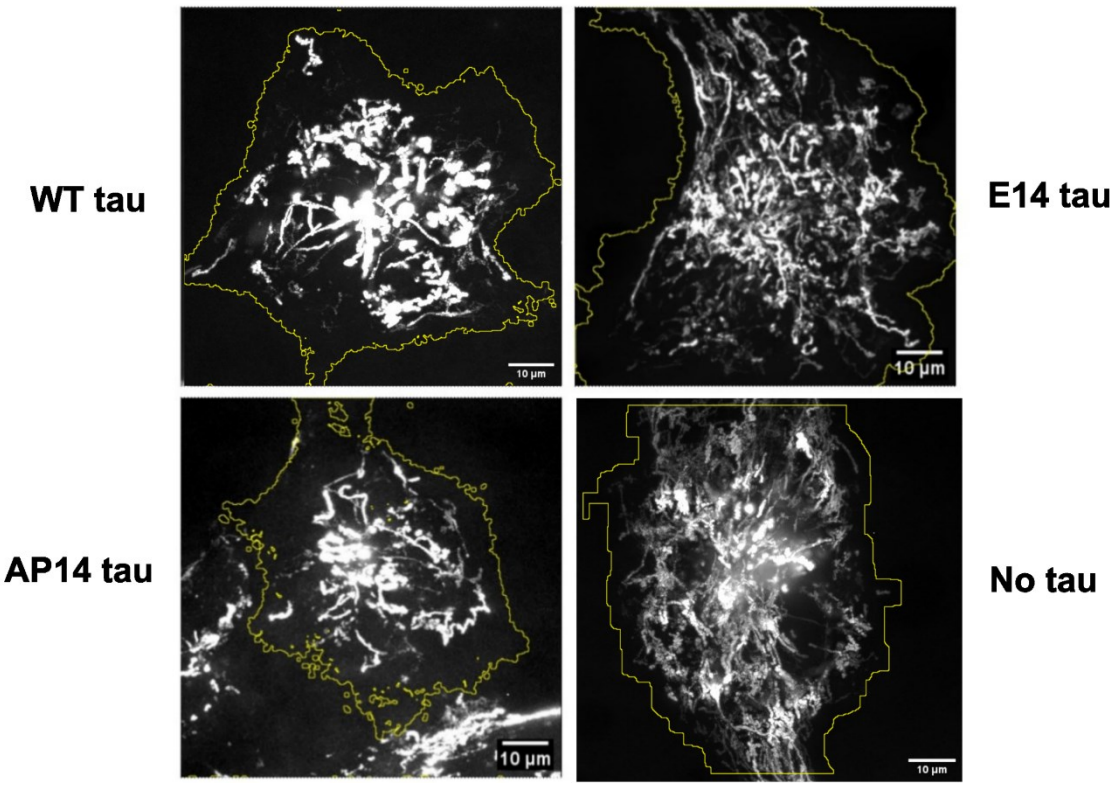

Figure 8: Trajectory plots showing lysosome motility in cells expressing different tau variants (WT, E14, and AP14) along with no tau cell in maximum projection format. The raw data was captured in a 90-second video and processed using FIJI with the Trackmate plugin to obtain the X, Y, and time coordinates of the trajectories. Motility analysis was conducted to assess the impact of tau on cargo motility.

2.4. Automated tracking using Trackmate:

Before tracking the trajectories, both the lysosomes and early endosomes movie raw data were corrected for photobleaching using the histogram matching algorithm in the bleach correction

plugin in ImageJ. The region of interest was generated based on the cell contour, and then the organelles were tracked using the ImageJ (National Institutes of Health) plugin, Trackmate (Ershov et al., 2022). The Laplacian of Gaussian (LoG) filter was used along with sub-pixel localization and median filter to detect the cargo first, and then using a simple Linear Assignment Problem (LAP) tracker to generate the trajectories made by the organelles. Based on the maximal velocity of the cargoes, the tracking parameters were set to linking distance (μm): gap-closing maximum distance (μm): gap-closing maximum frame gap of 1.5:1.5:1 for lysosomes and 1:1.2:3/5 (this is varied to connect the trajectories of motile dim quantum dots) for early endosomes. For the analysis, only the organelles detected in the movie's first frame are considered, and the trajectories should be at least greater than 5 frames to remove the false positive trajectories or very short trajectories.

2.5. Tau intensity quantification

To address the variability in tau-EGFP expression observed after transient transfection, a systematic approach was employed to quantify tau levels and investigate the role of tau in a dose-dependent manner. The intensity of eGFP fluorescence signal was used to measure tau expression, and ImageJ software was used for quantification. To obtain normalized tau intensity, the mean tau intensity of each cell was divided by the background mean intensity, which was measured in an area away from the cell. This normalization procedure aimed to reduce data variability and allow a more reliable comparison of tau expression levels across different cells. Throughout all experiments, rigorous control was exercised to maintain consistent experimental and imaging conditions within and across studies. This measure was taken to minimize potential sources of variability and ensure a reliable assessment of normalized tau intensity. Cells were categorized into three tau expression levels based on the normalized intensity values: low, medium, and high. The current analysis specifically

considered cells exhibiting low tau expression levels (normalized tau intensity < 5). This range of normalized intensity was chosen as it aligns with tau expression levels observed in distal and proximal axons of neurons, as demonstrated through tau immunostaining using tau-5 in iPSC-derived cortical neurons and COS-7 cells (Balabanian et al., 2022). We then further divided the low tau intensity into low expression (1 to 3) and high expression (3 to 5) for our analysis for our better understanding.

2.6. Tau binding and microtubule bundling analysis

Two MATLAB scripts were developed to investigate the interactions and bundling of microtubules involving tau protein. For assessing binding properties, the analysis was one by processing microtubule intensity data when bound with tau and the corresponding background intensity data. This facilitated the computation of the ratio of bound to unbound tau by individually dividing these values across the dataset. Subsequently, the mean ratio was calculated and presented through bar plots, categorized into low tau intensity (1 – 3 tau intensity) and high tau intensity (3 – 5 tau intensity) ranges.

For evaluating bundling properties, Gaussian components within the differential distribution of bound and unbound intensity values were identified and quantified. The implementation of the code commenced with the loading of experimental data, with a distinction between various conditions (WT, E14, AP14) and between bound and unbound states. The difference between bound and unbound tau was quantified, and the resulting data was visualized through a histogram. The code then employs Gaussian Mixture Model (GMM) fitting to the difference data using a range of Gaussian components (up to 10), and the Akaike Information Criterion (AIC) is utilized to determine the optimal number of components for the GMM model. The parameters of the GMM, including means and fraction bound to microtubules were estimated.

The GMM curve is superimposed on the histogram, revealing the fit quality. Additionally, areas under individual Gaussian components were found and their respective fractions were determined, providing key information on the proportion of bundles made in the presence of tau. Thus, the obtained GMM parameters were used to interpret and analyze microtubule bundling characteristics.

2.7. Motility analysis

The radius of gyration (Rg) measures the travelled distances of lysosomes or early endosomes from the center of their trajectory. Rg of the lysosome (from 90 seconds movies) and early endosome trajectories (from 30 seconds movies) was calculated with the following equation:

$$R_g = \sqrt{\frac{1}{n}\sum_{i}^{n}\left((x_i - \bar{X})^2 + (y_i - \bar{Y})^2\right)}$$

No minimum thresholds for Rg were applied when examing the motion of all lysosomes or early endosomes. The Rg code was developed and modified in MATLAB based on the scripts developed by Linda Balabanian (Balabanian et al., 2022).

$$MSD(n\Delta t) = \frac{1}{N-n}\sum_{i=i}^{N-n}[(x_{i+n} - x_i)^2 + (y_{i+n} - y_i)^2]$$

2D mean-squared displacement (MSD) was analyzed using MSDanalyzer in MATLAB (Tarantino et al., 2014). The MSD curves of lysosomes and early endosomes were transformed into a log-log scale to analyze their dynamic behaviour. Specifically, the first 10% of the log-log transformed MSD curves were subjected to linear fitting, covering a time window of 50

seconds for lysosomes and 15 seconds for early endosomes. The slope of the linear fit on a log-log plot, α, indicates the nature of the particle's movement ($\alpha < 1$ for stationary, $\alpha = 1$ for diffusive, and $\alpha > 1$ for processive motion). The fitting process was applied separately to each trajectory in the dataset. However, low-quality fits, indicated by a coefficient of determination (R2) below 0.8, were excluded from further analysis to ensure reliability. A weighted standard deviation approach was employed to calculate the standard error of the mean (SEM) for the obtained α values, considering the variability of the fitted α values. The SEM was then estimated by dividing the weighted standard deviation by the square root of the number of degrees of freedom (Tarantino et al., 2014).

We calculated a running-mean velocity to assess the motion of lysosomes and early endosomes, aiming to understand their average speed with pausing and the percentage of time spent pausing. For each trajectory, we calculated the total run length, which represents the overall distance covered by the cargo, and the total binding time, which accounts for the duration of the trajectory, including pauses. By dividing the trajectory's total distance by the trajectory's total time (with paused segments), we obtained the average speed of the cargo with pausing. To determine the percentage of time spent pausing, we identified pauses as time intervals with negligible movement based on a threshold of 0.01 units. The proportion of such pausing intervals to the total time of the trajectory yielded the percentage of time spent pausing. Smoothing techniques were applied to reduce noise, and statistical means were computed for average speed with pausing and percentage pausing across all trajectories to derive overall insights into the cargo dynamics. For the sliding means analysis of velocity with pausing and percentage pausing, bootstrapping was done on the data for 1000 iterations with a window size of 7 and the fraction of total data points in each bin of 0.04. The speed analysis code was

developed and modified in MATLAB based on the scripts developed by Linda Balabanian (Balabanian et al., 2022).

2.8. Analysis of lysosomal directionality and localization

Lysosome motility was classified based on the net directionality. This classification was determined by comparing the rho value of the first and last points in each lysosome's trajectory, where the rho value of a trajectory represents the mean distance of the trajectory points from the cell center. The rho value was normalized to standardize this measurement by dividing it by the distance from the cell center to the cell edge. It was estimated based on the cell's area using the formula: radius = $\sqrt{(\text{cell area}/\pi)}$. Lysosomes were categorized as stationary, moving outward (first rho point less than last rho point), or moving inward (first rho point greater than last rho point) based on their directionality. To quantify the distribution of stationary, outward, and inward-moving lysosomes, the percentages were calculated as the mean of cell means, accompanied by the standard error of the mean (SEM).

For the localization analysis, lysosomes were categorized into three regions based on their normalized rho values: peripheral (≥ 0.85), juxtanuclear ($0.5 \leq \text{rho} < 0.85$), and perinuclear ($< 0.5$). Similar to directionality, percentages of lysosomes in each category were calculated as the mean of cell means with SEM. The localization and directionality code were developed and modified in MATLAB based on the scripts developed by Linda Balabanian (Balabanian et al., 2022).

2.9. Statistical analysis

Using the bootstrapping method of 1000 iterations and with a 95% confidence interval (for determining the statistical significance), the normalized means of Rg and α values of lysosome and early endosome trajectories to normalized tau intensity (normalized to the background) were calculated and averaged with a bin size of 5 and 8 respectively along the x-axis (Chaubet et al., 2020). In this study, we employed bootstrapping with the resampling method, a robust statistical approach to assess the significance of differences between experimental groups (Control vs different tau groups and between the different tau groups in a pairwise manner). We did this for all our analyses, such as α, Rg, velocity, localization, and directionality analysis for both the lysosome and early endosome cargo. We normalized the data to ensure that any variations due to the total number of events were accounted for. We then bootstrapped with 1000 iterations for each group to create sampling distributions and obtained the bootstrap mean differences between the pairwise groups. The p-values were computed by plotting the histogram of bootstrap mean differences between the pairwise groups and checking if the histogram was greater than zero. A p-value threshold of 0.05 was used to determine statistical significance. If the tail of the histogram covers less than 0.05, it is considered significant, and if it is greater than 0.05, it is considered insignificant. All statistical tests were performed with MATLAB (MathWorks).

Chapter 3

3.1. Overview

Alzheimer's disease (AD) is a progressive neurodegenerative disease primarily characterized by the accumulation of abnormal protein aggregates of amyloid beta and tau in the brain (Chong et al., 2018; Kametani & Hasegawa, 2018; Sergeant et al., 2008). While much attention has been focused on how these aggregates contribute to neurodegeneration, less is understood about the role of hyperphosphorylated tau in affecting microtubule organization and intracellular transport. In this study, we examined 1) how hyperphosphorylated tau alters the organization of the microtubule cytoskeleton and 2) how hyperphosphorylated tau impacts the cargo transport of lysosomes and early endosomes. We hypothesize that hyperphosphorylated tau could destabilize microtubules, directly impacting cargo transport. This study showcases valuable insights into the role of hyperphosphorylated tau in intracellular transport and provides a methodological framework for further investigations in tau-related pathologies and cellular transport.

The cells rely on cytoskeletal elements, such as microtubules and motor proteins, for intracellular transport (Aiken & Holzbaur, 2021). Microtubules are polarized structures responsible for maintaining the cell structure and cargo transport. It comprises long, dynamic polymers of α- and β- tubulin heterodimers involved in growth and shrinkage cycles through dynamic instability (Balabanian et al., 2018; Brouhard & Rice, 2018; Horio & Murata, 2014; Mitchison & Kirschner, 1984; Muroyama & Lechler, 2017). Motor proteins, such as kinesins and dyneins, use ATP hydrolysis to generate mechanical forces, which enables them to move along the polarized microtubules and transport organelles to their respective destinations(Aiken & Holzbaur, 2021). Kinesins, including kinesin-1, -2, and -3, are considered anterograde

motors, carrying cargo toward the microtubule plus end (Hirokawa & Tanaka, 2015). While cytoplasmic dynein acts as a retrograde motor, moving cargoes toward the microtubule minus end (Maday et al., 2012). Cargoes can have different ratios of kinesins and dyneins, which help them move unidirectionally or bidirectionally along microtubules (Beaudet et al., 2023). This intracellular transport system is crucial in neurons as they are highly polarized cells with distinct subcellular compartments, including axons and dendrites, each requiring precise transport of essential cargo. Several mechanisms exist in regulating cargo transport, such as microtubule organization, post-translational modifications, and microtubule-associated proteins (MAPs) (Aiken & Holzbaur, 2021; Balabanian et al., 2018; Gendron, 2009). MAPs can regulate cargo transport by modulating the organization through lattice compaction and expansion, microtubule bundling and stability, and also by directly influencing motor proteins that move along the microtubule surface (Breuzard et al., 2013; Cario et al., 2022; Castle et al., 2020; Samsonov et al., 2004; Siahaan et al., 2019, 2022). Misregulation of MAPs, such as tau, can lead to defects in the organelle transport which are implicated in various neurological disorders, such as Alzheimer's disease (AD) (Ballatore et al., 2007; Noble et al., 2013; Yang et al., 2023).

Tau is a multifunctional MAP predominantly found in neurons, where it plays a critical role in maintaining microtubule stability and regulating their assembly and dynamics (Kent et al., 2020; Rodríguez-Martín et al., 2013a; Wang & Mandelkow, 2016; Yang et al., 2023). There are six isoforms of tau, which differ by the absence or presence of 0, 1 or 2 acidic inserts at the N-terminal and whether they contain 3 or 4 repeats of the tubulin-binding motif at the C-terminal region. So 4R-tau is based on the inclusion of exon 10, and 3R-tau is based on the exclusion of exon 10 (Gendron, 2009). Tau can exist in different states along microtubule surfaces, either static or diffusive, with 3R-tau being more static than 4R-tau in binding to

microtubules (McVicker et al., 2014b). Tau can form envelopes, which are patches of tau formed on the microtubule surface, that influence the behaviour of microtubules and motor proteins (Siahaan et al., 2022). Tau can regulate cargo transportation directly by interacting with the motors, such as short 3R tau isoform inhibiting kinesin-1 or indirectly by affecting the lattice properties, which affect motor binding and kinetics (McVicker et al., 2011, 2014b; Siahaan et al., 2019, 2022).

Tau can be phosphorylated at multiple sites by kinases, including fyn, glycogen synthase kinase 3 beta (GSK3β) and cyclin-dependent kinase 5 (CDK5), affecting its interaction with microtubules (Avila et al., 2012; Gendron, 2009; Xia et al., 2021b). Phosphorylation of tau leads to additional negative charges being added to the protein, reducing the tau affinity for microtubules, and this could also destabilize the envelopes on the microtubule surface, affecting the lattice compaction (Siahaan et al., 2022). Tau phosphorylation also alters its effects on motor protein by differentially regulating cargoes driven by kinesin-3 motors, as shown using monophosphomimetic Y18E tau (Balabanian et al., 2022; Stern et al., 2017). Different phosphorylation sites have varying effects, influencing tau to unbind from microtubules or form aggregates, which could impact cargo motility. Dysregulation of tau, such as hyperphosphorylation, has been implicated in the pathogenesis of Alzheimer's diseases and other tauopathies (Duquette et al., 2021; Rodríguez-Martín et al., 2013a; Shahpasand et al., 2012). The hyperphosphorylation of tau could drastically reduce tau affinity to microtubules, leading to microtubule destabilization, a hallmark of neurodegenerative diseases (Gendron, 2009; Xia et al., 2021b)

The precise mechanisms underlying how hyperphosphorylated tau impacts the transport of organelles in the context of neurodegenerative diseases remain unclear. Understanding these

mechanisms is crucial, as defects in intracellular transport significantly affect neuronal function and survival (Hoover et al., 2010). We employed a live-cell imaging technique using COS-7 cells exogenously expressing tau to address this. This method enabled us to isolate the effects of tau. We examined E14 tau, which mimics 14 Alzheimer's disease-relevant phosphorylation sites (Hoover et al., 2010), and compared it to WT tau and phosphoresistive AP14 tau. We used Total Internal Reflection Fluorescent (TIRF) microscopy to facilitate cargo tracking and then quantified the impact of the three tau constructs on microtubule organization and cargo transport. Here, we show that phosphomimetic E14 tau was predominantly cytosolic due to its weak affinity towards microtubules, showing lower microtubule bundling and weakly inhibiting lysosome and early endosome transport compared to phosphoresistive AP14 tau. These results suggest that hyperphosphorylation may relieve tau-mediated inhibition of transport, as hyperphosphorylated tau has a weakened effect on microtubule organization and on motor protein motility.

3.2. Experimental findings

3.2.1. Phosphomimetic E14 tau is less enriched on microtubules compared to phosphoresisitive AP14 tau:

Our study aims to investigate the effect of tau hyperphosphorylation on cargo motility. We expressed WT, E14 and AP14 tau in COS-7 fibroblast cells and examined how they were bound to the microtubules. We selected COS-7 cells as their flat morphology facilitates high-resolution imaging and recording of organelle motility using TIRF (Total Internal Reflection Fluorescence) microscopy. Further, COS-7 cells do not endogenously express tau, enabling us to isolate differences in cytoskeletal organization and intracellular transport due to tau expression.

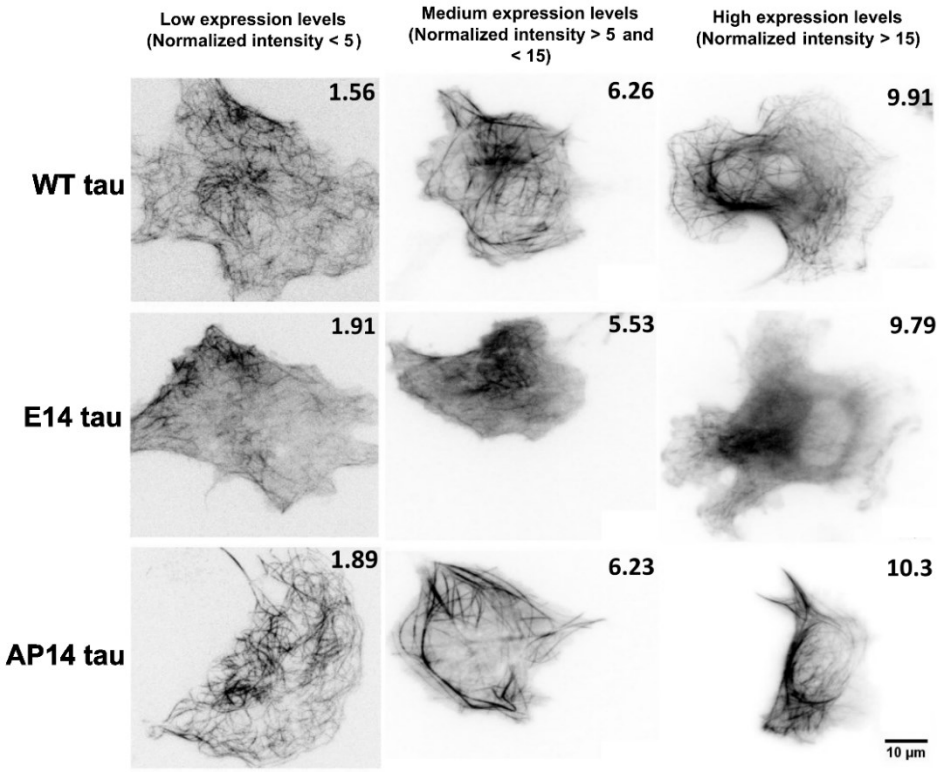

Figure 9: Phosphomimetic E14 tau is less enriched on microtubules compared to phosphoresisitive AP14 tau. Transient tau expression resulted in variable expression levels (low, medium, and high expression). Tau binds tightly to microtubules in the case of WT tau and AP14 tau (much more strongly) compared to E14 tau. E14 tau is enriched in the cytosol and expression results in less microtubule bundling.

To reduce the variability in our data analysis and to investigate the roles of tau in a dose-dependent manner, we normalized our tau intensities. To do so, we first quantified tau expression levels of the cells and then subsequently normalized against the background intensity outside the cell (see Methods). We categorized the intensity level into three categories: low levels of tau expression (normalized tau intensity < 5) (Fig. 9, 1st column), cells expressing medium levels of tau intensity (5 ≤ normalized tau intensity < 10) (Fig. 9, 2nd column) and finally high levels of tau expression (normalized tau intensity ≥ 10) and exhibit cell-wide cytosolic signal (Fig. 9, 3rd column). Interestingly, cells expressing E14 tau showed elevated cytosolic tau even at low expression levels. As expression increased, cytosolic E14 tau levels rose without affecting cell morphology. AP14 tau demonstrated robust binding to microtubules, leading to multiple microtubules bundles even at lower expression levels qualitatively. With increasing expression, AP14 tau exhibited stronger tau-microtubule interactions and more microtubule bundles, resulting in smaller cell sizes. Similar observation

can be made on WT tau as they bind to microtubules, bundle them, and show cytosolic tau at increasing tau levels. AP14 tau acts more robust, particularly at low tau expression levels, with consistently low cytosolic tau levels across all ranges. Hence, through qualitative inspection, the microtubule dynamics were significantly altered in AP14 tau, followed by WT tau and E14 tau due to their different tau binding abilities.

To further analyze how these three tau types affect microtubule dynamics and cargo transport, we focused on low tau expression levels for cargo motility analysis, which exhibited a radial microtubule organization. Low tau expression levels closely correspond to the endogenous tau levels in neuronal axons (Balabanian et al., 2022). With this, we focused on the binding and bundling abilities of the three tau types at an increasing tau intensity range (i.e., from tau intensity of 1 to 3 to tau intensity of 3 to 5).

3.2.2. E14 tau binds more weakly to microtubules and exhibit impaired bundling capacity compared to AP14 tau:

To analyse the effect of WT, E14 and AP14 tau on microtubule properties, we calculated the amount of tau bound to microtubules, as a proportion of unbound tau at lower and higher tau intensity (Fig. 10A). The results revealed that E14 tau had a significantly reduced ability to attach to microtubules in comparison to WT tau and AP14 (Bootstrapping-derived p-value is < 0.001 for normalized tau intensity ranges 1-3 and 3-5). When considering WT and AP14 tau, higher tau intensity correlated with an increased tau binding ratio. At lower tau intensity, AP14 demonstrated a stronger microtubule binding compared to WT tau ($p = 0.003$), but this similarity shifted at higher tau intensity ($p = 0.07$) (Fig. 10A). This aligns with previous

research on phosphomimetic and phosphoresistive tau types (Balabanian et al., 2022; Boumil et al., 2020; Rodríguez-Martín et al., 2013a).

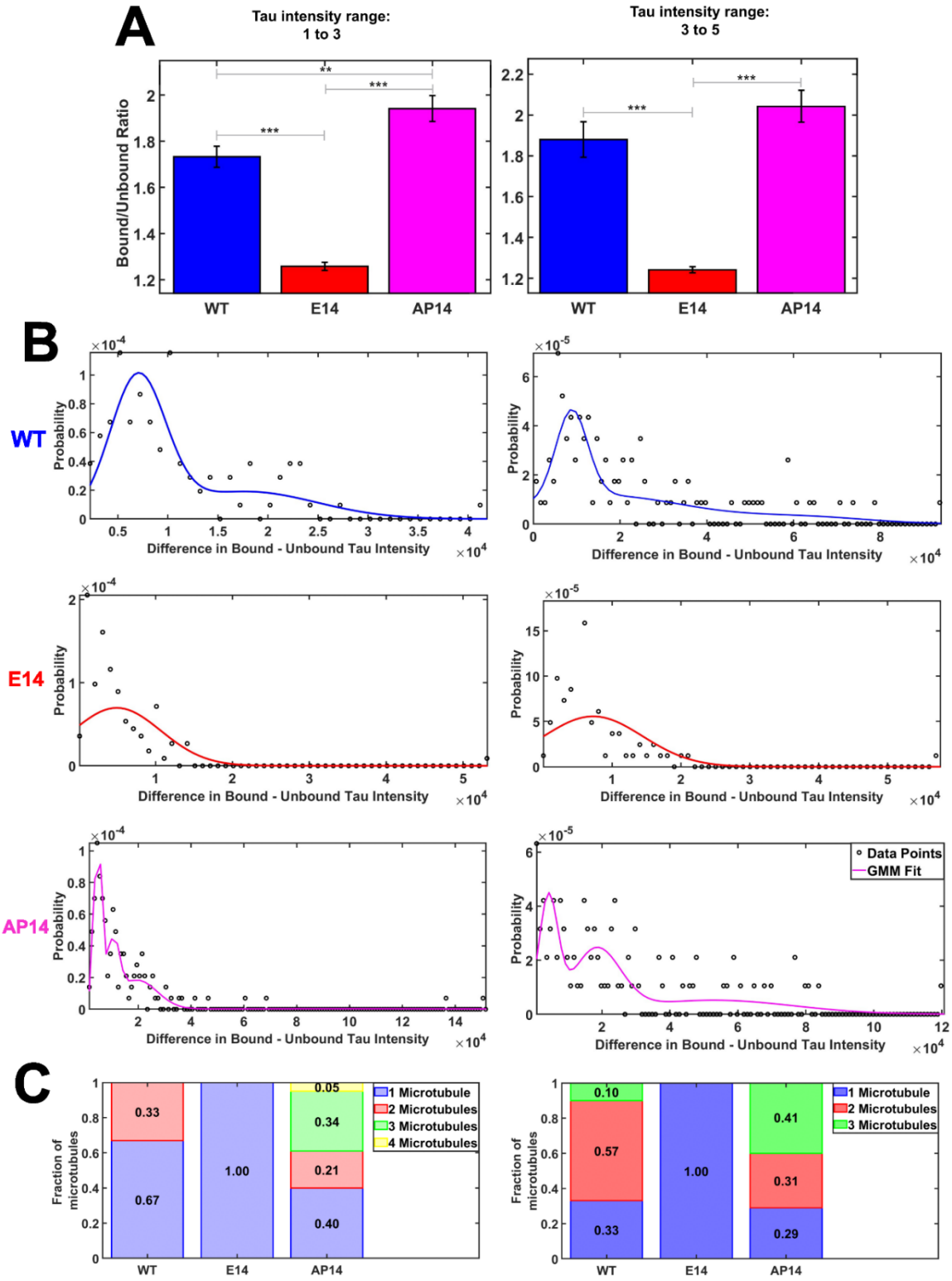

Figure 10: E14 tau binds more weakly to microtubules and exhibit impaired bundling capacity compared to AP14 tau. A. Quantification of tau-bound/unbound on microtubules (mean ± SEM) for tau intensity 1 to 3 and tau intensity 3 to 5. E14 tau shows impaired tau binding compared to AP14 and WT tau, which exhibit stronger

tau binding at increasing tau levels. However, AP14 and WT show similar tau binding at tau intensity 3 to 5. B & C. Tau bundling capacity of WT, E14, and AP14 tau. This was calculated by normalizing tau-bound microtubules against adjacent cytosolic tau. WT tau forms 2 microtubule bundles (fractions of bound tau: 0.67 and 0.33) and 3 microtubule bundles (fractions of bound tau: 0.33, 0.57, and 0.1) at tau intensity ranges 1 to 3 and 3 to 5, respectively. E14 tau, due to weak binding, does not form bundles at any tau as it is bound to only one microtubule. Conversely, AP14 tau exhibits prominent bundling, forming 4 microtubule bundles (fractions of bound tau: 0.40, 0.21, 0.34, and 0.05) and 3 microtubule bundles (fractions of bound tau: 0.29, 0.31 and 0.41) at tau intensity ranges 1 to 3 and 3 to 5, respectively. (WT tau: 11 cells - 220 tau bound/unbound datapoints; E14 tau: 15 cells – 194 tau bound/unbound datapoints; AP14 tau: 19 cells - 238 tau bound/unbound datapoints) (* $p < 0.05$, ** $p < 0.01$, *** $p < 0.001$, bootstrapping-derived p-value).

We also evaluated the three tau variants for their capability to bundle microtubules (Fig. 10B and 10C). As expected, following the binding ratio pattern, E14 tau exhibited reduced microtubule bundling ability, binding only to individual microtubules even at higher tau intensity. In contrast, both WT and AP14 tau displayed pronounced bundling at both tau intensities. Notably, AP14 exhibited robust bundling (four microtubules in a bundle) at lower tau intensity than WT tau (two microtubules in a bundle). This bundling capacity remained similar between AP14 and WT tau at higher tau intensity (three microtubules in a bundle). Overall, we found that there was a prominent increase tau-bound microtubules, which exhibits increased bundling capacity for AP14 compared to E14 tau.

3.2.3. E14 tau weakly inhibits lysosome transport compared to AP14 tau:

This study investigated lysosome motility in COS-7 cells using Lysotracker Deep imaged through TIRF microscopy. Lysosomes exhibit bidirectional motion driven by kinesin-1, kinesin-2, kinesin-3, and dynein (Guardia et al., 2016; Nagpal et al., 2023; Beaudet et al., 2023). We collected raw data on lysosome motion and processed it using Trackmate and MATLAB. We used mean-squared displacement (MSD) and Radius of gyration (Rg) to analyze lysosomal cargo motion. MSD and Rg were used to determine the motion type and the distance traveled by lysosomal cargoes, respectively. The slope of the MSD, α, quantifies processivity: $\alpha < 1$ for stationary, $\alpha = 1$ for diffusive, and $\alpha > 1$ for processive motion. Rg (square root of $[(1/n) * \Sigma((x_i - \bar{X})^2 + (y_i - \bar{Y})^2)]$) measures the distance travelled by cargo. While calculating Rg, every

trajectory holds equal weight. However, in calculating MSD, each delay period receives equal weight, leading to longer trajectories exerting greater influence than shorter ones. We also measured the speed with pausing and the percentage of lysosome pausing in the presence of the three tau types.

Based on the MSD and alpha plot (Fig. 11A & 11B, 95% confidence interval), three tau types tested led to reduced lysosome processivity as tau intensity increased (Bootstrapping-derived p-value is < 0.001 for normalized tau intensity ranges 1-3 and 3-5, between no tau and all tau types: WT, E14, AP14). This observation aligns with the Rg analysis (Fig. 11C, 95% confidence interval), where higher tau intensity decreased lysosome run length increased (Bootstrapping-derived p-value is < 0.001 for normalized tau intensity ranges 1-3 and 3-5, between no tau and all tau types: WT, E14, AP14).

At lower tau expression levels, E14 tau and WT tau weakly affected cargo processivity and run length. However, AP14 tau significantly inhibited lysosome processive motion ($p = 0.005$ for normalized tau intensity 1-3 and $p = 0.047$ for intensity 3-5) and run length ($p < 0.001$ for normalized tau intensity 1-3 and $p = 0.003$ for intensity 3-5) compared to E14 tau.

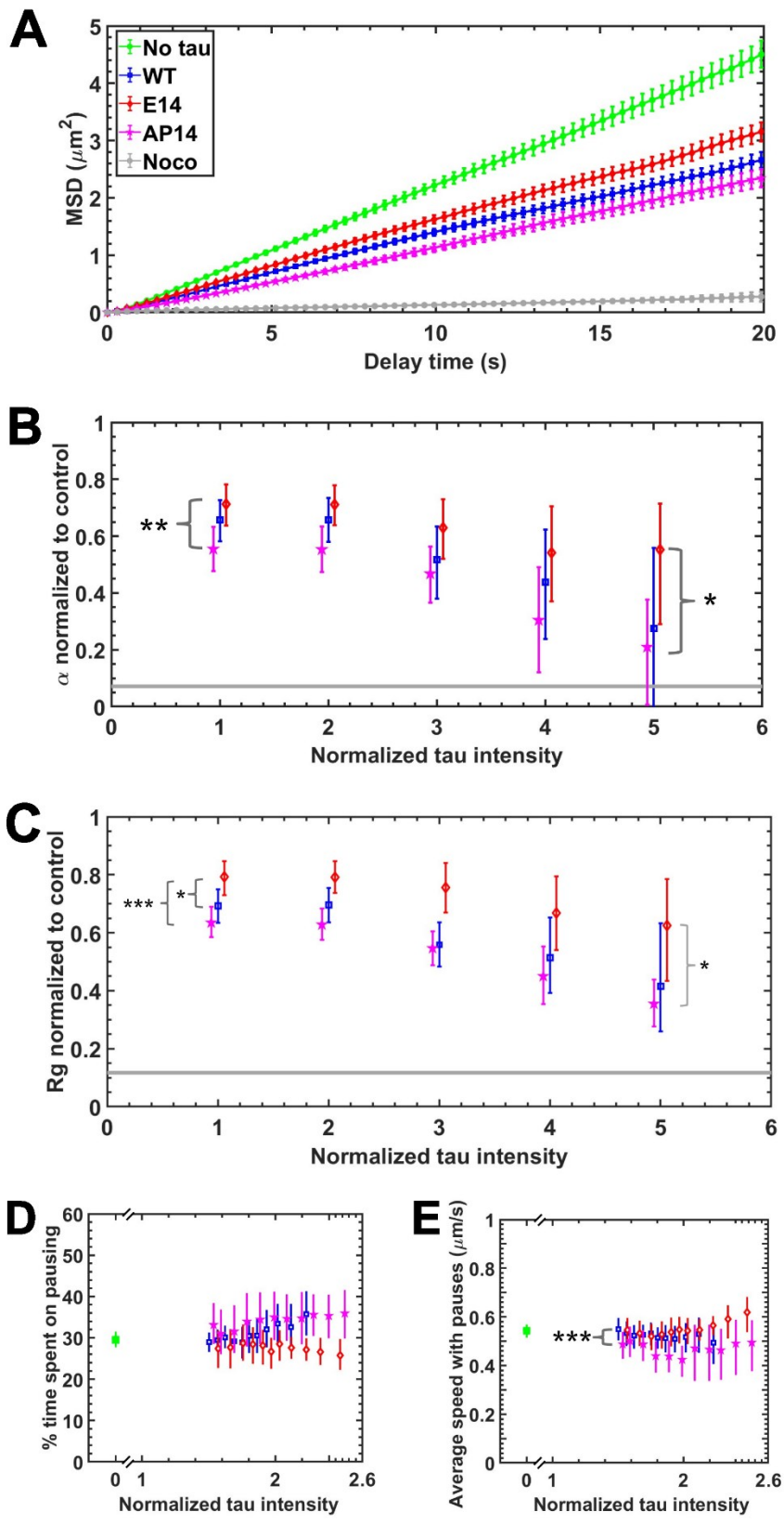

Figure 12: E14 tau weakly inhibits lysosome transport compared to AP14 tau. A. MSD plot of lysosomes under different tau types (WT, E14, and AP14 tau) and with 10 µM Nocodazole as a baseline (mean ± SEM). The three tau types inhibit lysosome transport compared to no tau condition. B. Comparison of tau types by plotting the MSD (α) slope against normalized tau intensity. AP14 tau shows stronger inhibition of lysosome motility than E14 tau across all tau ranges (p-value < 0.001 for normalized tau intensity ranges 1-3 and 3-5, between no tau and all tau types: WT, E14, AP14). C. Rg (run length) plotted against normalized tau intensity, demonstrating that all the three tau types inhibit lysosome run length, with AP14 tau being more inhibitory than E14 tau (p-value < 0.001 for normalized tau intensity ranges 1-3 and 3-5, between no tau and all tau types: WT, E14, AP14). D. Sliding means of % pausing shows increased lysosome pausing in AP14 tau compared to no tau condition (normalized tau intensity = 0) and WT and E14 tau at higher tau intensity levels. E. Sliding means of average speed with pauses of moving lysosome trajectories (Rg ≥ 0.5 µm) reveal initial speed reduction in AP14 tau. All three tau conditions exhibit speed reduction at higher tau levels, with AP14 tau showing more reduction than E14 tau, except for WT tau compared with no tau condition (normalized tau intensity = 0). Overall, the plots suggest that E14 tau weakly inhibits lysosome transport compared to AP14 tau. (Control: 45 cells; WT tau: 93 cells; E14 tau: 79 cells; AP14 tau: 75 cells; Nocodazole treated: 17 cells). (* $p < 0.05$, ** $p < 0.01$, *** $p < 0.001$, bootstrapping-derived p-value)

We also analyzed the speed without pausing, which refers to the average speed of cargo movement over a trajectory by considering only the time spent in motion and excluding pauses

(Fig. 11D), and the pausing percentage of the lysosomes (Fig. 11E) in the presence of tau. We consider both the motile and paused segments to calculate the speed with pausing. The average speed of lysosomes showed no variation initially except with AP14 tau ($p < 0.001$), which reduced the speed considerably. There is also a decrease in speed in the AP14 condition compared to WT and E14 tau ($p = 0.01$ for WT and $p < 0.001$ for E14) condition. This was supported by the increased percentage of pausing by the lysosome in the presence of AP14 tau. However, the percentage of pausing increases along with a reduction in the speed of the lysosomes with increasing tau expression levels of all tau types except for WT tau ($p = 0.01$ for E14 and $p < 0.001$ for AP14) and between the tau types as well ($p = 0.021$ for WT and E14, $p = 0.002$ for WT and AP14, $p = 0.033$ for E14 and AP14).

These results and MSD and Rg show that AP14 tau inhibits the lysosome motility strongly, whereas E14 tau weakly inhibits the lysosome motility. Because of the inability of the E14 tau to bind to the microtubule due to its high negativity because of glutamate groups (which mimic phosphorylation), it reduces the competition with the motor proteins for binding. It thereby helps in maintaining the cargo transport rather than inhibiting it.

3.2.4. Tau alters the localization and directionality of the lysosomes, with E14 tau weakly influencing the lysosome movement than AP14 tau:

Based on measuring the distance travelled by the lysosomes from the cell center and the radius of gyration of the lysosome motility, we classified the directionality into three types: inward, outward, and stationary motility (Fig. 12A). Since most kinesins drive the cargo towards the cell periphery and dyneins drive the cargo towards the MTOC, tau affects kinesins (kinesin-1 and kinesin-3) significantly compared to dyneins depending on their phosphorylation status. The presence of tau increased stationary cargoes and reduced both outward and inward-moving

lysosome cargoes compared to no tau condition (Bootstrapping-derived p-value is < 0.001 for WT and AP14 tau compared to no tau condition for outward, inward and stationary motility; and p = 0.012, < 0.001 and 0.021 for E14 compared to no tau condition for outward, inward and stationary motility). E14 tau weakly inhibited outward-based lysosomes compared to WT tau (p = 0.042). AP14 tau significantly increased stationary cargoes (p = 0.005) and inhibited outward-based motile lysosomes (p = 0.008) compared to E14 tau due to AP14 tau's ability to bind tightly with microtubules and act as a barrier for motor proteins.

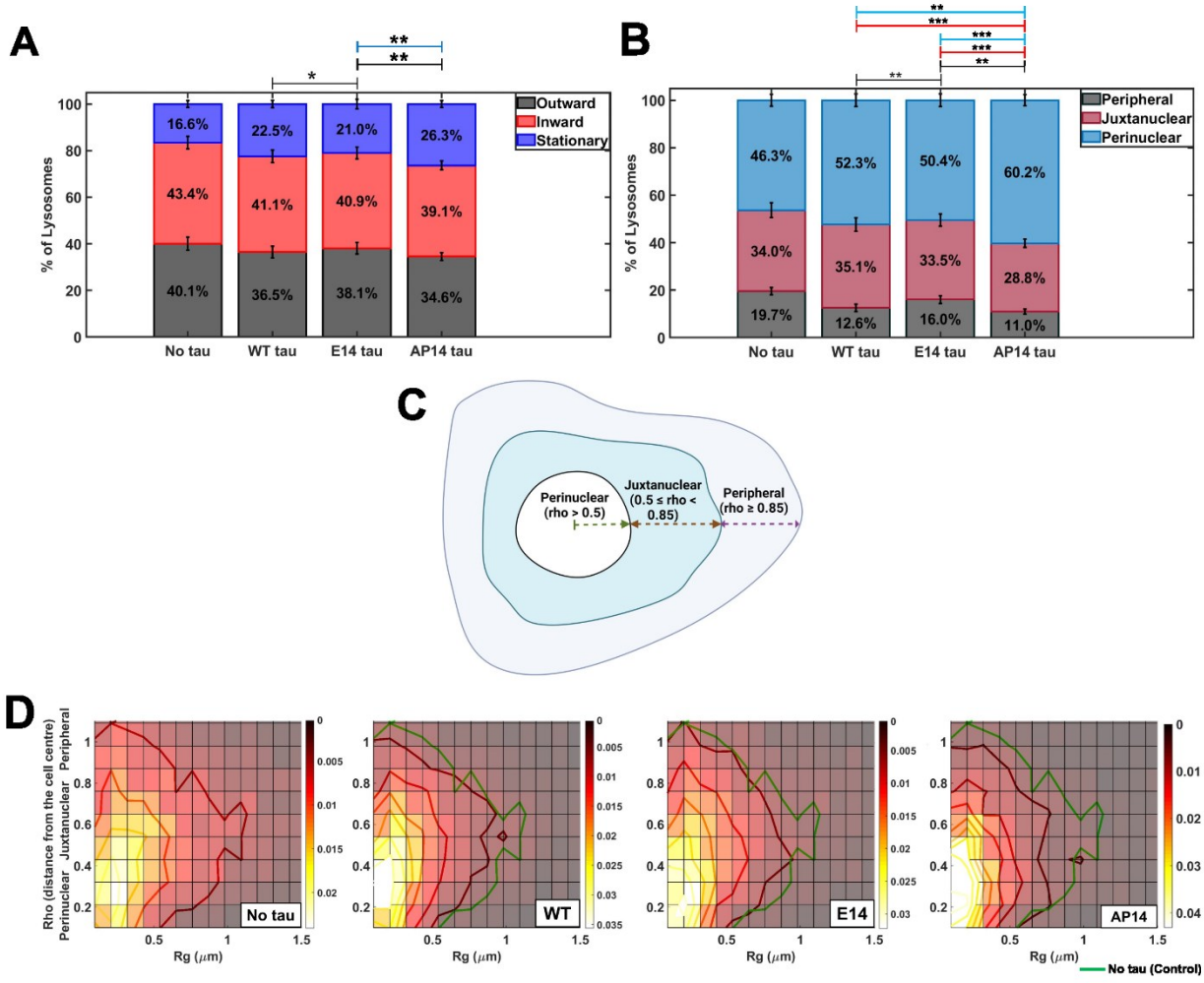

Figure 12: **E14 tau weakly influences lysosome localization and directionality compared to AP14 tau. A.** Bar plot (mean ± SEM) showing lysosome distribution under different tau types: outward (grey), inward (red), and stationary (blue). Introducing different tau types increases stationary cargoes and decreases outward and inward cargoes. **B.** Bar plot (mean ± SEM) illustrating lysosome directionality: peripheral (grey), juxtanuclear (red), and perinuclear (blue). AP14 tau has a stronger effect on outward and stationary cargoes than E14 tau, leading to increased perinuclear and reduced peripheral cargoes. **C.** Schematic diagram of the lysosome localization based on Rho. Rho can be described as the average distance of every trajectory from the center of the

cell, which is then adjusted relative to the cell's average radius. So, the cell region is classified as perinuclear (rho < 0.5), juxtanuclear (0.5 ≤ rho < 0.85), and peripheral (rho ≥ 0.85). **D.** Heatmap plot displaying the lysosome distribution (Rho – distance from the cell center) and Rg (run-length). All the three tau types reduce lysosome run length, with AP14 tau concentrating lysosomes in the perinuclear region and fewer in juxtanuclear and peripheral areas than E14 tau. (Control: 45 cells; WT tau: 93 cells; E14 tau: 79 cells; AP14 tau: 75 cells). (* $p < 0.05$, ** $p < 0.01$, *** $p < 0.001$, bootstrapping-derived p-value)

Lysosome localization dynamics (Fig. 12B & Fig. 12C) were analyzed across sub-cellular regions: perinuclear, juxtanuclear, and peripheral. All three tau types notably reduced peripheral and increased perinuclear lysosomes, aligning with tau inhibiting the outward-based cargoes primarily driven by kinesins (p-value is < 0.001 for WT, E14 and AP14 tau compared to no tau condition for peripheral, and perinuclear localization). AP14 tau alone had reduced juxtanuclear cargoes ($p < 0.001$). These results were expected as more outward-based cargoes were inhibited as kinesins primarily drove them, directing them toward the perinuclear space.

Previous studies indicated kinesin-1 and kinesin-3 transport along acetylated and tyrosinated microtubules, respectively, with tau affecting these motors depending on phosphorylation status, which explains the observed effects (Balabanian et al., 2017; Lipka et al., 2016; McVicker et al., 2014a; Verhey & Hammond, 2009). AP14 tau had a more prominent effect, diverting cargoes from peripheral and juxtanuclear space, resulting in increased perinuclear localization compared to E14 tau ($p = 0.002$, 0.001 and < 0.001 for peripheral, juxtanuclear, and perinuclear localization compared between E14 and AP14). E14 tau showed increased peripheral than WT tau ($p = 0.004$). AP14 tau showed greater perinuclear and reduced juxtanuclear localization of lysosomes than WT tau ($p < 0.001$ and 0.003 for juxtanuclear and perinuclear localization compared between WT and AP14 tau). Heatmap plots (Fig. 12D) further confirmed alterations in lysosome distribution due to tau presence, with AP14 tau leading to more concentrated perinuclear lysosomes than E14 tau. Overall, AP14 tau exerted more potent inhibition on

kinesin-driven lysosomes, resulting in increased perinuclear localization compared to the weak inhibition of E14 tau.

3.2.5. Phosphomimetic and phosphoresistive tau inhibit the motility of early endosomes:

In this study, we investigated the impact of hyperphosphomimetic E14 tau on early endosome motility, which is driven by kinesin-1, kinesin-2, kinesin-3, and dynein. Using TIRF to image the early endosomes labelled by Qdot 565-EGF in COS-7 cells, we obtained the raw data on early endosome motility (Zajac et al., 2013). Trajectories were extracted using Trackmate and further analyzed in MATLAB for MSD, Rg, and velocity analysis.

Like lysosomes, early endosome processivity decreased with increasing tau intensity for AP14 tau, as evident from the MSD and α plot (Fig. 13A & Fig. 13B; Bootstrapping-derived p-value is 0.027 and 0.001 for AP14 tau normalized tau intensity 1-3 and intensity 3-5 respectively compared to no tau condition). This result also agreed with Rg analysis (Fig. 13C; $p < 0.001$ and $p = 0.021$ for AP14 for normalized tau intensity 1-3 and intensity 3-5 respectively compared to no tau condition). In contrast, E14 and WT tau did not affect processivity drastically compared to the no-tau condition ($p = 0.098$ for WT tau and $p = 0.303$ for E14 tau for normalized tau intensity 1-3 and $p = 0.296$ for WT tau and $p = 0.114$ for E14 tau for intensity 3-5). However, WT tau and E14 tau influenced Rg by decreasing it, suggesting that early endosome processivity was not affected but their displacement was cut short in the presence of WT tau and E14 tau compared to no tau condition ($p = 0.006$ for WT tau and 0.012 for E14 tau for normalized tau intensity 1-3 and $p = 0.005$ for WT tau and $p < 0.001$ for E14 tau for intensity 3-5). The results for 4RS WT tau in our study agree with those for 3RS WT tau in the previous study, where the trends for α and Rg are similar (Balabanian et al., 2022).

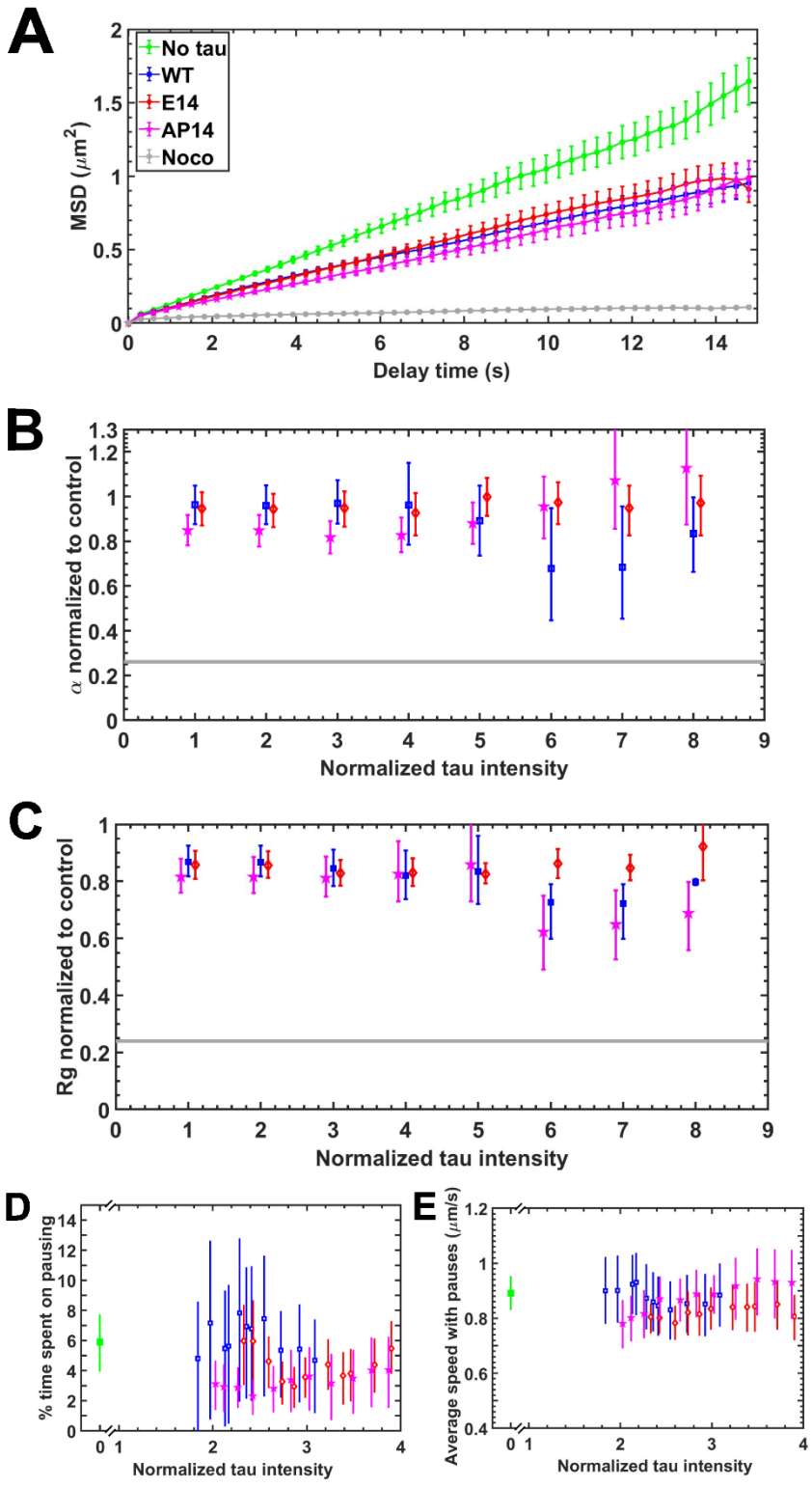

Figure 13: AP14 and E14 tau s inhibits the motility of early endosomes. A. MSD plot of lysosomes under different tau types – WT, E14 and AP14 tau was plotted along with 10 µM Nocodazole, which abolishes the early endosome transport, was used as a baseline measurement for comparison (mean ± SEM). AP14 tau inhibit early endosome transport but E14 and WT tau does not (p-value is 0.027 and 0.001 for AP14 tau normalized tau intensity 1-3 and intensity 3-5 respectively compared to no tau condition). **B.** For a clearer comparison between tau types, the slope of MSD, α, was plotted against normalized tau intensity (considering only the delay time of 6 seconds from the MSD analysis). This plot showed that AP14 inhibited early endosome motility strongly with WT and E14 showing weak inhibition. **C.** Rg plot showed that all three tau types inhibit the run length, with AP14 tau being more inhibitory than E14 tau at lower tau intensity levels (p-value: AP14 ($p < 0.001$, $p = 0.021$) and WT ($p = 0.006$) vs. E14 tau ($p = 0.012$) for intensity 1-3, and for AP14 ($p = 0.006$) and WT ($p = 0.005$) vs. E14 tau ($p < 0.001$) for intensity 3-5 compared to the no tau condition.). **D &E.** Sliding means of % pausing and sliding means of average speed without pauses of moving early endosome trajectories (Rg ≥ 0.5 µm) show no effect in the presence of any tau types except at the low expression level of E14 tau. Overall, all the plots suggest that E14 tau weakly inhibits the early endosome transport compared to AP14 tau. (Control: 45 cells; WT tau: 52 cells; E14 tau: 58 cells; AP14 tau: 51 cells; Nocodazole treated: 14 cells). (* $p < 0.05$, ** $p < 0.01$, *** $p < 0.001$, bootstrapping-derived p-value)

When comparing the tau types, we found that AP14 tau significantly inhibited the run length of early endosomes compared to E14 and WT tau at lower tau levels ($p = 0.01$ for WT and AP14 and $p = 0.016$ for E14 and AP14 tau for tau intensity 1 - 3). However, there was no significant difference at high tau levels ($p = 0.286$ for E14 and AP14, and $p = 0.457$ for WT and AP14 for intensity 3 – 5). This suggests that AP14 tau could compete strongly with early endosomes for binding to microtubules and might disrupt the efficient movement of early endosomes along microtubules, resulting in reduced processivity and shorter run lengths.

We also examined speed with pausing (Fig. 13D) and pausing percentage of early endosomes (Fig. 13E) in the presence of tau. WT and AP14 tau did not affect average speed and pausing percentages with increasing intensity. E14 tau initially decreased average speed with pausing ($p = 0.036$), accompanied by a higher pausing percentage, but showed no further impact later at high tau levels ($p = 0.6$). These findings indicate that early endosomes navigate by briefly pausing and continuing their travel, suggesting they stay attached to microtubules, but their motility is affected in the presence of the three tau types.

In summary, AP14 tau strongly impacts early endosome processivity and run length. We suggest that AP14 inhibits by competing with the early endosomes for microtubule binding at lower tau levels, reducing their processivity and displacement compared to E14 tau. In contrast, E14 tau has a more subtle effect, influencing the displacement of the early endosomes without significantly altering the rate of movement. This shows that early endosome is more sensitive in its motility in the presence of WT, AP14 and E14 tau. This supports the results from the previous study on 3RS WT tau and Y18E tau as the trends for processivity and displacement were similar (Balabanian et al., 2022).

3.2.6. AP14 tau more strongly alters the directionality and localization of early endosomes than E14 tau:

We analyzed the directionality of the early endosomes (Fig. 14A). As expected, due to the nature of early endosomes, all three tau forms increased the level of stationary early endosomes, with AP14 tau showing the most significant effect (Bootstrapping-derived p-value is 0.003, 0.003 and < 0.001 for WT, E14 and AP14 respectively compared to no tau condition). Additionally, the presence of tau reduced outward-moving early endosomes (p-value = 0.017, 0.039 and < 0.001 for WT, E14 and AP14, respectively, compared to no tau condition). AP14 tau alone exhibited a prominent decrease in both the outward-moving and inward-moving early endosomes (p = 0.004 for inward). When comparing with other tau types, it was found that E14 tau and WT tau have more outward-moving cargoes and fewer stationary cargoes than AP14 tau condition (p = 0.012 and 0.005 for WT compared to AP14 for outward and stationary cargoes and p = 0.003 and 0.002 for E14 compared to AP14 for outward and stationary cargoes).

Localization dynamics of early endosomes (Fig. 14B and 14C) showed prominent reductions in juxtanuclear cargo levels with all three tau forms (p-value = 0.001, 0.005 and 0.001 for WT, E14 and AP14, respectively, compared to no tau condition). WT and E14 tau showed increased peripheral cargoes (p-value = 0.023 and 0.039 for WT and E14, respectively, compared to no tau condition). AP14 showed a prominent increase in perinuclear cargoes (p = 0.008). There was also a prominent increase in perinuclear early endosomes in the AP14 tau condition compared to WT and E14 (p-value = 0.001 and 0.043 comparing WT and AP14 and p = 0.043 and 0.026 for comparing E14 and AP14 for peripheral and perinuclear localization). Heatmap plots (Fig. 14D) further confirmed altered distributions of early endosomes with tau. WT and E14 tau exhibited more peripheral and fewer perinuclear early endosomes than AP14 tau.

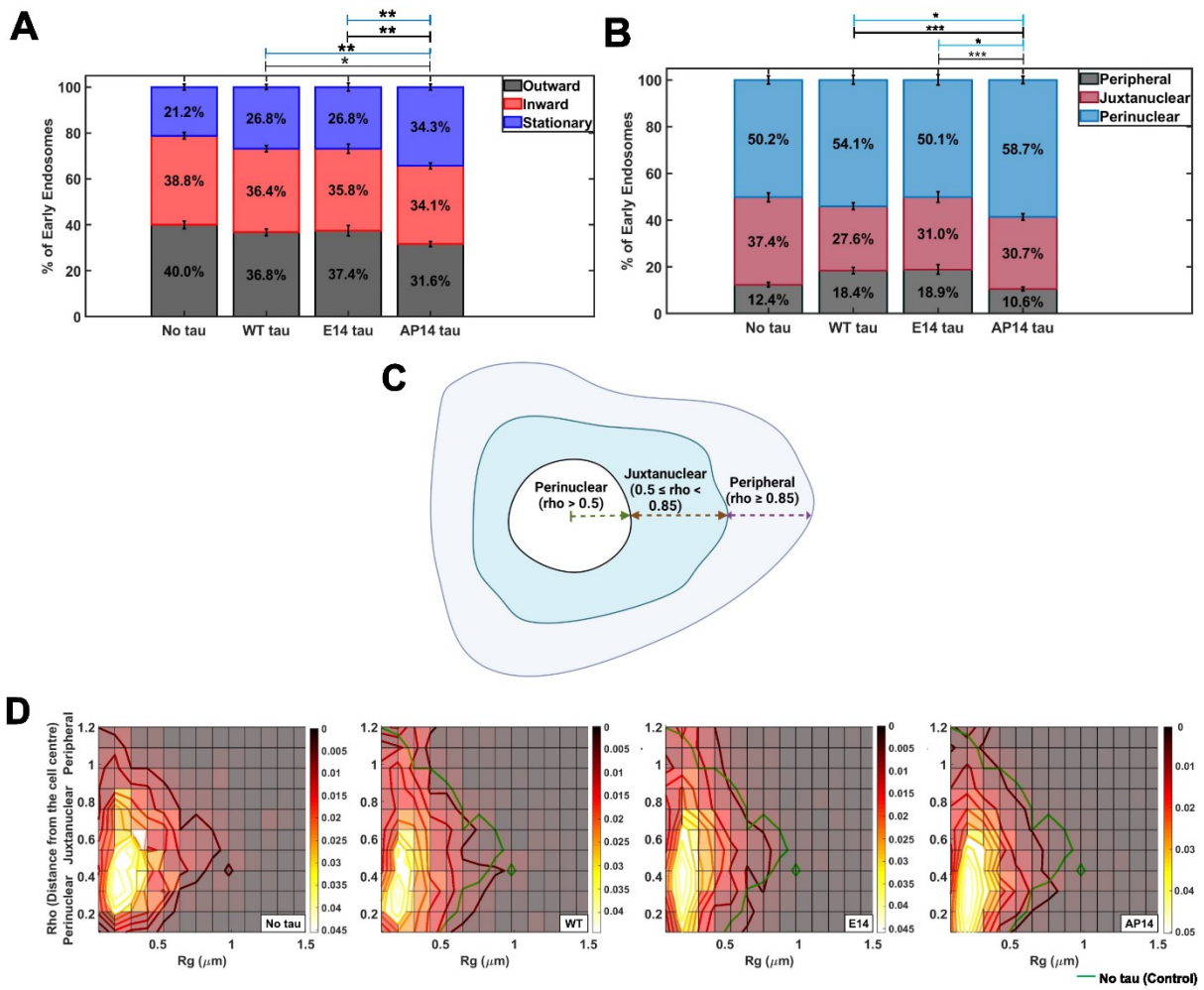

Figure 14: AP14 tau alters the directionality and localization of early endosomes more strongly compared to E14 tau. A. Bar plot (mean ± SEM) illustrating the distribution of early endosomes under different tau types: outward (grey), inward (red), and stationary (blue). The introduction of different tau types increased stationary cargoes (0.003, 0.003 and < 0.001 for WT, E14 and AP14) and decreased outward cargo endosomes (p-value = 0.017, 0.039 and < 0.001 for WT, E14 and AP14, respectively, compared to no tau condition). Additionally, inward-moving cargoes were affected in the AP14 tau condition (p = 0.004). **B.** Bar plot (mean ± SEM) shows the directionality of early endosomes: peripheral (grey), juxtanuclear (red), and perinuclear (blue). All three tau types affect perinuclear cargoes (p-value = 0.001, 0.005 and 0.001 for WT, E14 and AP14). AP14 tau had a more substantial effect, leading to more perinuclear early endosomes than E14 tau (p = 0.008). E14 and WT tau conditions showed more peripheral early endosomes than no-tau (p-value = 0.023 and 0.039 for WT and E14) and AP14 tau conditions (p-value = 0.001 and 0.043 comparing WT and AP14 and p = 0.043 and 0.026 for comparing E14 and AP14 for peripheral and perinuclear localization). **C.** Schematic diagram of the early endosome localization based on Rho. Rho can be described as the average distance of every trajectory from the center of the cell, which is then adjusted relative to the cell's average radius. So, the cell region is classified as perinuclear (rho < 0.5), juxtanuclear (0.5 ≤ rho < 0.85), and peripheral (rho ≥ 0.85). **D.** Heatmap plot displaying the early endosome distribution (Rho – distance from the cell center) and Rg (run-length). All three tau types reduced the run length, with AP14 tau concentrating early endosomes in the perinuclear region more than E14 tau, consistent with the observations in lysosome cargoes. (Control: 45 cells; WT tau: 52 cells; E14 tau: 58 cells; AP14 tau: 51 cells). (* p < 0.05, ** p <0.01, *** p < 0.001, bootstrapping-derived p-value).

In summary, the tight interaction of AP14 tau with microtubules and its ability to influence the microtubule lattice properties can act as a motor barrier, leading to a more pronounced effect

on early endosomes than E14 and WT tau. The reason why early endosomes are more sensitive to tau compared to lysosomes is due to fewer motor subsets driving the early endosomes. So AP14 tau had a more pronounced inhibitory effect. Also, our results on early endosome motility, localization, and directionality analysis showed that the early endosomes were more sensitive to E14 tau than the lysosomes, corresponding to the results based on monophosphomimetic Y18E tau in the previous study (Balabanian et al., 2022). The effects of E14 were weaker but still showed inhibitory effects on the early endosomes. This inhibitory result is interesting as it suggests that the phosphorylation of tau may target early endosomes in the signalling pathway regardless of the number of phosphorylated sites that tau possesses.

Chapter 4

4. Discussion

Intracellular transport and regulation are critical to sustaining cellular signalling and endocytic pathways. Microtubule-associated proteins, such as tau, play a pivotal role in this regulation by differentially regulating organelles and modulating microtubule properties (Balabanian et al., 2018; Gendron, 2009). However, the impact of tau phosphorylation and hyperphosphorylation on microtubule organization and cargo transport remains limited. Our study aimed to elucidate how aberrant tau phosphorylation disrupts microtubule binding, bundling, and cargo transport to understand the defective organelle transport observed in neurodegenerative diseases such as Alzheimer's disease. For our experiments, we chose low tau expression levels as they are comparable to neuronal tau levels. Our findings reveal that phosphomimetic E14 tau is predominantly cytosolic and weakly inhibits lysosomes, unlike phosphoresistive AP14, which inhibits cargo strongly. Phosphorylation relieves the inhibition of lysosome transport by tau, suggesting phosphorylation could be a protective response to sustain cargo transport rather than disrupt it. We also found that the early endosomes were sensitive to E14 tau compared to lysosomes, suggesting that phosphorylated tau could specifically target the early endocytic and signalling pathway.

Before we build upon our investigation into how tau hyperphosphorylation affects microtubule organization and cargo transport, we recognized the significance of tau expression levels in cells and choosing the appropriate expression level for our analysis. Tau expression levels have distinct effects on cellular functions, and understanding these effects is crucial for studying its role in physiology. Physiological levels of tau in neurons help maintain normal microtubule dynamics, ensuring proper cargo transportation within the cell. Moderate increases in tau

expression can lead to enhanced microtubule stabilization, which may influence cargo transport as found in neurons. However, when tau expression levels become excessively high, it can result in severe cytoskeletal distortions and the formation of abnormal microtubule bundles not typically observed under normal conditions. These extreme alterations can significantly impair organelle motility and disrupt the normal balance of cellular functions (Balabanian et al., 2022; Montejo de Garcini et al., 1994). Therefore, studying tau at levels comparable to those found in neurons is essential for considering its physiological impact (Balabanian et al., 2022).

4.1. Impact of E14 tau on microtubule binding and stability

We employed live-cell imaging and spatiotemporal analysis of lysosomes and early endosomes to examine their response to WT, E14 and AP14 tau. Our results show clear differences in all three tau types affecting motor proteins due to their ability to interact with the microtubules. We expected tau hyperphosphorylation to decrease microtubule binding due to increased negative charge from added phosphate groups (we used phosphomimetic constructs where glutamate groups mimic phosphate groups). Thus, we hypothesized that E14 tau, being highly negatively charged, would exhibit reduced microtubule interaction and greater diffusive characteristics (Rodríguez-Martín et al., 2013; Stern et al., 2017). Indeed, our observations supported this hypothesis, as E14 tau showed a cytosolic distribution and limited microtubule binding compared to AP14 tau, which firmly bound to microtubules at physiological expression levels. This result suggests that E14 tau might impair microtubule elongation and stabilization, but other MAPs, such as MAP6, could still help to support microtubule stability (Baas & Qiang, 2019; Qiang et al., 2018). Tau phosphorylation could also affect envelope formation and stability (Siahaan et al., 2019).

Previous research considered the role of tau in influencing microtubule lattice compaction through cooperative binding and locally enriching to form concentrated tau envelopes (Siahaan et al., 2019, 2022). This compaction changes the mechanical properties of the microtubules and, thereby, enhances the affinity of additional tau molecules within the envelope. Lattice compaction also affects the binding of kinesin motors and depolymerases like spastin to the microtubules (Siahaan et al., 2019) (Siahaan et al., 2022; Verhey & Ohi, 2023). It was also found that phosphorylated tau can result in slower formation of tau envelopes and destabilization of existing envelopes (Karhanová & Lánský, 2023). The inability of E14 tau to bind to microtubules could impact its capacity to bundle microtubules and form envelopes, which may enhance the binding of kinesins to the microtubule due to less competition of tau. Motor proteins such as kinesin-1 can transiently modify and expand the GDP-tubulin lattice to be more like the GTP-tubulin lattice to promote its binding and walking. This structural change can also induce damage to the lattice and may lead to microtubule fragmentation. Hyperphosphorylated tau might fail to recognize the GDP-tubulin lattice, thereby affecting the regulation of severing enzymes and motor proteins and disrupting microtubules (Castle et al., 2020). Hence, cytosolic tau may affect the microtubule stability directly by failing to make envelopes and indirectly by letting enzymes destabilize the microtubules. Furthermore, cytosolic tau could contribute to aggregate formation, directly interfering with transport (Avila et al., 2012; Hoover et al., 2010; Rodríguez-Martín et al., 2013; Stern et al., 2017). However, the current study focused on the hyperphosphorylated tau and not on tau tangles. We then focused on tau hyperphosphorylation on organelle transport.

4.2. Impact of tau hyperphosphorylation on cargo transport

Our laboratory previously showed that tau phosphorylation at Y18 relieves the inhibition of kinesin-1, improving cargo processivity and run-length of lysosomes. However, it was also

found that the tau phosphorylation differentially regulates cargoes such as peripheral lysosomes and early endosomes by selectively inhibiting kinesin-3, which drives them. But this was the case for monophosphomimetic Y18E tau, which models tau phosphorylation in healthy cells (Balabanian et al., 2022; Chaudhary et al., 2018; McVicker et al., 2011; Stern et al., 2017).

When tau is hyperphosphorylated, we hypothesized that it could disrupt the cargo transport strongly due to the changes in the microtubule properties and loss of affinity to the microtubule lattice, in contrast to Y18E tau. We examined the effect of phosphomimetic E14, phosphoresistive AP14, and wild-type WT tau on lysosome and early endosome motility. We found that all three tau types impacted the cargo transport processivity and localization compared to no-tau conditions. AP14 tau exhibited the most potent inhibitory effect, affecting cargo outward and inward movements and promoting stronger perinuclear localization. E14 tau, on the other hand, had a milder effect on the transport, suggesting that its reduced microtubule binding might have an initially protective role, sustaining cargo transport rather than impeding it completely, as initially hypothesized. We also found that E14 tau targets the early endosomes like Y18E and it shows that tau phosphorylation targets the signalling pathway of the cells, regardless of the number of phosphorylated sites.

The alignment of our findings with studies on different phosphomimetic tau forms reinforces the significance of phosphorylation in modulating tau interaction with microtubules and its implications for intracellular transport dynamics.

4.3. Considerations from previous studies on tau hyperphosphorylation

Findings from the research on phosphomimetic E18 and E27 tau (with 18 and 27 phosphomimetic sites) in Chinese hamster ovary (CHO) cells align with our results

(Rodríguez-Martín et al., 2013; Stern et al., 2017). There was a significant reduction in microtubule binding properties 24 hours after E18 and E27 tau transfection in cells, even at high tau concentrations. In contrast, WT tau and AP18 tau (with 18 phosphoresistive sites) exhibited strong microtubule binding, leading to bundling, even at low tau concentrations. This was the same as in our case with AP14 and E14 tau, wherein AP14 tau showed prominent microtubule binding and bundling compared to E14 tau at physiological tau levels. In the same study, CHO cells transfected with E18 and E27 tau exhibited increased motile phosphomimetic tau particles in axonal transport compared to WT tau. However, the velocity, number, and duration of pauses remained consistent between these forms of tau, which shows that the effect of tau hyperphosphorylation had a weak or less impact on tau transport.

Boumil et al. (2020) explored E18 tau's phosphomimetic variant in neurons. This study demonstrated that cells expressing E18 tau exhibited elongated neurites compared to controls, potentially due to reduced neurofilament levels, which hinder neurite stabilization. In line with this, our study observed that E14 tau did not significantly impact cell morphology, unlike AP14 and WT tau, which led to reduced cell size through microtubule bundling. Boumil et al. (2020) also indicated that WT and AP18 tau overexpression increased acetylated microtubules, suggesting their role in microtubule stabilization. Additionally, E18 tau showed less impact on anterograde axonal transport, promoting continued neurite elongation. In our study, E14 tau had a milder effect on anterograde outward motility than AP14 and WT tau, indicating that hyperphosphorylated tau's influence on cargo transport can transcend its lower microtubule stabilization. These studies demonstrated reduced microtubule binding and bundling for hyperphosphorylated tau, highlighting the significance of phosphorylation in regulating tau's association with microtubules. Furthermore, our study's impact on neurite outgrowth and axonal transport dynamics echoes previous work involving E18 tau (Boumil et al., 2020). it

can be noted that WT and AP14 could increase the acetylation of the microtubules based on the experiments done on AP18 and WT tau in another study (Boumil et al., 2020). While our study on tau hyperphosphorylation provides valuable insights into the disease pathogenesis, limitations should be acknowledged.

4.4. Limitations and final summary

Although our COS-7 cell model offers insights, validating results in neuronal systems is essential. The complexity of tau phosphorylation necessitates further exploration to determine which phosphorylation sites significantly influence the regulatory properties of tau. Additionally, while our E14 tau model captures disease-relevant phosphorylation sites, other phosphorylation events may impact tau's behaviour. Since we also know that Alzheimer's disease is a mixed tauopathic disease (initially 4R-tau predominant followed by 3R-tau predominant), it is hard to replicate the exact disease condition in our cell model study. However, it would be interesting to elucidate how hyperphosphorylation in different isoforms could affect the microtubule properties and cargo transport in neurons. Future investigations in neurons can enhance our understanding of tau-mediated cargo transport regulation. Thus, our research can be considered a preliminary insight into the vast field of tauopathic disease progression.

One question arises: What happens when hyperphosphorylated tau is introduced into neurons? We anticipate results similar to those observed in COS-7 cells. However, interactions between endogenous tau in neurons and hyperphosphorylated tau may occur. It is possible that hyperphosphorylated tau may induce abnormal phosphorylation of wild-type tau through prion-like spreading (Kundel et al., 2018). This phenomenon can lead to the spread of pathological tau aggregates within neurons, contributing to the formation of neurofibrillary

tangles and affecting neuronal health (Strang et al., 2019). However, since we used phosphomimetic tau constructs to express the hyperphosphorylated tau mimics, we may not observe the tangle formation in neurons as we did not observe this in the COS-7 model cell line. But before proceeding with experimenting on neurons with endogenous tau, it would be easier to work with neurons that express no tau (Tau knocked-out neurons) to establish and confirm the results we obtained from COS-7 analysis. This approach allows us to establish a baseline and subsequently investigate and test the prion-spread hypothesis and other mechanisms using the phosphomimetic constructs.

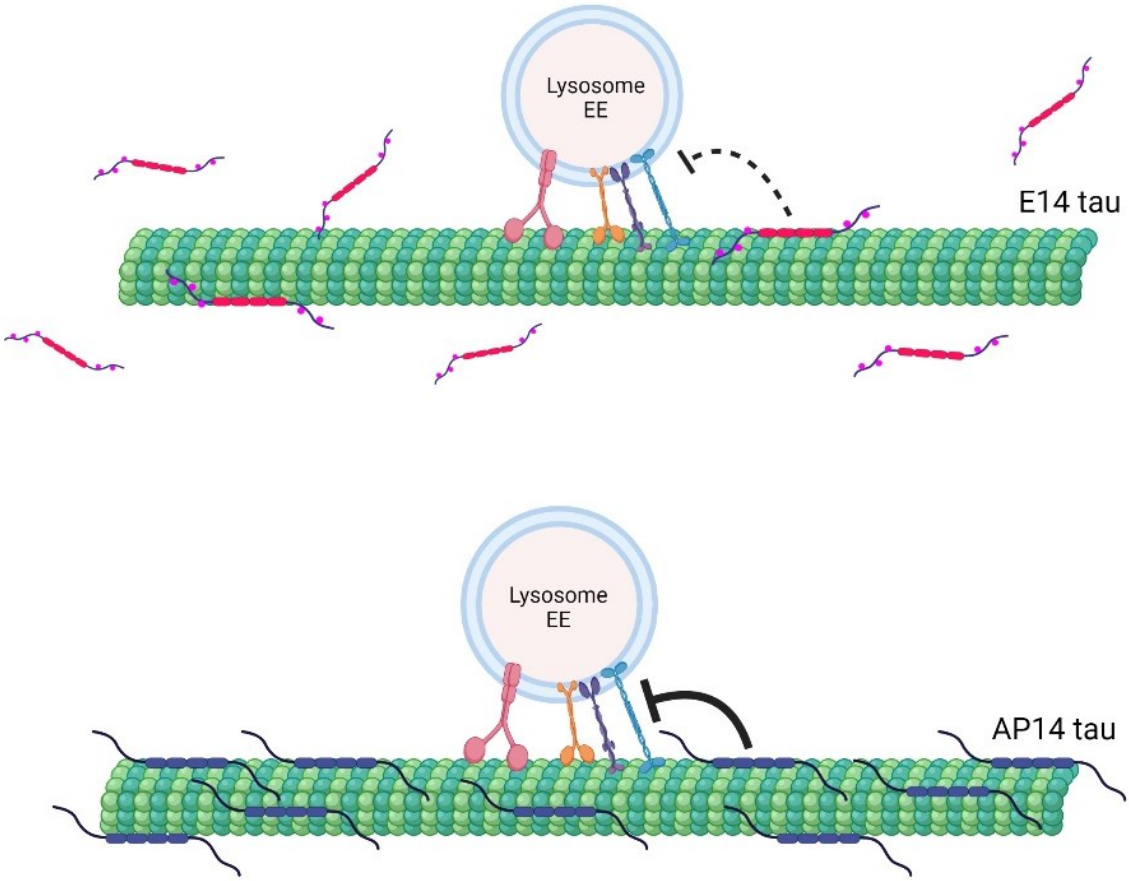

Figure 15: Summary of the effect of tau hyperphosphorylation on cargo transport. E14 tau mimics phosphorylation at 14 AD-relevant sites, and due to its high negative charge, it has a weak binding capacity toward microtubules. Thus, they are cytosolic, reducing the competition to bind to microtubules against the cargo-carrying motor proteins. This allows the cargo transport to be uninterrupted partly. On the other hand, AP14 is phosphoresistive and binds to microtubules readily, thereby directly resisting the motor proteins carrying cargo by competing for the microtubule sites. This shows that the hyperphosphorylated tau may not cause dysregulation in cargo transport, so they may not be as toxic as initially thought.

In summary, our findings contribute to understanding the differential effects of various tau forms on intracellular transport processes (Fig. 15). We showed that E14 tau exhibited a weaker binding to the microtubules, reduced bundling ability, and weaker inhibitory response on cargo transport than AP14 tau. This suggests that E14 tau may protect cargo movement without directly hindering motor proteins like AP14 and WT tau. These results provide insights into the complexity of hyperphosphorylated tau-mediated regulation and its implications for neurodegenerative diseases.

Chapter 5

5.1. Conclusion

In this study, we investigated the effects of phosphomimetic E14 tau, wild-type (WT) tau, and phosphoresistive AP14 tau on the organization of microtubules and their role in regulating organelle transport within cells. We found that these tau types influenced organelle transport in distinct ways, likely due to their varying interactions with microtubules Specifically, E14 tau, which mimics 14 phosphorylation sites linked to Alzheimer's disease, had unique properties (Hoover et al., 2010). Due to its highly negative charge, it did not bind strongly to the microtubules. As a result, it was ineffective in bundling microtubules together and weakly inhibits the movement of organelles compared to AP14 tau. Thus, our study highlights the intricate relationship between tau protein phosphorylation, the organization of microtubules, and their interactions with cargoes carried by the motor proteins.

Surprisingly, our findings challenged our initial expectations of hyperphosphorylated tau directly involved in defective organelle transport. Despite its hyperphosphorylated nature, E14 tau exhibited only modest inhibition on the transport of lysosomes and early endosomes. This nuanced response suggests an initial protective mechanism to sustain the flow of cargo transport.

As we reflect on our research, several compelling questions arise that merit further exploration in tau hyperphosphorylation research. For example, 1) How does hyperphosphorylated tau affect individual motor proteins carrying organelles? 2) Are there differential effects of hyperphosphorylation on different isoforms of tau (i.e., 3R hyperphosphorylated tau vs. 4R hyperphosphorylated tau)? 3) Due to its weak interaction, how does hyperphosphorylated tau

alter microtubule polymerization and depolymerization rates? 4) Do tau tangles found in the later stages of the disease destabilize the microtubules and affect organelle transport? 5) Does tau hyperphosphorylation affect other cellular processes that could indirectly impact axonal transport, leading to defective cargo transport? There are many more questions in this field that we hope to uncover soon, and this would help us provide suitable biomarkers and treatment strategies for mitigating the devastating impacts of Alzheimer's disease.

For our future work on E14 tau, we can further build our knowledge of hyperphosphorylated tau by understanding the mechanism of tau hyperphosphorylation and also experimenting with different phosphomimetic variants and their effects on individual motor proteins and iPSC-derived neurons.

5.2. Future work

The research presented in this thesis has shed light on the intricate relationship between tau hyperphosphorylation and its impact on microtubule organization and intracellular cargo transport dynamics. While our study has provided valuable insights, there remain several avenues for future research that can further advance our understanding of tau-related pathologies and their role in cellular activities. We outline these potential research directions and the proposed experiments below:

5.2.1. Investigating the Impact of Tau Phosphomimetic Variants

Our study has focused on a single phosphomimetic tau variant, i.e. E14 tau and it served as a simple yet valuable tool for simulating hyperphosphorylation-related changes in tau behaviour and its effect on cellular functions. Future investigations can expand upon this approach by exploring additional phosphomimetic tau variants that mimic specific phosphorylation patterns

associated with Alzheimer's disease. Though there are numerous combinations of hyperphosphorylated tau sites in Alzheimer's disease, we can gain a more comprehensive understanding of the relationship between tau phosphorylation states and disease progression through a systematic examination of specific variants, such as AT8, E18 and other phosphomimetic tau models.

5.2.2. Elucidating the Molecular Mechanisms of Tau Hyperphosphorylation

While we know that hyperphosphorylation of tau is a key event in the progression of Alzheimer's disease, the precise molecular mechanism of tau hyperphosphorylation still remains a topic of ongoing investigation. It is also unclear how and if hyperphosphorylation of tau directly leads to aggregation, which in turn leads to neuronal death. Future research can delve deeper into the mechanisms by which kinases, such as GSK-3β, phosphorylate tau at specific sites and their effect on cellular functions. It would also be interesting to understand how the dysfunction of phosphatases affects the balance between phosphorylation and dephosphorylation of tau.

It is also important to note that the molecular mechanisms underlying tauopathic diseases, such as Alzheimer's, are not solely linked to reduced tau binding and microtubule stability but they involve a huge variety of other cellular functions. Thus, tau's role is far more intricate than simply stabilizing axonal microtubules, and understanding its complex functions and structures is crucial for exploring its involvement in both normal neuronal function and disease states(Cario & Berger, 2023). Understanding the intricacies of tau phosphorylation and the factors that modulate it can provide critical insights into the early stages of tauopathic diseases. It is also important to study various other post-translational modifications (PTMs) such as

ubiquitination, acetylation, methylation, GlcNAcetylation, and potentially other molecular factors besides phosphorylation, which might contribute to the toxicity associated with tau and its aggregates (Wegmann et al., 2021). Exploring the kinase-substrate relationships, potential inhibitors, and the effects of altering PTM patterns on tau function should be pursued to gain clarity in our understanding of neurodegenerative diseases.

5.2.3. Optical trapping experiment on understanding the effect of E14 tau on different motor proteins in cargo transport

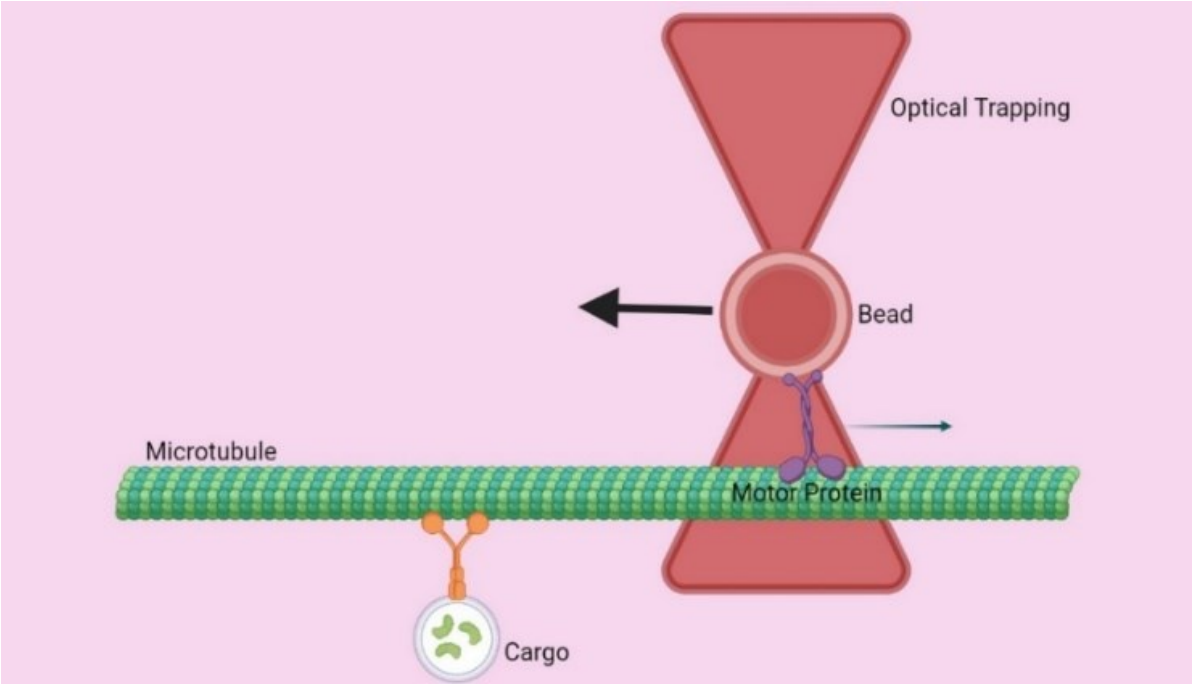

Figure 16: Optical Trapping experiment. Optical trapping experiment for measuring the force production by trapping a microsphere using a near-infrared optical trapping beam through a high numerical aperture microscope objective lens. The microsphere is covalently bound to a single motor that moves along the microtubule. The motor pulls the trapped microsphere with force and displaces the sphere, and these parameters are measured using an interferometer. [Image created using Biorender]

Employing single-molecule motility assays such as the Optical Trapping technique using nanodiamonds on live cells to measure the processivity of the motor proteins such as kinesin-1, kinesin-2, kinesin-3 and dynein in the presence of E14 tau will help us understand how the

hyperphosphorylated tau biases the different motors carrying the cargoes. The cells can be transfected with WT and E14 tau, along with nanodiamonds. The optical trapping system can be arranged after performing the necessary calibration to correct any oscillations and fluctuations in the cells due to the heterogeneous viscoelastic environment of the cells (Fig. 16). Nanodiamonds can be used as the probes as they possess desirable properties for live cell trapping experiments, such as small size, higher refractive index, and biocompatibility (Zhou et al., 2017).

This research will provide us with an understanding of how a robust transport occurs along the axonal microtubules when the microtubules are heavily decorated with tau and how the aberrant tau phosphorylation contributes to defective transport in AD, which could mark the early stage of the disease pathogenesis.

5.2.4. Experiments with iPSC-derived neurons

Tau is primarily found in the axons of neurons. It would be interesting to know the effect of phosphomimetic E14 tau on the motility of lysosomes and other cargo. Tau-knockout AIW2-2 iPSC cell lines can be used to perform similar experiments as done with COS-7 cell lines to discern the effects. Localization of tau in iPSC-derived neurons will be of interest, as tau, though primarily localized in axons, is altered in a disease condition. A previous study has shown that tau exhibited a motile punctate structure along the axons in transfected neurons (Rodríguez-Martín et al., 2013). It was shown to be redistributed to the somatodendritic sites, the primary sites for synaptic-based communication and a pathological marker of early tauopathic disease (Hoover et al., 2010) and so how the transport of organelles is affected here will provide us more information about the pathogenesis of early AD. (Noble et al., 2013)

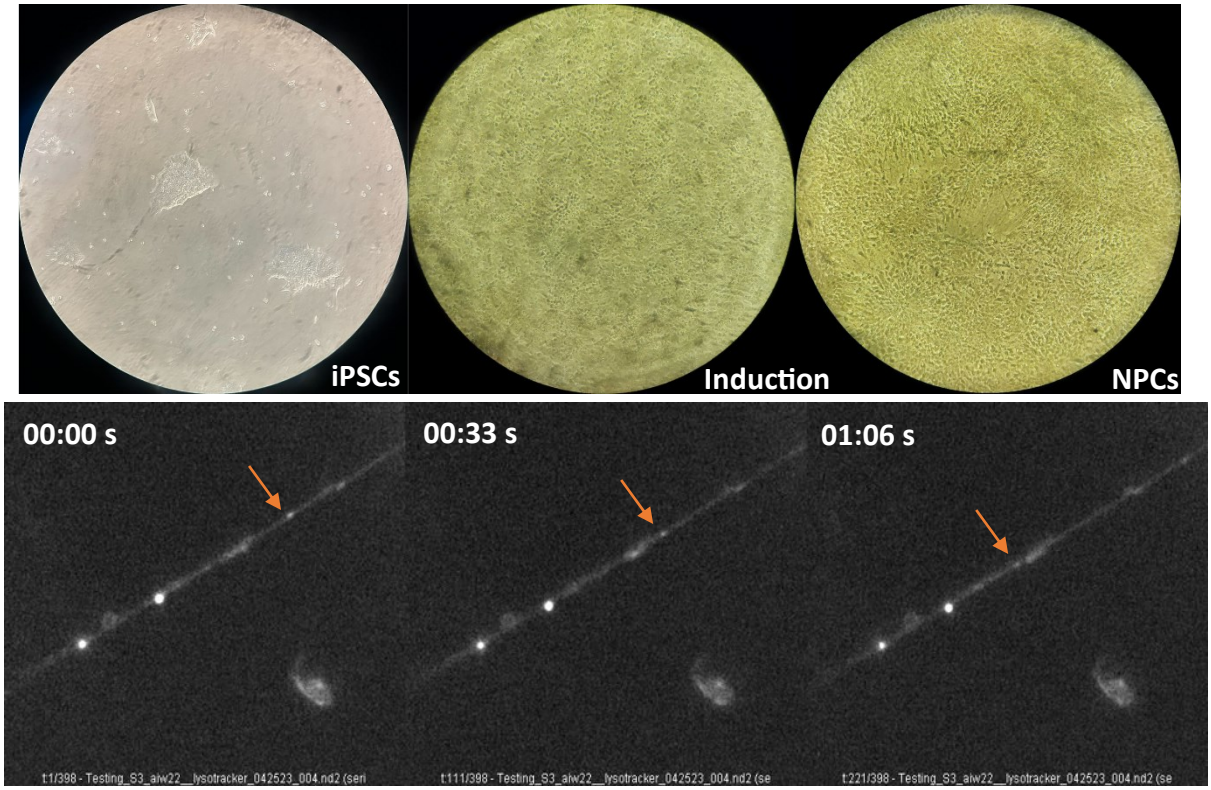

Figure 17: Culturing AIW2-2 iPSCs and inducing them to become neuronal progenitor cells (NPCs) and eventually into neurons. A. AIW2-2 iPSCs in the stem cell stage. After the first split, the iPSCs were maintained in induction media (induction stage). After multiple rounds of split and maintaining in induction media for about a month, neural progenitor cells (NPCs), which have small projections, were spotted. These were then cultured in specialized differentiation media to obtain the cortical neurons. (Magnification varies from 40x to 100x for each image) **B.** Time series image snapshots of axonal transport of lysosomes (using Lysotracker Deep Red) in neurons. Single lysosome motility was marked with an orange arrow.

In conclusion, using a phosphomimetic tau construct, our study provides a comprehensive analysis of the impact of hyperphosphorylated tau on microtubule interactions and cargo transport dynamics. By elucidating the effects of E14 tau, we unravel the intricate mechanisms underlying neurodegenerative diseases. This research lays the foundation for further exploration into the complex interactions within cells and their implications for pathological conditions like Alzheimer's disease. This concludes my thesis work.

In addition to my thesis work, I collaborated with my lab colleagues on two mini-projects, which I will discuss in the next chapter.

Chapter 6

6. Contributions to other projects

6.1. Tau Differentially Regulates the Transport of Early Endosomes and Lysosomes

This project aimed to perform specific experiments on WT tau and phosphomimetic Y18E tau and their effect on lysosomes for aiding a manuscript submission upon reviewers' feedback. The first part of the work involved using nocodazole-treated cells to observe and compare the effect of tau to the complete inhibition of microtubule dynamics in COS7 cell lines and quantify the mean-squared displacement and radius of gyration between the two conditions. Two different concentrations of Nocodazole were used to treat the cells: 1 uM and 10 uM, and the COS-7 cells were incubated with the Nocodazole for 15 minutes before being imaged with Lysotracker with the same parameters and settings used (check the methodology – lysosome imaging). At higher nocodazole concentration (10 uM), the lysosome motility was less processive (wobbling movement by lysosomes as noted qualitatively) and had reduced run length as it was known that nocodazole affects the microtubule stability, therefore destabilizes it, and thereby affect the motility.

The second part of the work involves observing the effect of WT and Y18E tau on lysosome motility at different Z-sectioning of the COS-7 cell lines. This was done to show that the effect of tau was throughout the cell and not limited to the plane of the TIRF image**.** Using Zeiss Elyra 7 structure illumination microscopy (SIM), Z-sectioning time-series experiments on COS-7 cells were performed. COS-7 cells were plated on FluoroDish Cell Culture Dish (World Precision Instruments) with 0.17 mm glass coverslip thickness. The cells were transfected with DNA plasmid a day before the imaging experiment. On the day of imaging, the cells were incubated with 50 nM Lysotracker Deep Red (Invitrogen) in complete DMEM media for 10

minutes and then washed with the Leibovitz's L-15 media with 10% (v/v) FBS (Gibco). Then the cells were imaged in Leibovitz's L-15 media at 37C using Zeiss Elyra 7 wide field-based super-resolution microscope with a PCO edge sCMOS camera. Alpha Plan-Apochromat 63× (NA - 1.46) oil objective was used to image the cells, which were imaged in Apotome mode. And fibre coupled solid-state lasers (561 nm – 50% of 75 mW) and diode-pumped solid-state lasers (642 nm – 50% of 75 mW) were used as the light source. A time series movie was recorded at 50 ms per frame with 15 Z- stacks at a range of 6 um with an interval between each stack is 0.403 um. Like TIRF experiments, the cells were imaged within 1 hour following the lysotracker staining.

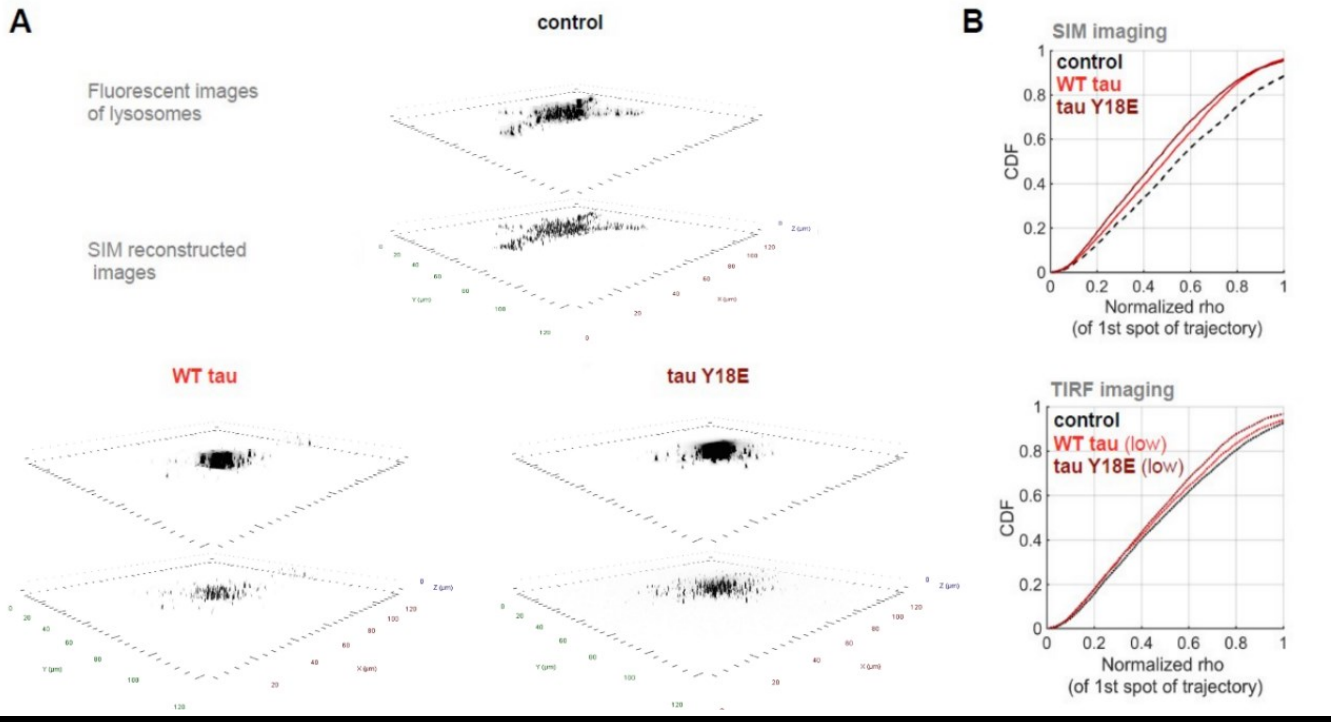

Figure 18: 3D Structured Illumination Microscopy (SIM) image of lysosome cargoes in COS-7. A. 3D SIM reconstructed images show the localization of lysosomes throughout the entire cell volume for control, WT tau transfected cell and Y18E transfected cells. **B.** CDF plots comparing the normalized rho (which indicates the distance travelled by the lysosome from the cell center) obtained from TIRF imaging and SIM imaging show the same response. All these results show that Y18E tau inhibits lysosome localization in the cell periphery. Image taken from Balabanian et al., 2022.

Using Zeiss Zen Blue software, the data were analyzed, and 3D reconstructed spatial images of the lysosome motility in the cell were generated (Fig. 18A). This project was done in collaboration with Linda Balabanian, Dominique Lessard, Pamela Yaninska, Muriel Sebastien, Samuel Wang, Piper Stevens, Paul Wiseman, Christopher Berger, and Adam Hendricks (Manuscript accepted; mentioned in the bibliography and cited in this proposal work) (Balabanian et al., 2022).

6.2. Characterizing Motor Protein Motility Using Optogenetic Inhibition

One of the important questions that require focus in the field of intracellular protein trafficking is why there are multiple motors required for an organelle for robust transport in a cell. This is necessary to address as the collective action of the motor proteins and coordination among themselves is mainly unexplored as this project proposes that each motor has a distinct role to play in the transport of organelles.

So, in this project, an optogenetic system using the LOVTRAP system was employed in which each motor protein (kinesin-1, kinesin-2, kinesin-3, and dynein) involved in transporting early endosomes, late endosomes, and lysosomes, were temporally inhibited to understand how the vesicles in the endocytic pathway rely on the unique set of motors and their coordination to drive the cargo to the right destination (Fig. 19). Upon inhibiting specific motors, it was expected that there would be a directional switch in the cargo transport and so it would be helpful to visualize this switch. The velocity parameter can provide information on the bidirectionality switches over time that the motor proteins undergo when carrying cargo in a cell. Hence, my work in this project aimed to develop a velocity MATLAB code that identifies the directional switch.

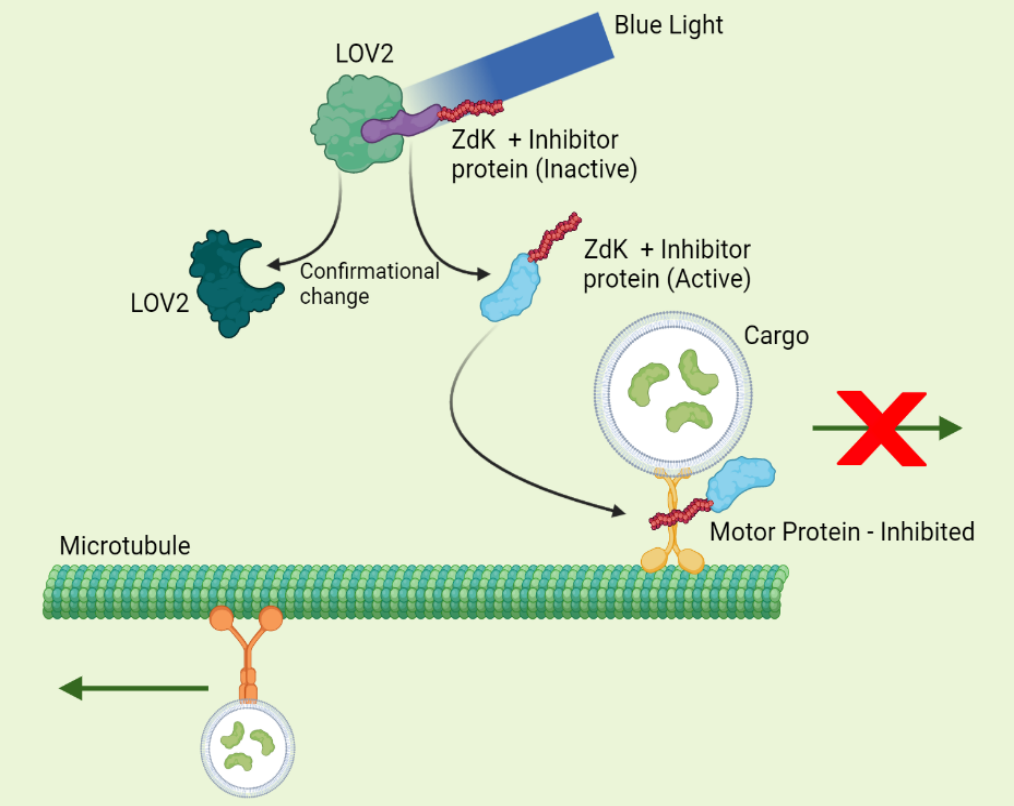

Figure 19: Characterizing motor protein motility using optogenetic inhibition. This schematic diagram shows how the optogenetic LOVTRAP system can be used to control the activity of motor proteins. When the blue light is shone on the LOV2 protein, it undergoes a conformational change that activates the ZDK + inhibitor protein complex. This complex then binds to the motor protein, inhibiting its activity. When the blue light is turned off, the LOV2 protein returns to its inactive state and the motor protein is no longer inhibited. [Image created using Biorender]

Using Trackmate, X and Y coordinates, and the time duration of each motor trajectory in a cell was obtained. Using MATLAB and the trackmate, the 2D position of the individual trajectories was calculated. The trajectories which span less than 400 timeframes were discarded. This is done to choose the trajectories that span in 2 conditions (dark state – normal uninhibited state and lit state – inhibited state). The sliding window algorithm was employed to analyze the data, reducing the computational power by breaking the large array into smaller sub-arrays. So, this algorithm calculated the average velocity of the individual trajectories with a window size of 15 seconds. The average of all the trajectories was calculated by focusing on the 20 seconds before the inhibition as it best represented the conditions of the motor motility moments before the optogenetic inhibition. The average velocity was then categorized into 3 parts: Positive

velocity (velocity ≥ 0.01 um/s), negative velocity (velocity ≤ - 0.01 um/s) and neutral velocity (0.01 um/s < velocity < -0.01 um/s). This differentiation helped us understand the change in the motor protein directionality and processivity before and upon optogenetic inhibition (Fig. 20).

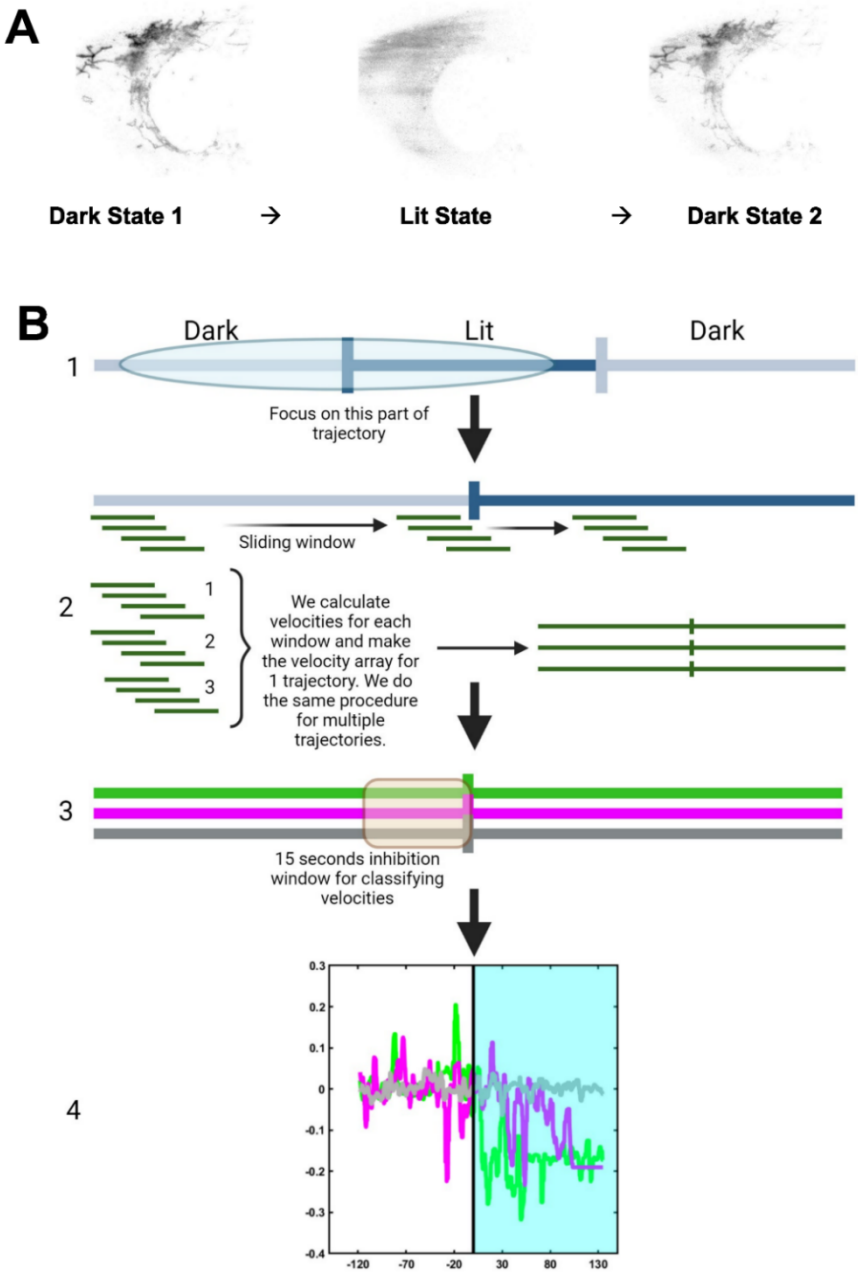

Figure 20: Optogenetic system and developing the velocity code to visualize the directionality switch of the motor protein. A. Time series snapshots of the reversible LOVTRAP optogenetic inhibitor system to inhibit specific motor proteins. At dark state 1, LOV2-Zdk complex-bound motor inhibitory peptide is attached to the mitochondria. Upon blue light illumination, the complex dissociates, and the Zdk-inhibitory peptide spreads in the cytosol to inhibit the motor protein of interest. When the blue light illumination is stopped, the Zdk-inhibitory peptide binds to the LOV2 to reform the complex, and this optogenetic inhibition can be repeated. **B.** Schematic diagram of how the velocity code works. 1) We focus on the trajectory data of the specific motor protein of interest that has undergone the first transition from the dark to the lit state. 2) We break down the trajectory into multiple

windows of specific size using the sliding window algorithm and calculate the velocity for each window to get a velocity array for a single trajectory. We do the same procedure for multiple trajectories. 3) To categorize the velocities as Positive velocity (velocity ≥ 0.01 um/s), negative velocity (velocity ≤ - 0.01 um/s) and neutral velocity (0.01 um/s < velocity < -0.01 um/s), the velocity in the 15 seconds before inhibition was considered, representing the state of motor motility right before inhibition. After categorization, we average all the velocities that are positive, negative, and neutral and plot them for visualization. 4) The line plot will show the directionality of the specific motor protein before the inhibition, and the directionality switch it faces after the optogenetic inhibition, which is helpful to characterize the motor proteins carrying specific cargoes. Image taken from Nagpal et al., 2023 and created using Biorender.

Upon employing this code, it was observed that when inhibiting specific motors transiently, the cargo in motion can undergo a directional switch (Fig. 19). This code helped visualize the temporally controlled optogenetic inhibition effect. This project was done in collaboration with Sahil Nagpal, Samuel Wang, Florian Berger and Adam Hendricks (manuscript submitted for review) (Nagpal et al., 2023).

7. Bibliography

Aiken, J., & Holzbaur, E. L. F. (2021). Cytoskeletal regulation guides neuronal trafficking to effectively supply the synapse. In *Current Biology* (Vol. 31, Issue 10, pp. R633–R650). Cell Press. https://doi.org/10.1016/j.cub.2021.02.024

Alushin, G. M., Lander, G. C., Kellogg, E. H., Zhang, R., Baker, D., & Nogales, E. (2014). High-Resolution Microtubule Structures Reveal the Structural Transitions in αβ-Tubulin upon GTP Hydrolysis. *Cell*, *157*(5), 1117–1129. https://doi.org/https://doi.org/10.1016/j.cell.2014.03.053

Anthis, N. J., Haling, J. R., Oxley, C. L., Memo, M., Wegener, K. L., Lim, C. J., Ginsberg, M. H., & Campbell, I. D. (2009). β Integrin Tyrosine Phosphorylation Is a Conserved Mechanism for Regulating Talin-induced Integrin Activation*. *Journal of Biological Chemistry*, *284*(52), 36700–36710. https://doi.org/https://doi.org/10.1074/jbc.M109.061275

Armstrong, M. J., Litvan, I., Lang, A. E., Bak, T. H., Bhatia, K. P., Borroni, B., Boxer, A. L., Dickson, D. W., Grossman, M., Hallett, M., Josephs, K. A., Kertesz, A., Lee, S. E., Miller, B. L., Reich, S. G., Riley, D. E., Tolosa, E., Tröster, A. I., Vidailhet, M., & Weiner, W. J. (2013). Criteria for the diagnosis of corticobasal degeneration. *Neurology*, *80*(5), 496. https://doi.org/10.1212/WNL.0b013e31827f0fd1

Avila, J., León-Espinosa, G., García, E., García-Escudero, V., Hernández, F., & Defelipe, J. (2012). Tau phosphorylation by GSK3 in different conditions. In *International Journal of Alzheimer's Disease*. https://doi.org/10.1155/2012/578373

Baas, P. W., & Qiang, L. (2019). Tau: It's Not What You Think. *Trends in Cell Biology*, *29*(6), 452–461. https://doi.org/https://doi.org/10.1016/j.tcb.2019.02.007

Balabanian, L., Berger, C. L., & Hendricks, A. G. (2017). Acetylated Microtubules Are Preferentially Bundled Leading to Enhanced Kinesin-1 Motility. *Biophysical Journal*, *113*(7), 1551–1560. https://doi.org/https://doi.org/10.1016/j.bpj.2017.08.009

Balabanian, L., Chaudhary, A. R., & Hendricks, A. G. (2018). Traffic control inside the cell: microtubule-based regulation of cargo transport How do PTMs control microtubule track stability and direct cargo trafficking? *The Biochemist*, *40*(2), 14–17. http://portlandpress.com/biochemist/article-pdf/40/2/14/851779/bio040020014.pdf

Balabanian, L., Lessard, D. V, Swaminathan, K., Yaninska, P., Sébastien, M., Wang, S., Stevens, P. W., Wiseman, P. W., Berger, C. L., & Hendricks, A. G. (2022). Tau differentially regulates the transport of early endosomes and lysosomes. *Molecular Biology of the Cell*, *33*(13), ar128. https://doi.org/10.1091/mbc.E22-01-0018

Ballatore, C., Lee, V. M. Y., & Trojanowski, J. Q. (2007). Tau-mediated neurodegeneration in Alzheimer's disease and related disorders. In *Nature Reviews Neuroscience* (Vol. 8, Issue 9, pp. 663–672). https://doi.org/10.1038/nrn2194

Barbier, P., Zejneli, O., Martinho, M., Lasorsa, A., Belle, V., Smet-Nocca, C., Tsvetkov, P. O., Devred, F., & Landrieu, I. (2019). Role of Tau as a Microtubule-Associated Protein: Structural and Functional Aspects. *Frontiers in Aging Neuroscience*, *11*. https://www.frontiersin.org/articles/10.3389/fnagi.2019.00204

Barghorn, S., Zheng-Fischhöfer, Q., Ackmann, M., Biernat, J., von Bergen, M., Mandelkow, E.-M., & Mandelkow, E. (2000). Structure, Microtubule Interactions, and Paired Helical Filament Aggregation by Tau Mutants of Frontotemporal Dementias. *Biochemistry*, *39*(38), 11714–11721. https://doi.org/10.1021/bi000850r

Beaudet, D., Berger, C. L., & Hendricks, A. G. (2023). *Tau inhibits the long-range, dynein-mediated motility of early phagosomes (To be submitted)*.

Bechstedt, S., Lu, K., & Brouhard, G. J. (2014). Doublecortin Recognizes the Longitudinal Curvature of the Microtubule End and Lattice. *Current Biology*, *24*(20), 2366–2375. https://doi.org/https://doi.org/10.1016/j.cub.2014.08.039

Bertrand, J., Plouffe, V., Sénéchal, P., & Leclerc, N. (2010). The pattern of human tau phosphorylation is the result of priming and feedback events in primary hippocampal neurons. *Neuroscience*, *168*(2), 323–334. https://doi.org/https://doi.org/10.1016/j.neuroscience.2010.04.009

Boumil, E. F., Vohnoutka, R. B., Lee, S., & Shea, T. B. (2020). Tau interferes with axonal neurite stabilization and cytoskeletal composition independently of its ability to associate with microtubules. *Biology Open*, *9*(9), bio052530. https://doi.org/10.1242/bio.052530

Bowles, K. R., Pugh, D. A., Pedicone, C., Oja, L., Weitzman, S. A., Liu, Y., Chen, J. L., Disney, M. D., & Goate, A. M. (2023). Development of MAPT S305 mutation models exhibiting

elevated 4R tau expression, resulting in altered neuronal and astrocytic function. *BioRxiv*, 2023.06.02.543224. https://doi.org/10.1101/2023.06.02.543224

Breuzard, G., Hubert, P., Nouar, R., De Bessa, T., Devred, F., Barbier, P., Sturgis, J. N., & Peyrot, V. (2013). Molecular mechanisms of Tau binding to microtubules and its role in microtubule dynamics in live cells. *Journal of Cell Science*, *126*(13), 2810–2819. https://doi.org/10.1242/jcs.120832

Brouhard, G. J., & Rice, L. M. (2018). Microtubule dynamics: an interplay of biochemistry and mechanics. *Nature Reviews Molecular Cell Biology*, *19*(7), 451–463. https://doi.org/10.1038/s41580-018-0009-y

Cario, A., & Berger, C. L. (2023). Tau, microtubule dynamics, and axonal transport: New paradigms for neurodegenerative disease. *BioEssays*, *45*(8), 2200138. https://doi.org/https://doi.org/10.1002/bies.202200138

Cario, A., Savastano, A., Wood, N. B., Liu, Z., Previs, M. J., Hendricks, A. G., Zweckstetter, M., & Berger, C. L. (2022). The pathogenic R5L mutation disrupts formation of Tau complexes on the microtubule by altering local N-terminal structure. *Proceedings of the National Academy of Sciences*, *119*(7), e2114215119. https://doi.org/10.1073/pnas.2114215119

Castle, B. T., McKibben, K. M., Rhoades, E., & Odde, D. J. (2020). Tau Avoids the GTP Cap at Growing Microtubule Plus-Ends. *IScience*, *23*(12), 101782. https://doi.org/https://doi.org/10.1016/j.isci.2020.101782

Chang, C.-W., Shao, E., & Mucke, L. (2021). Tau: Enabler of diverse brain disorders and target of rapidly evolving therapeutic strategies. *Science*, *371*(6532), eabb8255. https://doi.org/10.1126/science.abb8255

Chapelet, G., Béguin, N., Castellano, B., Grit, I., de Coppet, P., Oullier, T., Neunlist, M., Blottière, H., Rolli-Derkinderen, M., Le Dréan, G., & Derkinderen, P. (2023). Tau expression and phosphorylation in enteroendocrine cells. *Frontiers in Neuroscience*, *17*. https://www.frontiersin.org/articles/10.3389/fnins.2023.1166848

Chaubet, L., Chaudhary, A. R., Heris, H. K., Ehrlicher, A. J., & Hendricks, A. G. (2020). Dynamic actin cross-linking governs the cytoplasm's transition to fluid-like behavior.

Molecular Biology of the Cell, *31*(16), 1744–1752. https://doi.org/10.1091/mbc.E19-09-0504

Chaudhary, A. R., Berger, F., Berger, C. L., & Hendricks, A. G. (2018). Tau directs intracellular trafficking by regulating the forces exerted by kinesin and dynein teams. *Traffic*, *19*(2), 111–121. https://doi.org/10.1111/tra.12537

Chen, J., Kanai, Y., Cowan, N. J., & Hirokawa, N. (1992). Projection domains of MAP2 and tau determine spacings between microtubules in dendrites and axons. *Nature*, *360*(6405), 674–677. https://doi.org/10.1038/360674a0

Chong, F. P., Ng, K. Y., Koh, R. Y., & Chye, S. M. (2018). Tau Proteins and Tauopathies in Alzheimer's Disease. *Cellular and Molecular Neurobiology*, *38*(5), 965–980. https://doi.org/10.1007/s10571-017-0574-1

Combs, B., Mueller, R. L., Morfini, G., Brady, S. T., & Kanaan, N. M. (2019). Tau and Axonal Transport Misregulation in Tauopathies. In *Advances in Experimental Medicine and Biology* (Vol. 1184, pp. 81–95). Springer. https://doi.org/10.1007/978-981-32-9358-8_7

Dixit, R., Ross, J. L., Goldman, Y. E., & Holzbaur, E. L. F. (2008). Differential Regulation of Dynein and Kinesin Motor Proteins by Tau. *Science*, *319*(5866), 1086–1089. https://doi.org/10.1126/science.1152993

D'Souza, I., & Schellenberg, G. D. (2005). Regulation of tau isoform expression and dementia. *Biochimica et Biophysica Acta (BBA) - Molecular Basis of Disease*, *1739*(2), 104–115. https://doi.org/https://doi.org/10.1016/j.bbadis.2004.08.009

Duquette, A., Pernègre, C., Veilleux Carpentier, A., & Leclerc, N. (2021). Similarities and Differences in the Pattern of Tau Hyperphosphorylation in Physiological and Pathological Conditions: Impacts on the Elaboration of Therapies to Prevent Tau Pathology. In *Frontiers in Neurology* (Vol. 11). Frontiers Media S.A. https://doi.org/10.3389/fneur.2020.607680

Ershov, D., Phan, M.-S., Pylvänäinen, J. W., Rigaud, S. U., Le Blanc, L., Charles-Orszag, A., Conway, J. R. W., Laine, R. F., Roy, N. H., Bonazzi, D., Duménil, G., Jacquemet, G., & Tinevez, J.-Y. (2022). TrackMate 7: integrating state-of-the-art segmentation algorithms into tracking pipelines. *Nature Methods*, *19*(7), 829–832. https://doi.org/10.1038/s41592-022-01507-1

Fernández-Nogales, M., & Lucas, J. J. (2020). Altered Levels and Isoforms of Tau and Nuclear Membrane Invaginations in Huntington's Disease. *Frontiers in Cellular Neuroscience*, *13*. https://www.frontiersin.org/articles/10.3389/fncel.2019.00574

Fish, K. N. (2022). Total Internal Reflection Fluorescence (TIRF) Microscopy. *Current Protocols*, *2*(8), e517. https://doi.org/https://doi.org/10.1002/cpz1.517

Fletcher, D. A., & Mullins, R. D. (2010). Cell mechanics and the cytoskeleton. *Nature*, *463*(7280), 485–492. https://doi.org/10.1038/nature08908

Gendron, T. F. (2009). The role of tau in neurodegeneration. *Molecular Neurodegeneration*, *4*(1). https://doi.org/10.1186/1750-1326-4-13

Genova, M., Grycova, L., Puttrich, V., Magiera, M. M., Lansky, Z., Janke, C., & Braun, M. (2023). Tubulin polyglutamylation differentially regulates microtubule-interacting proteins. *The EMBO Journal*, *42*(5), e112101. https://doi.org/https://doi.org/10.15252/embj.2022112101

Goedert, M., Eisenberg, D. S., & Crowther, R. A. (2017). Propagation of Tau Aggregates and Neurodegeneration. *Annual Review of Neuroscience*, *40*(1), 189–210. https://doi.org/10.1146/annurev-neuro-072116-031153

Goedert, M., Spillantini, M. G., Jakes, R., Rutherford, D., & Crowther, R. A. (1989). Multiple isoforms of human microtubule-associated protein tau: sequences and localization in neurofibrillary tangles of Alzheimer's disease. *Neuron*, *3*(4), 519–526. https://doi.org/https://doi.org/10.1016/0896-6273(89)90210-9

Guha, S., Johnson, G. V. W., & Nehrke, K. (2020). The Crosstalk Between Pathological Tau Phosphorylation and Mitochondrial Dysfunction as a Key to Understanding and Treating Alzheimer's Disease. *Molecular Neurobiology*, *57*(12), 5103–5120. https://doi.org/10.1007/s12035-020-02084-0

Guo, T., Noble, W., & Hanger, D. P. (2017). Roles of tau protein in health and disease. *Acta Neuropathologica*, *133*(5), 665–704. https://doi.org/10.1007/s00401-017-1707-9

Guo, W., Stoklund Dittlau, K., & Van Den Bosch, L. (2020). Axonal transport defects and neurodegeneration: Molecular mechanisms and therapeutic implications. *Seminars in Cell & Developmental Biology*, *99*, 133–150. https://doi.org/https://doi.org/10.1016/j.semcdb.2019.07.010

Hallinan, G. I., Vargas-Caballero, M., West, J., & Deinhardt, K. (2019). Tau Misfolding Efficiently Propagates between Individual Intact Hippocampal Neurons. *The Journal of Neuroscience*, *39*(48), 9623. https://doi.org/10.1523/JNEUROSCI.1590-19.2019

Hamano, T., Enomoto, S., Shirafuji, N., Ikawa, M., Yamamura, O., Yen, S. H., & Nakamoto, Y. (2021). Autophagy and tau protein. In *International Journal of Molecular Sciences* (Vol. 22, Issue 14). MDPI AG. https://doi.org/10.3390/ijms22147475

Hanger, D. P., & Noble, W. (2011). Functional implications of glycogen synthase kinase-3-mediated tau phosphorylation. In *International Journal of Alzheimer's Disease*. https://doi.org/10.4061/2011/352805

Harada, A., Oguchi, K., Okabe, S., Kuno, J., Terada, S., Ohshima, T., Sato-Yoshitake, R., Takei, Y., Noda, T., & Hirokawa, N. (1994). Altered microtubule organization in small-calibre axons of mice lacking tau protein. *Nature*, *369*(6480), 488–491. https://doi.org/10.1038/369488a0

Hinrichs, M. H., Jalal, A., Brenner, B., Mandelkow, E., Kumar, S., & Scholz, T. (2012). Tau Protein Diffuses along the Microtubule Lattice*. *Journal of Biological Chemistry*, *287*(46), 38559–38568. https://doi.org/https://doi.org/10.1074/jbc.M112.369785

Hirokawa, N., & Tanaka, Y. (2015). Kinesin superfamily proteins (KIFs): Various functions and their relevance for important phenomena in life and diseases. *Experimental Cell Research*, *334*(1), 16–25. https://doi.org/https://doi.org/10.1016/j.yexcr.2015.02.016

Hoeprich, G. J., Mickolajczyk, K. J., Nelson, S. R., Hancock, W. O., & Berger, C. L. (2017). The axonal transport motor kinesin-2 navigates microtubule obstacles via protofilament switching. *Traffic*, *18*(5), 304–314. https://doi.org/https://doi.org/10.1111/tra.12478

Hoeprich, G. J., Thompson, A. R., McVicker, D. P., Hancock, W. O., & Berger, C. L. (2014). Kinesin's neck-linker determines its ability to navigate obstacles on the microtubule surface. *Biophysical Journal*, *106*(8), 1691–1700. https://doi.org/10.1016/j.bpj.2014.02.034

Hoover, B. R., Reed, M. N., Su, J., Penrod, R. D., Kotilinek, L. A., Grant, M. K., Pitstick, R., Carlson, G. A., Lanier, L. M., Yuan, L. L., Ashe, K. H., & Liao, D. (2010). Tau Mislocalization to Dendritic Spines Mediates Synaptic Dysfunction Independently of

Neurodegeneration. *Neuron*, *68*(6), 1067–1081. https://doi.org/10.1016/j.neuron.2010.11.030

Horio, T., & Murata, T. (2014). The role of dynamic instability in microtubule organization. *Frontiers in Plant Science*, *5*. https://www.frontiersin.org/articles/10.3389/fpls.2014.00511

Hyttinen, J. M. T., Niittykoski, M., Salminen, A., & Kaarniranta, K. (2013). Maturation of autophagosomes and endosomes: A key role for Rab7. *Biochimica et Biophysica Acta (BBA) - Molecular Cell Research*, *1833*(3), 503–510. https://doi.org/https://doi.org/10.1016/j.bbamcr.2012.11.018

Iqbal, K., Liu, F., & Gong, C.-X. (2016). Tau and neurodegenerative disease: the story so far. *Nature Reviews Neurology*, *12*(1), 15–27. https://doi.org/10.1038/nrneurol.2015.225

Jovanov-Milošević, N., Petrović, D., Sedmak, G., Vukšić, M., Hof, P. R., & Šimić, G. (2012). Human fetal tau protein isoform: Possibilities for Alzheimer's disease treatment. *The International Journal of Biochemistry & Cell Biology*, *44*(8), 1290–1294. https://doi.org/https://doi.org/10.1016/j.biocel.2012.05.001

Kametani, F., & Hasegawa, M. (2018). Reconsideration of Amyloid Hypothesis and Tau Hypothesis in Alzheimer's Disease. *Frontiers in Neuroscience*, *12*. https://www.frontiersin.org/articles/10.3389/fnins.2018.00025

Kanai, Y., Chen, J., & Hirokawa, N. (1992). Microtubule bundling by tau proteins in vivo: analysis of functional domains. *The EMBO Journal*, *11*(11), 3953–3961. https://doi.org/https://doi.org/10.1002/j.1460-2075.1992.tb05489.x

Karhanová, A., & Lánský, Z. (2023). *Role of tau phosphorylation in formation of tau envelopes* [Univerzita Karlova (Faculty of Science)]. https://dspace.cuni.cz/handle/20.500.11956/181446

Katrukha, E. A., Jurriens, D., Salas Pastene, D. M., & Kapitein, L. C. (2021). Quantitative mapping of dense microtubule arrays in mammalian neurons. *ELife*, *10*, e67925. https://doi.org/10.7554/eLife.67925

Katsinelos, T., Zeitler, M., Dimou, E., Karakatsani, A., Müller, H.-M., Nachman, E., Steringer, J. P., Ruiz de Almodovar, C., Nickel, W., & Jahn, T. R. (2018). Unconventional Secretion

Mediates the Trans-cellular Spreading of Tau. *Cell Reports*, *23*(7), 2039–2055. https://doi.org/https://doi.org/10.1016/j.celrep.2018.04.056

Kellogg, E. H., Hejab, N. M. A., Poepsel, S., Downing, K. H., DiMaio, F., & Nogales, E. (2018). Near-atomic model of microtubule-tau interactions. *Science*, *360*(6394), 1242–1246. https://doi.org/10.1126/science.aat1780

Kent, S. A., Spires-Jones, T. L., & Durrant, C. S. (2020). The physiological roles of tau and Aβ: implications for Alzheimer's disease pathology and therapeutics. *Acta Neuropathologica*, *140*(4), 417–447. https://doi.org/10.1007/s00401-020-02196-w

Kundel, F., Hong, L., Falcon, B., McEwan, W. A., Michaels, T. C. T., Meisl, G., Esteras, N., Abramov, A. Y., Knowles, T. J. P., Goedert, M., & Klenerman, D. (2018). Measurement of Tau Filament Fragmentation Provides Insights into Prion-like Spreading. *ACS Chemical Neuroscience*, *9*(6), 1276–1282. https://doi.org/10.1021/acschemneuro.8b00094

Lessard, D. V., Zinder, O. J., Hotta, T., Verhey, K. J., Ohi, R., & Berger, C. L. (2019). Polyglutamylation of tubulin's C-terminal tail controls pausing and motility of kinesin-3 family member KIF1A. *Journal of Biological Chemistry*, *294*(16), 6353–6363. https://doi.org/10.1074/jbc.RA118.005765

Lipka, J., Kapitein, L. C., Jaworski, J., & Hoogenraad, C. C. (2016). Microtubule-binding protein doublecortin-like kinase 1 (DCLK1) guides kinesin-3-mediated cargo transport to dendrites. *The EMBO Journal*, *35*(3), 302–318. https://doi.org/https://doi.org/10.15252/embj.201592929

Liu, F., & Gong, C.-X. (2008). Tau exon 10 alternative splicing and tauopathies. *Molecular Neurodegeneration*, *3*(1), 8. https://doi.org/10.1186/1750-1326-3-8

Loubéry, S., Wilhelm, C., Hurbain, I., Neveu, S., Louvard, D., & Coudrier, E. (2008). Different Microtubule Motors Move Early and Late Endocytic Compartments. *Traffic*, *9*(4), 492–509. https://doi.org/https://doi.org/10.1111/j.1600-0854.2008.00704.x

Maday, S., Wallace, K. E., & Holzbaur, E. L. F. (2012). Autophagosomes initiate distally and mature during transport toward the cell soma in primary neurons. *Journal of Cell Biology*, *196*(4), 407–417. https://doi.org/10.1083/jcb.201106120

Martin, L., Latypova, X., Wilson, C. M., Magnaudeix, A., Perrin, M.-L., Yardin, C., & Terro, F. (2013). Tau protein kinases: Involvement in Alzheimer's disease. *Ageing Research Reviews*, *12*(1), 289–309. https://doi.org/https://doi.org/10.1016/j.arr.2012.06.003

Maurage, C.-A., Sergeant, N., Ruchoux, M.-M., Hauw, J.-J., & Delacourte, A. (2003). Phosphorylated serine 199 of microtubule-associated protein tau is a neuronal epitope abundantly expressed in youth and an early marker of tau pathology. *Acta Neuropathologica*, *105*(2), 89–97. https://doi.org/10.1007/s00401-002-0608-7

McVicker, D. P., Chrin, L. R., & Berger, C. L. (2011). The Nucleotide-binding State of Microtubules Modulates Kinesin Processivity and the Ability of Tau to Inhibit Kinesin-mediated Transport*. *Journal of Biological Chemistry*, *286*(50), 42873–42880. https://doi.org/https://doi.org/10.1074/jbc.M111.292987

McVicker, D. P., Hoeprich, G. J., Thompson, A. R., & Berger, C. L. (2014a). Tau interconverts between diffusive and stable populations on the microtubule surface in an isoform and lattice specific manner. *Cytoskeleton*, *71*(3), 184–194. https://doi.org/https://doi.org/10.1002/cm.21163

McVicker, D. P., Hoeprich, G. J., Thompson, A. R., & Berger, C. L. (2014b). Tau interconverts between diffusive and stable populations on the microtubule surface in an isoform and lattice specific manner. *Cytoskeleton*, *71*(3), 184–194. https://doi.org/https://doi.org/10.1002/cm.21163

Mitchison, T., & Kirschner, M. (1984). Dynamic instability of microtubule growth. *Nature*, *312*(5991), 237–242. https://doi.org/10.1038/312237a0

Monroy, B. Y., Sawyer, D. L., Ackermann, B. E., Borden, M. M., Tan, T. C., & Ori-McKenney, K. M. (2018). Competition between microtubule-associated proteins directs motor transport. *Nature Communications*, *9*(1), 1487. https://doi.org/10.1038/s41467-018-03909-2

Montejo de Garcini, E., de la Luna, S., Dominguez, J. E., & Avila, J. (1994). Overexpression of tau protein in COS-1 cells results in the stabilization of centrosome-independent microtubules and extension of cytoplasmic processes. *Molecular and Cellular Biochemistry*, *130*(2), 187–196. https://doi.org/10.1007/BF01457399

Mueller, R. L., Combs, B., Alhadidy, M. M., Brady, S. T., Morfini, G. A., & Kanaan, N. M. (2021). Tau: A Signaling Hub Protein. *Frontiers in Molecular Neuroscience*, *14*. https://www.frontiersin.org/articles/10.3389/fnmol.2021.647054

Muroyama, A., & Lechler, T. (2017). Microtubule organization, dynamics and functions in differentiated cells. *Development*, *144*(17), 3012–3021. https://doi.org/10.1242/dev.153171

Nagpal, S., Wang, S., Swaminathan, K., Berger, F., & Hendricks, A. G. (2023). *Optogenetic control of kinesins-1,-2,-3, and dynein reveals their specific roles in vesicular transport (Submitted)*.

Niewidok, B., Igaev, M., Sündermann, F., Janning, D., Bakota, L., & Brandt, R. (2016). Presence of a carboxy-terminal pseudorepeat and disease-like pseudohyperphosphorylation critically influence tau's interaction with microtubules in axon-like processes. *Molecular Biology of the Cell*, *27*(22), 3537–3549. https://doi.org/10.1091/mbc.E16-06-0402

Noble, W., Hanger, D., Miller, C., & Lovestone, S. (2013). The Importance of Tau Phosphorylation for Neurodegenerative Diseases. *Frontiers in Neurology*, *4*. https://www.frontiersin.org/articles/10.3389/fneur.2013.00083

Pu, J., Guardia, C. M., Keren-Kaplan, T., & Bonifacino, J. S. (2016). Mechanisms and functions of lysosome positioning. *Journal of Cell Science*, *129*(23), 4329–4339. https://doi.org/10.1242/jcs.196287

Qiang, L., Sun, X., Austin, T. O., Muralidharan, H., Jean, D. C., Liu, M., Yu, W., & Baas, P. W. (2018). Tau Does Not Stabilize Axonal Microtubules but Rather Enables Them to Have Long Labile Domains. *Current Biology*, *28*(13), 2181-2189.e4. https://doi.org/https://doi.org/10.1016/j.cub.2018.05.045

Rodríguez-Martín, T., Cuchillo-Ibáñez, I., Noble, W., Nyenya, F., Anderton, B. H., & Hanger, D. P. (2013a). Tau phosphorylation affects its axonal transport and degradation. *Neurobiology of Aging*, *34*(9), 2146–2157. https://doi.org/https://doi.org/10.1016/j.neurobiolaging.2013.03.015

Rodríguez-Martín, T., Cuchillo-Ibáñez, I., Noble, W., Nyenya, F., Anderton, B. H., & Hanger, D. P. (2013b). Tau phosphorylation affects its axonal transport and degradation.

Neurobiology of Aging, *34*(9), 2146–2157. https://doi.org/10.1016/j.neurobiolaging.2013.03.015

Rosenberg, K. J., Ross, J. L., Feinstein, H. E., Feinstein, S. C., & Israelachvili, J. (2008). Complementary dimerization of microtubule-associated tau protein: Implications for microtubule bundling and tau-mediated pathogenesis. *Proceedings of the National Academy of Sciences*, *105*(21), 7445–7450. https://doi.org/10.1073/pnas.0802036105

Samsonov, A., Yu, J.-Z., Rasenick, M., & Popov, S. V. (2004). Tau interaction with microtubules in vivo. *Journal of Cell Science*, *117*(25), 6129–6141. https://doi.org/10.1242/jcs.01531

Scholey, J. M. (2013). Kinesin-2: A Family of Heterotrimeric and Homodimeric Motors with Diverse Intracellular Transport Functions. *Annual Review of Cell and Developmental Biology*, *29*(1), 443–469. https://doi.org/10.1146/annurev-cellbio-101512-122335

Sergeant, N., Bretteville, A., Hamdane, M., Caillet-Boudin, M.-L., Grognet, P., Bombois, S., Blum, D., Delacourte, A., Pasquier, F., Vanmechelen, E., Schraen-Maschke, S., & Buée, L. (2008). Biochemistry of Tau in Alzheimer's disease and related neurological disorders. *Expert Review of Proteomics*, *5*(2), 207–224. https://doi.org/10.1586/14789450.5.2.207

Shahpasand, K., Uemura, I., Saito, T., Asano, T., Hata, K., Shibata, K., Toyoshima, Y., Hasegawa, M., & Hisanaga, S. (2012). Regulation of Mitochondrial Transport and Inter-Microtubule Spacing by Tau Phosphorylation at the Sites Hyperphosphorylated in Alzheimer's Disease. *The Journal of Neuroscience*, *32*(7), 2430. https://doi.org/10.1523/JNEUROSCI.5927-11.2012

Siahaan, V., Krattenmacher, J., Hyman, A. A., Diez, S., Hernández-Vega, A., Lansky, Z., & Braun, M. (2019). Kinetically distinct phases of tau on microtubules regulate kinesin motors and severing enzymes. *Nature Cell Biology*, *21*(9), 1086–1092. https://doi.org/10.1038/s41556-019-0374-6

Siahaan, V., Tan, R., Humhalova, T., Libusova, L., Lacey, S. E., Tan, T., Dacy, M., Ori-McKenney, K. M., McKenney, R. J., Braun, M., & Lansky, Z. (2022). Microtubule lattice spacing governs cohesive envelope formation of tau family proteins. *Nature Chemical Biology*, *18*(11), 1224–1235. https://doi.org/10.1038/s41589-022-01096-2

Stern, J. L., Lessard, D. V, Hoeprich, G. J., Morfini, G. A., & Berger, C. L. (2017). Phosphoregulation of Tau modulates inhibition of kinesin-1 motility. *Molecular Biology of the Cell*, *28*(8), 1079–1087. https://doi.org/10.1091/mbc.e16-10-0728

Strang, K. H., Golde, T. E., & Giasson, B. I. (2019). MAPT mutations, tauopathy, and mechanisms of neurodegeneration. *Laboratory Investigation*, *99*(7), 912–928. https://doi.org/https://doi.org/10.1038/s41374-019-0197-x

Tan, R., Lam, A. J., Tan, T., Han, J., Nowakowski, D. W., Vershinin, M., Simó, S., Ori-McKenney, K. M., & McKenney, R. J. (2019). Microtubules gate tau condensation to spatially regulate microtubule functions. *Nature Cell Biology*, *21*(9), 1078–1085. https://doi.org/10.1038/s41556-019-0375-5

Tarantino, N., Tinevez, J.-Y., Crowell, E. F., Boisson, B., Henriques, R., Mhlanga, M., Agou, F., Israël, A., & Laplantine, E. (2014). TNF and IL-1 exhibit distinct ubiquitin requirements for inducing NEMO–IKK supramolecular structures. *Journal of Cell Biology*, *204*(2), 231–245. https://doi.org/10.1083/jcb.201307172

Tarawneh, R., & Holtzman, D. M. (2012). The clinical problem of symptomatic Alzheimer disease and mild cognitive impairment. *Cold Spring Harbor Perspectives in Medicine*, *2*(5). https://doi.org/10.1101/cshperspect.a006148

Tarhan, M. C., Orazov, Y., Yokokawa, R., Karsten, S. L., & Fujita, H. (2013). Biosensing MAPs as “roadblocks”: kinesin-based functional analysis of tau protein isoforms and mutants using suspended microtubules (sMTs). *Lab on a Chip*, *13*(16), 3217–3224. https://doi.org/10.1039/C3LC50151E

Toral-Rios, D., Pichardo-Rojas, P. S., Alonso-Vanegas, M., & Campos-Peña, V. (2020). GSK3β and Tau Protein in Alzheimer’s Disease and Epilepsy. In *Frontiers in Cellular Neuroscience* (Vol. 14). Frontiers Media S.A. https://doi.org/10.3389/fncel.2020.00019

Tripathi, T., Prakash, J., & Shav-Tal, Y. (2019). Phospho-Tau Impairs Nuclear-Cytoplasmic Transport. *ACS Chemical Neuroscience*, *10*(1), 36–38. https://doi.org/10.1021/acschemneuro.8b00632

Verhey, K. J., & Hammond, J. W. (2009). Traffic control: regulation of kinesin motors. *Nature Reviews Molecular Cell Biology*, *10*(11), 765–777. https://doi.org/10.1038/nrm2782

Verhey, K. J., & Ohi, R. (2023). Causes, costs and consequences of kinesin motors communicating through the microtubule lattice. *Journal of Cell Science*, *136*(5), jcs260735. https://doi.org/10.1242/jcs.260735

Vershinin, M., Carter, B. C., Razafsky, D. S., King, S. J., & Gross, S. P. (2007). Multiple-motor based transport and its regulation by Tau. *Proceedings of the National Academy of Sciences*, *104*(1), 87–92. https://doi.org/10.1073/pnas.0607919104

Vershinin, M., Xu, J., Razafsky, D. S., King, S. J., & Gross, S. P. (2008). Tuning Microtubule-Based Transport Through Filamentous MAPs: The Problem of Dynein. *Traffic*, *9*(6), 882–892. https://doi.org/https://doi.org/10.1111/j.1600-0854.2008.00741.x

Wang, Y., & Mandelkow, E. (2016). Tau in physiology and pathology. *Nature Reviews Neuroscience*, *17*(1), 22–35. https://doi.org/10.1038/nrn.2015.1

Wegmann, S., Biernat, J., & Mandelkow, E. (2021). A current view on Tau protein phosphorylation in Alzheimer's disease. *Current Opinion in Neurobiology*, *69*, 131–138. https://doi.org/https://doi.org/10.1016/j.conb.2021.03.003

Xia, Y., Prokop, S., & Giasson, B. I. (2021a). "Don't Phos Over Tau": recent developments in clinical biomarkers and therapies targeting tau phosphorylation in Alzheimer's disease and other tauopathies. *Molecular Neurodegeneration*, *16*(1), 37. https://doi.org/10.1186/s13024-021-00460-5

Xia, Y., Prokop, S., & Giasson, B. I. (2021b). "Don't Phos Over Tau": recent developments in clinical biomarkers and therapies targeting tau phosphorylation in Alzheimer's disease and other tauopathies. *Molecular Neurodegeneration*, *16*(1), 37. https://doi.org/10.1186/s13024-021-00460-5

Xia, Y., Prokop, S., Gorion, K.-M. M., Kim, J. D., Sorrentino, Z. A., Bell, B. M., Manaois, A. N., Chakrabarty, P., Davies, P., & Giasson, B. I. (2020). Tau Ser208 phosphorylation promotes aggregation and reveals neuropathologic diversity in Alzheimer's disease and other tauopathies. *Acta Neuropathologica Communications*, *8*(1), 88. https://doi.org/10.1186/s40478-020-00967-w

Yang, X., Ma, Z., Lian, P., Xu, Y., & Cao, X. (2023). Common mechanisms underlying axonal transport deficits in neurodegenerative diseases: a mini review. *Frontiers in Molecular Neuroscience*, *16*. https://www.frontiersin.org/articles/10.3389/fnmol.2023.1172197

Yogev, S., Cooper, R., Fetter, R., Horowitz, M., & Shen, K. (2016). Microtubule Organization Determines Axonal Transport Dynamics. *Neuron*, *92*(2), 449–460. https://doi.org/https://doi.org/10.1016/j.neuron.2016.09.036

Yu, Y., Run, X., Liang, Z., Li, Y., Liu, F., Liu, Y., Iqbal, K., Grundke-Iqbal, I., & Gong, C.-X. (2009). Developmental regulation of tau phosphorylation, tau kinases, and tau phosphatases. *Journal of Neurochemistry*, *108*(6), 1480–1494. https://doi.org/https://doi.org/10.1111/j.1471-4159.2009.05882.x

Zajac, A. L., Goldman, Y. E., Holzbaur, E. L. F., & Ostap, E. M. (2013). Local cytoskeletal and organelle interactions impact molecular-motor-driven early endosomal trafficking. *Current Biology*, *23*(13), 1173–1180. https://doi.org/10.1016/j.cub.2013.05.015

Zhou, L.-M., Xiao, K.-W., Chen, J., & Zhao, N. (2017). Optical levitation of nanodiamonds by doughnut beams in vacuum. *Laser & Photonics Reviews*, *11*(2), 1600284. https://doi.org/https://doi.org/10.1002/lpor.201600284

8. Appendix

8.1. Supplementary image

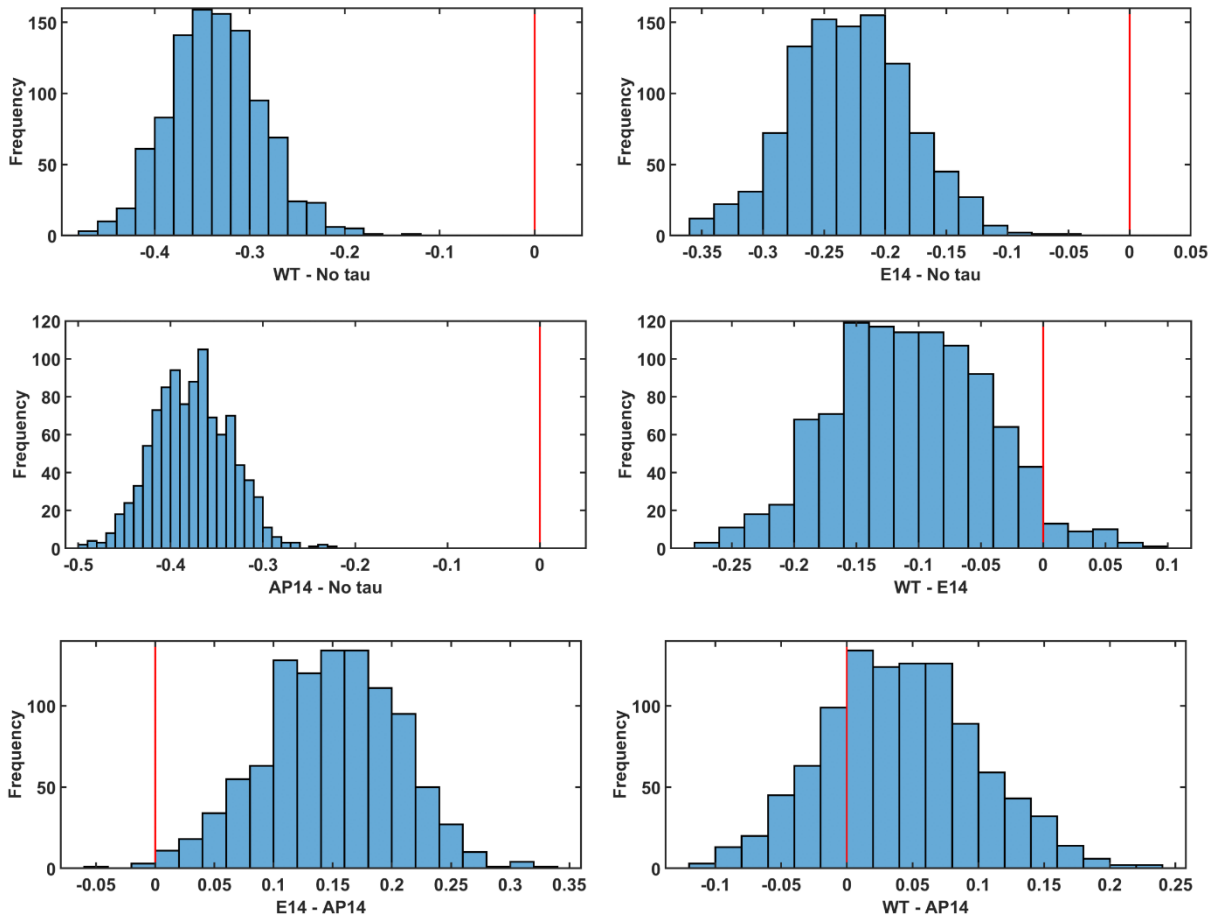

Figure S1: This figure illustrates the results of statistical significance analysis performed using p-value determination by the bootstrapping resampling method. Each plot's x-axis represents a specific parameter (alpha, Rg, velocity, localization parameters, and directionality parameters), while the y-axis displays the frequency based on 1000 bootstrapping iterations. P-values were calculated by examining whether the histogram of bootstrap mean differences between pairwise groups exceeded zero. Statistical significance was determined using a threshold of 0.05: if the histogram's tail covered less than 0.05, it was considered significant; if it exceeded 0.05, it was considered insignificant. Here, we specifically focused on Rg within the tau range of 3 to 5 for lysosomes. This was performed for other parameters at different tau ranges (1 to 3 and 3 to 5).

8.2. Protocol - Zeiss Elyra 7 Structure Illumination Microscopy (SIM)

A) Sample Preparation:

1. Transfected cells were cultivated on FluoroDish Cell Culture Dishes (World Precision Instruments) with 0.17 mm glass coverslip thickness. They were subsequently incubated in complete DMEM media with 50 nM Lysotracker Deep Red (Invitrogen) for 10 minutes.
2. Cells were then washed with Leibovitz's L-15 Medium (no phenol red) (Gibco), supplemented with 10% (v/v) FBS, followed by further incubation in the same medium for 5 minutes while preparing the microscope for imaging.
3. Place the cell culture dish in the Elyra 7 microscope chamber. Clean the microscope lens using lens cleaning paper before positioning the dish. Apply a small drop of special Zeiss immersion oil.

B) Microscope Setup:

1. Power on the computer, the heat chamber, and the microscope.
2. Verify the proper sealing of the chamber by checking for the illuminated orange light at the back. If the light is not on, reseal the chamber gently.
3. Launch the Zeiss Zen Black SR 3.0 software and initiate the system by clicking 'Start System.' Create a user profile to save your future chosen settings and parameters.
4. In the 'Locate' tab, configure the number of Z-stacks (1 for tau imaging, 15 for lysosome imaging – corresponding to 6 µm) and time series (cycles – 0 for tau, 30 for lysosomes). Enable these options accordingly before imaging.

5. Enable the desired laser types (488, 642, and 561 nm lasers) in the Laser window. Adjust laser output in laser properties.
6. Proceed to 'Imaging Setup,' choose Apotome mode, confirm the activation of camera 1 (TV1), and select appropriate lenses and filters (SBS LP 560 and BP 495-550 + BP 570-620 for tau, SBS LP 560 and BP 420-480 + L 655 for lysosomes). Utilize Alpha Plan-Apochromat 63× (NA - 1.46) oil objective lens for imaging the cells (other objectives can be used depending on your purpose).
7. In the 'Acquisition Parameter' window, enable 3-phase imaging by selecting 'Acquisition Mode.' Ensure proper incubation by enabling the heating system and setting the temperature to 37°C.

C) Image Acquisition:

Imaging Tau in Cells:

1. With parameters set, commence imaging by first focusing on tau. Use brightfield mode (WF mode) in 'Imaging Setup' to locate cells and adjust zoom for optimal focus.
2. In the 'Multidimensional Acquisition' window, choose Z-Stack and click the 'Center' button to maintain focus. Opt for [Leap] mode for imaging.
3. Under 'Acquisition Parameter,' select the desired laser for tau imaging (561 nm – 50% of 75 mW) in "Channels." Set exposure time at 50 ms per frame.
4. To acquire the image, click 'Start Experiment' in the Experiment Manager window. Verify Z-position, 3 phases, and adjust image contrast below the image viewer (changing contrast is not recommended but okay for visualization. Before saving, revert it to the default settings).
5. Save the image as a .czi file.

Imaging Lysosomes in Cells:

1. Like tau imaging, image lysosomes without changing the plane of focus.
2. Select Z-Stack in the 'Multidimensional Acquisition' window and opt for [Leap] mode. Given 15 Z-Stacks, maintain an interval of about 0.403 µm throughout.
3. Under 'Acquisition Parameter,' choose the desired laser for lysosome imaging (642 nm – 50% of 75 mW) in "Channels." Maintain an exposure time of 50 ms per frame.
4. Initiate image acquisition by clicking 'Start Experiment' in the Experiment Manager window. Check 15 Z-positions, 3 phases, and adjust image contrast if needed.
5. Save the file as a .czi file.

D) Image Processing:

1. After saving lysosome czi data, launch Zeiss Zen 3.0 SR software. In the Methods option, use SIM to batch-process images by specifying the folder location.
2. Save the resulting images as _SIM.czi files.
3. As files might be too large for direct analysis, use custom Macros code in FIJI (link in Github) to trim images to the desired time series. Save as .TIFF files for analysis with Trackmate and MATLAB.

E) 3D Image Reconstruction:

1. For 3D image reconstruction, utilize raw and SIM data of lysosomes (not post-Macros processed data).
2. Load the desired lysosome czi file (SIM or raw data) into Zeiss Zen Blue software. The image will appear in the display viewer. Access the 3D mode on the side (some versions may offer a 2.5D option).

3. Beneath the display viewer, various options like dimensions, navigation, colour mapping, and display are available. Adjust X, Y, and Z positions to orient the image for optimal 3D visualization.
4. Invert the image colours (black and white) using colour mapping after alignment.
5. Reference scales and grids can be added for contextual reference through options in the display tab.
6. Once aligned and colored, save the image as a TIFF file.